Hemodialysis vascular access failure: novel pathophysiological mechanisms and therapeutic strategies

by

Taisiya Bezhaeva

Hemodialysis vascular access failure: novel pathophysiological mechanisms and therapeutic strategies

ISBN: 978-94-6380-202-4

Cover design: Zhenya Pashkina and Taisiya Bezhaeva

Layout and printing: proeschriftmaken.nl

Hemodialysis vascular access failure: novel pathophysiological mechanisms and therapeutic strategies

Proefschrift

ter verkrijging van graad van doctor aan de Universiteit Leiden, op gezag van de Rector Magnificus Prof. Mr. C.J.J.M. Stolker,

volgens besluit van het College voor Promoties

ter verdedigen op 7 maart 2019

klokke 16:15 uur

door

Taisiya Bezhaeva

Geboren te Moskou

in 1986

Promotores	Prof. Dr. A.J. van Zonneveld
	Prof. Dr. P.H.A. Quax
Co-Promotores	Dr. J.I. Rotmans
Promotiecommissie	Prof. Dr. T. Lee
	University of Alabama at Birmingham, United States
	Prof. Dr. M.J.T.H. Goumans
	Prof. Dr. E.S.G. Stroes
	Academic Medical Center, Amsterdam, the Netherlands
	Prof. Dr. J.F. Hamming

The research described in this thesis was supported by a grant by the Leiden University Medical Center.
Financial support by the Dutch Kidney Foundation and the Dutch Heart Foundation is gratefully acknowledged.
Publication of the thesis was further supported by Proteon Therapeutics.

Table of Contents

Chapter 1

General introduction

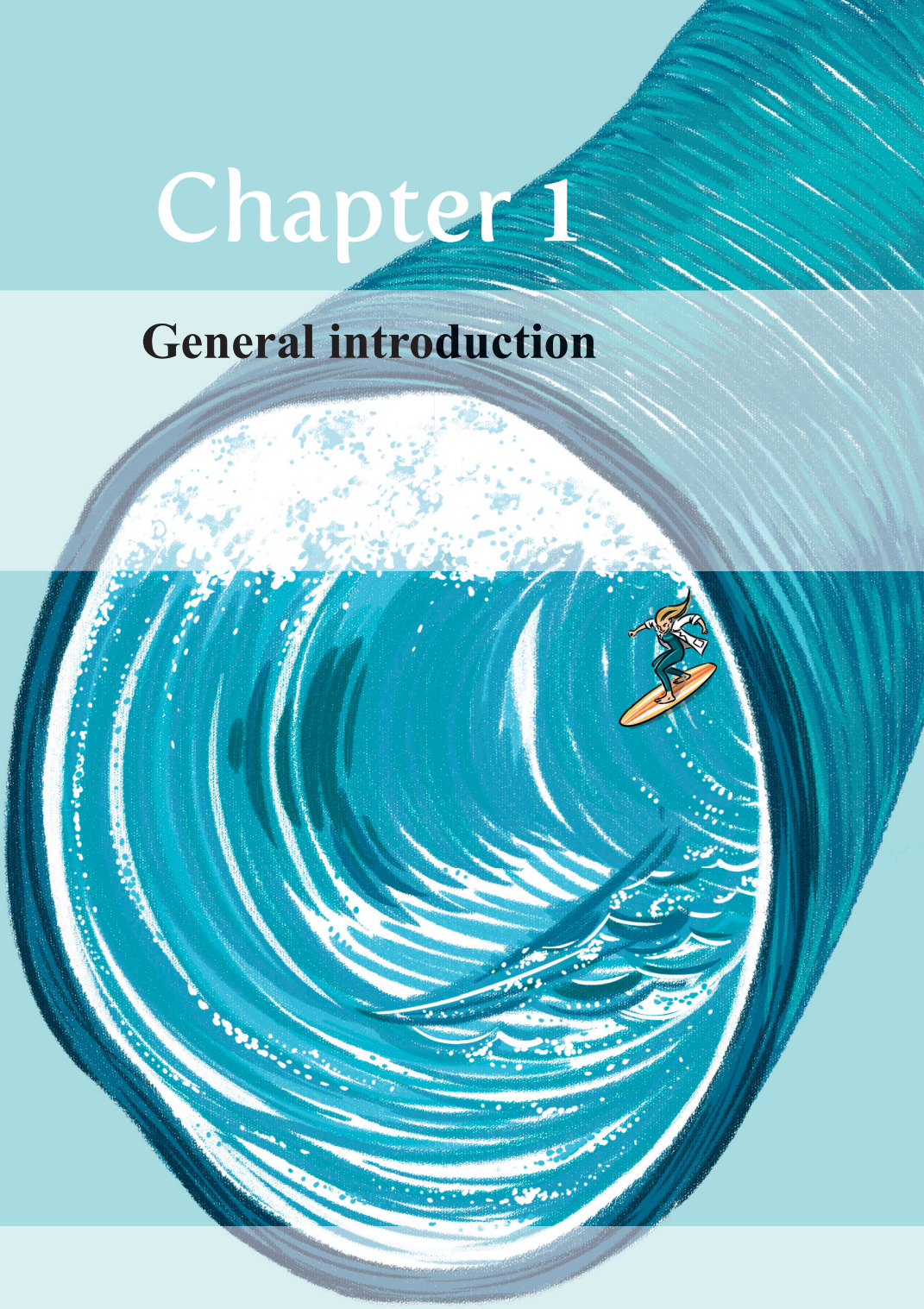

What is end stage renal disease?

The kidneys are complex organs traditionally known for their role in excretion of waste and excess water from the body. Besides, they also perform a spectrum of other functions essential for health such as helping to maintain blood pressure and assuring bone integrity. As they carry out these functions the kidneys work cooperatively and interactively with other organs systems, particularly the cardiovascular system.

Kidney disease can ultimately lead to the loss of kidney function and it can develop rapidly—acute kidney injury (AKI) or have long term pathology—chronic kidney disease (CKD).

Diabetic nephropathy followed by hypertension are the most common causes of CKD. When not treated, CKD can progress to end-stage renal disease (ESRD). ESRD is a terminal illness defined as having a glomerular filtration rate less than 15 mL/min. The development of CKD and its progression to ESRD remains a major source of reduced quality of life and significant premature mortality. Over the last decades the number of ESRD patients steadily increased worldwide. In the Netherlands, on January 2017, there were 17.132 ESRD patients and each year there are about 2000 new reported cases of ESRD[1].

ESRD is fatal without renal replacement therapy (RRT).

How kidney failure treated and what is renal replacement therapy?

Kidney failure may be treated with hemodialysis (HD), peritoneal dialysis (PD) or kidney transplantation. On January 2017, in the Netherlands 32% (5450) patients were on HD and 63% (10812) received kidney transplant[1].

In hemodialysis treatment, extracorporeal removal of waste products and extraction of fluids is carried out directly via the blood, whereas peritoneal dialysis is carried out via the peritoneal cavity.

Treatment with HD may be performed at a dialysis unit or at home. In-center HD treatments are usually performed three times a week. Home HD and PD is generally done daily at home.

According to the 2017 United States Annual Renal Data Report[2] in 82% of the countries, HD is still the most common way of renal replacement therapy.

What is hemodialysis vascular access?

To be able to start hemodialysis therapy, a proper access site to a blood vessel with a high blood flow is required.

When urgent or emergent HD is needed central venous catheter (CVC) represent the only means for vascular access option (Figure 1a). However, this direct form of vascular access is not preferred for chronic dialysis treatment due to high risk of infections and central venous stenosis[3,4].

To create a vascular access point in the upper extremity is preferred approach. Anatomical superficial location of veins in the low arm makes percutaneous cannulation easier and more suitable for regular use.

However, the blood flow in the low arm veins is not high enough for efficient dialysis. To allow high blood flow so that large amount of blood can pass through the dialyzer, a surgical connection between high pressure arterial system with a low pressure venous system is needed. A direct connection between the native artery and vein is called an arteriovenous fistula (AVF) (Figure 1b), when a prosthetic interposition between an artery and a vein is used it is called an arteriovenous graft (AVG) (Figure 1c).

According to the National Kidney Foundation Kidney Disease Outcomes Quality Initiative (NKF KDOQI)[5], the placement of AVFs is currently regarded as the best available option for permanent vascular access, especially because of the lower rate of mortality, infections, thrombotic complications and a higher patency when compared to AVGs or CVCs[6-8]. However, a downside of the AVF is that it needs to be planned at least one or two months before starting HD, a time required for the proper "maturation" of the AVF.

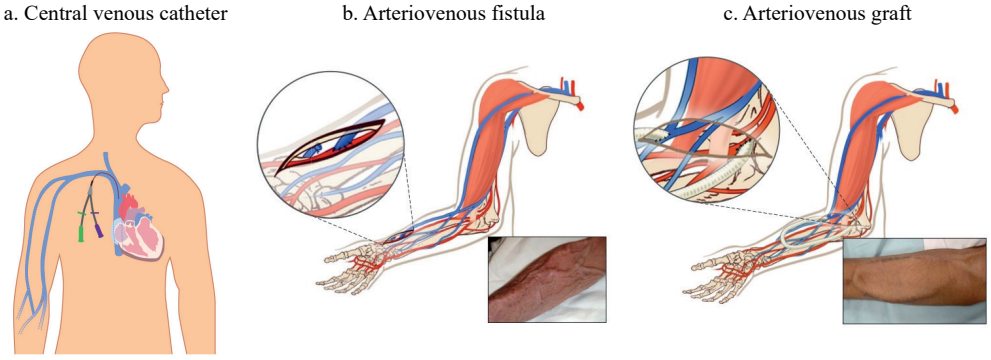

Figure 1. Types of hemodialysis vascular access.
adapted from Atlas of Dialysis Vascular Access, Tushar J. Vachharajani

What is arteriovenous fistula maturation?

According to the NKF KDOQI guidelines an AVF is matured and functional when the fistula has the flow of > 600 mL/min, the vein has a minimum diameter of 6 mm[2] and does not exceed the depth of 6 mm, and the margins are clearly identifiable.

For an AVF to successfully mature several functional and structural adaptations to the inflow artery and outflow vein are required. The connection of a low-pressure vein to the high-pressure arterial circulation results in an immediate increase of blood flow and wall shear stress (WSS) through both the inflow artery and the outflow vein[9-11].

On a biological level, changes in WSS and wall tension are sensed by vascular endothelial cells, that convert hemodynamic stimuli into biochemical signals such as production of nitric oxide (NO) and growth factors that can trigger relaxation of vascular smooth muscle cells (VSMCs) resulting in acute vasodilatation[12-14].

Upregulation of matrix metalloproteinases (MMPs) results in matrix degradation and restructuring of the vascular scaffold leading to luminal expansion[15] but also to thickening especially of the venous wall[16,17]. Finally, successful vascular remodeling restores WSS toward normal levels in a vessel with increased blood flow and helps maintain luminal diameter[18-20], a key hallmark of successful AVF remodeling.

Current concept of AVF maturation postulates that both, degrees of intimal hyperplasia (IH), which thickens the venous wall, narrows the luminal area, and predisposes to intravascular thrombosis together with adaptive restructuring of the vascular wall (outward remodeling [OR]), leading to luminal expansion of the arteriovenous conduct will ultimately determine luminal dimensions, fistula flow and patency[21,22] (Figure 2).

What does it mean an arteriovenous fistula maturation failure?

While AVFs remain the most common vascular access, complications related to vascular access are one of the most common causes of hospitalization and morbidity in hemodialysis patients with approximately of $1 billion spent annually on health care costs[23].

The utility of AVFs is hampered by two distinct causes of failure: (1) initial failure to mature, and (2) dysfunction of mature AVFs due to stenotic lesions in the venous outflow tract.

Recent quantitative study of the outcomes of fistula patency and maturation reports that the primary and secondary patency rates for fistulas at one year is an average 64%, and 79% respectively. For fistulas that were reported as mature, mean time to maturation was 3.5 months, however only 26% of created fistulas were reported as mature at 6 months and 21% of fistulas were abandoned without use[24].

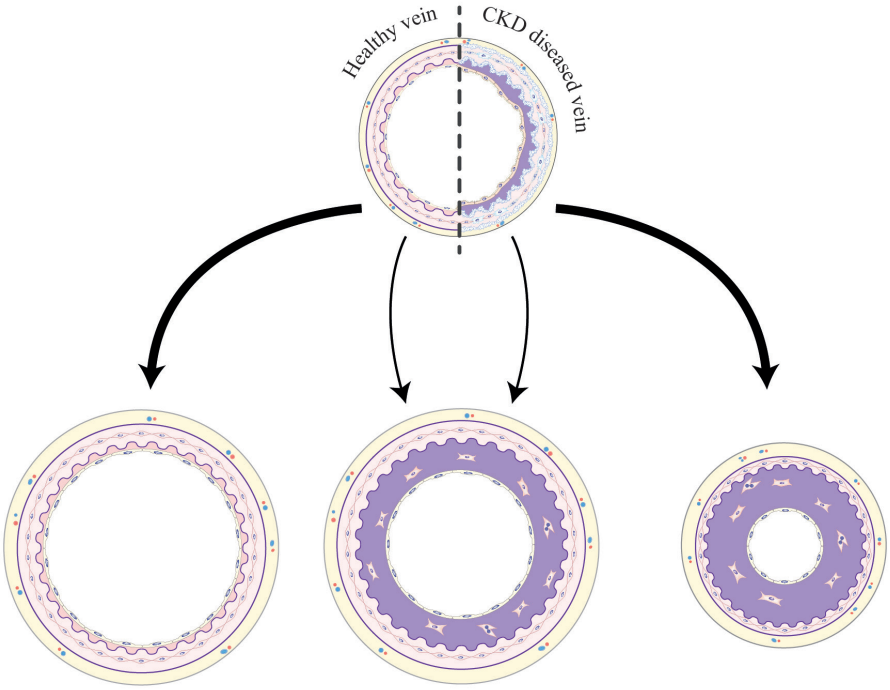

Figure 2. Vascular remodelling after fistula creation.
Healthy vein has the potential for successful outward remodelling (top left), whereas adequate maturation may be partially hindered by CKD-induced pre-existing intimal hyperplasia (IH) (top right). The net resultant of IH and outward remodelling may determine ultimate luminal calibre. adapted from Rothuizen *et al.*, Nephrol Dial Transplant. 2013 May;28(5):1085-92

The exact mechanisms that lead to AVF maturation failure remain unknown, but both impaired OR and formation of IH are regarded as primary contributors to this pathophysiology[21].

As previously discussed, the creation of an AVF results in an increase in shear stress, which causes vascular dilation in an attempt to return shear stress levels back to normal. As we try to create AVF in patients with severe vascular disease, it is possible that this conventional dogma may not always hold true. As an example, vascular calcification seen in elderly patients with diabetes mellitus, prevents endothelium to secrete mediators that are required for flow-mediated vasodilation.

Geometrical configuration of AVF may cause creation of difference in shear stress levels across the venous segment. In particular, at the site of arteriovenous anastomosis there are regions of low shear stress prone to inflammation. Increase in inflammation activates deposition of extracellular matrix (ECM) proteins, production of cytokines and growth factors, activation of proliferation and migration of VSMCs—all together creating focal areas of intimal hyperplasia and vasoconstriction[25-27]. There is an ongoing debate

about the anatomical origin of cells that are responsible for venous stenotic lesions in arteriovenous fistulas[28-32]. This issue will be further elaborated in **chapter 5** of this thesis.

The fact that AVF being the most favored access, exhibits failure rates that are among the highest for any elective surgical procedure, underscores the enormity of the issue of hemodialysis access dysfunction.
The focus of this thesis will be primarily on the novel strategies to prevent arteriovenous fistula maturation failure.

Are there other alternatives to vascular access besides an arteriovenous fistula?

As mentioned before, patients with ESRD require surgery to create a vascular access site for hemodialysis. For this purpose, native veins are generally preferred due to superior patency rates when compared to prosthetic grafts, but often unavailable due to preexisting vascular pathology often seen in patients with CKD[33,34]. The failure of synthetic vascular grafts predominantly results from the development of intimal hyperplasia ultimately leading to graft occlusion, and a relatively high risk of infectious complications[3,35,36].

In recent years, tissue engineering strategies have made substantial progress to improve vascular access. Tissue engineered blood vessels could offer a better alternative to synthetic AV-grafts, when it is not possible to create an AV-fistula. Indeed, tissue engineered blood vessels (TEBVs) can be tailor-made, are devoid of pre-existing vascular diseases and have the potential to adapt to changing hemodynamic conditions.

Can we engineer vascular tissue?

Several strategies to develop tissue engineered grafts have been described[37]. The majority of these approaches include complex *in vitro* preparation steps, decellularized scaffolds, or the incorporation of synthetic materials to generate TEBV. Ideally, vascular replacement should comprise of completely autologous cellular tissue, to avoid host-immune reaction and hold the ability to remodel *in vivo*.

In our research group we developed a novel method to generate TEBVs by utilizing the foreign body response directed towards subcutaneously implanted polymeric rod that culminates in the formation of a fibrocellular tissue capsule (TC). Upon extraction of the polymer rod several weeks after implantation, the remaining tissue capsule is grafted into the vasculature, whereupon it differentiates into a blood vessel[38].

Thus far, the origin of cells in these TCs remained unknown. In **chapter 6** of this thesis, this topic will be discussed further.

Scope of this thesis

Previously, we established a unique murine model of arteriovenous fistula, which has a configuration similar to the one most frequently used in humans (venous end-to-arterial side)[25]. This thesis includes subsequent studies of this model designed to evaluate new therapeutic strategies aimed to improve patency of AV-fistulas and to unravel the pathophysiology of AVF failure.

In addition, we further expand our understanding on the cellular origin of tissue capsules for autologous tissue engineering, as an alternative to AV-grafts.

It is known that the process of vascular adaptation after AVF creation is associated with an excessive inflammatory response characterized by the infiltration of macrophages and lymphocytes as well as the up regulation of pro-inflammatory cytokines[30,39].

In chapter 2 and 3 of this thesis we further examined the contribution of inflammation to AVF failure.

In **chapter 2** we studied the complex role of toll-like receptor 4 (TLR4) homologue -RP105 in AVF remodeling. Here we hypothesized that in mice deficient for RP105 pro-inflammatory TLR4 signaling is upregulated, which results in worsening of AVF maturation.

We created AVFs in RP105 deficient mice to study the effect on AVF maturation *in vivo*. In addition, in series of *in vitro* studies we defined cell-specific effects of RP105 on macrophages and VSMCs.

In another study, described in **chapter 3**, we evaluated the feasibility and efficacy of prednisolone—a potent anti-inflammatory drug. To improve local biological activity and reduce systemic side-effects prednisolone was encapsulated in liposomes, a potent vehicle for targeted drug delivery to inflamed organs.

In **chapter 4** we assessed the role of the relaxin (RLN2) pathway in AVF remodeling. Relaxin is a hormone exhibiting its action on the vasculature via interaction with its receptor (RXFP1), resulting in vasodilatation, ECM remodeling and decreased inflammation—favorable effects for successful AVF maturation. In view of the emerging role of the RLN2-RXFP1 axis in vascular remodeling and inflammation, we examined the consequences of disturbing this hormone-receptor balance in AVF maturation. For this purpose, we used murine AVF model in which we studied the effect of RXFP1 deficiency on fistula remodeling. Furthermore, we determined the effects of RXFP1 deficiency on the phenotype and function of VSMCs *in vitro*.

The pathophysiology of arteriovenous fistula maturation failure is associated with impaired outward remodeling and intimal hyperplasia[21]. In **chapter 5**, based on the work of Liang and co-workers[29] the on-going debate about the cellular origin of cells forming intimal hyperplasia and venous stenosis in AVFs is discussed.

In parallel with testing new therapeutics to improve maturation and patency of native AVFs, our group is working on developing TEBVs, which could offer a suitable alternative for arteriovenous conduits, circumventing the limitations of synthetic grafts and avoiding the need for maturation of fistulas.

In **chapter 6**, a lineage tracing study is described to elucidate the contribution of bone marrow derived cells to TEBV formation. We established a rat model where cells of the hematopoietic lineage are labeled with green fluorescent protein. For the clinical application of the *in situ* engineered vascular grafts, we focus on patients with ESRD that require a vascular access for hemodialysis. Therefore, we combined bone marrow lineage tracing with a model of CKD to investigate the effect of chronic kidney failure on tissue capsule composition.

Finally, **chapter 7** gives an overall summary of the research presented in this thesis and discusses future prospective on vascular access for hemodialysis to reduce morbidity in ESRD patients.

Reference List

1. Renine.nl. RENINE-year-report. Online Source (2016).
2. usrds.org. The United States Renal Data System Annual Report. Online Source (2017).
3. Roy-Chaudhury, P., et al. Venous neointimal hyperplasia in polytetrafluoroethylene dialysis grafts. Kidney international 59, 2325-2334 (2001).
4. Roy-Chaudhury, P., et al. Back to the future: how biology and technology could change the role of PTFE grafts in vascular access management. Seminars in dialysis 25, 495-504 (2012).
5. www.ajkd.org/content/kdoqiguidelines. KDOQI Guidelines/Commentaries. American Journal of Kidney Diseases.
6. Clinical practice guidelines for vascular access. American journal of kidney diseases : the official journal of the National Kidney Foundation 48 Suppl 1, S248-273 (2006).
7. Gibson, K.D., et al. Vascular access survival and incidence of revisions: a comparison of prosthetic grafts, simple autogenous fistulas, and venous transposition fistulas from the United States Renal Data System Dialysis Morbidity and Mortality Study. Journal of vascular surgery 34, 694-700 (2001).
8. Santoro, D., et al. Vascular access for hemodialysis: current perspectives. International journal of nephrology and renovascular disease 7, 281-294 (2014).
9. Saucy, F., et al. Is intra-operative blood flow predictive for early failure of radiocephalic arteriovenous fistula? Nephrology, dialysis, transplantation : official publication of the European Dialysis and Transplant Association - European Renal Association 25, 862-867 (2010).
10. Vita, J.A., et al. Flow-induced arterial remodeling relates to endothelial function in the human forearm. Circulation 117, 3126-3133 (2008).
11. Ene-Iordache, B., et al. Radial artery remodeling in response to shear stress increase within arteriovenous fistula for hemodialysis access. Endothelium : journal of endothelial cell research 10, 95-102 (2003).
12. Miller, V.M. & Burnett, J.C., Jr. Modulation of NO and endothelin by chronic increases in blood flow in canine femoral arteries. The American journal of physiology 263, H103-108 (1992).
13. Garanich, J.S., Pahakis, M. & Tarbell, J.M. Shear stress inhibits smooth muscle cell migration via nitric oxide-mediated downregulation of matrix metalloproteinase-2 activity. American journal of physiology. Heart and circulatory physiology 288, H2244-2252 (2005).
14. Tronc, F., et al. Role of matrix metalloproteinases in blood flow-induced arterial enlargement: interaction with NO. Arteriosclerosis, thrombosis, and vascular biology 20, E120-126 (2000).
15. Corpataux, J.M., Haesler, E., Silacci, P., Ris, H.B. & Hayoz, D. Low-pressure environment and remodelling of the forearm vein in Brescia-Cimino haemodialysis access. Nephrology, dialysis, transplantation : official publication of the European Dialysis and Transplant Association - European Renal Association 17, 1057-1062 (2002).
16. Chan, C.Y., Chen, Y.S., Ma, M.C. & Chen, C.F. Remodeling of experimental arteriovenous fistula with increased matrix metalloproteinase expression in rats. Journal of vascular surgery 45, 804-811 (2007).
17. Langer, S., et al. Functional and structural response of arterialized femoral veins in a rodent AV fistula model. Nephrology, dialysis, transplantation : official publication of the European Dialysis and Transplant Association - European Renal Association 24, 2201-2206 (2009).
18. Girerd, X., et al. Remodeling of the radial artery in response to a chronic increase in shear stress. Hypertension (Dallas, Tex. : 1979) 27, 799-803 (1996).

19. Ben Driss, A., Benessiano, J., Poitevin, P., Levy, B.I. & Michel, J.B. Arterial expansive remodeling induced by high flow rates. The American journal of physiology 272, H851-858 (1997).
20. Dammers, R., et al. The effect of flow changes on the arterial system proximal to an arteriovenous fistula for hemodialysis. Ultrasound in medicine & biology 31, 1327-1333 (2005).
21. Rothuizen, T.C., et al. Arteriovenous access failure: more than just intimal hyperplasia? Nephrology, dialysis, transplantation : official publication of the European Dialysis and Transplant Association - European Renal Association 28, 1085-1092 (2013).
22. Lee, T. & Misra, S. New Insights into Dialysis Vascular Access: Molecular Targets in Arteriovenous Fistula and Arteriovenous Graft Failure and Their Potential to Improve Vascular Access Outcomes. Clinical journal of the American Society of Nephrology : CJASN 11, 1504-1512 (2016).
23. Schon, D., DeLozier, T. & Patel, N. Comparison of procedure cost for thrombectomy of arteriovenous fistulas and grafts. Seminars in dialysis 26, 344-348 (2013).
24. Bylsma, L.C., Gage, S.M., Reichert, H., Dahl, S.L.M. & Lawson, J.H. Arteriovenous Fistulae for Haemodialysis: A Systematic Review and Meta-analysis of Efficacy and Safety Outcomes. European journal of vascular and endovascular surgery : the official journal of the European Society for Vascular Surgery 54, 513-522 (2017).
25. Wong, C.Y., et al. Vascular remodeling and intimal hyperplasia in a novel murine model of arteriovenous fistula failure. Journal of vascular surgery (2013).
26. Krishnamoorthy, M.K., et al. Hemodynamic wall shear stress profiles influence the magnitude and pattern of stenosis in a pig AV fistula. Kidney international 74, 1410-1419 (2008).
27. Roy-Chaudhury, P., et al. Pathogenetic role for early focal macrophage infiltration in a pig model of arteriovenous fistula (AVF) stenosis. The journal of vascular access 15, 25-28 (2014).
28. Roy-Chaudhury, P., et al. Cellular phenotypes in human stenotic lesions from haemodialysis vascular access. Nephrology, dialysis, transplantation : official publication of the European Dialysis and Transplant Association - European Renal Association 24, 2786-2791 (2009).
29. Liang, M., et al. Migration of smooth muscle cells from the arterial anastomosis of arteriovenous fistulas requires Notch activation to form neointima. Kidney international 88, 490-502 (2015).
30. Wang, Y., et al. Venous stenosis in a pig arteriovenous fistula model--anatomy, mechanisms and cellular phenotypes. Nephrology, dialysis, transplantation : official publication of the European Dialysis and Transplant Association - European Renal Association 23, 525-533 (2008).
31. Tanaka, K., et al. Circulating progenitor cells contribute to neointimal formation in nonirradiated chimeric mice. FASEB journal : official publication of the Federation of American Societies for Experimental Biology 22, 428-436 (2008).
32. Misra, S., et al. Adventitial remodeling with increased matrix metalloproteinase-2 activity in a porcine arteriovenous polytetrafluoroethylene grafts. Kidney international 68, 2890-2900 (2005).
33. Lee, T., et al. Comparative analysis of cellular phenotypes within the neointima from vein segments collected prior to vascular access surgery and stenotic arteriovenous dialysis accesses. Seminars in dialysis 27, 303-309 (2014).
34. Friedl, R., et al. Intimal hyperplasia and expression of transforming growth factor-beta1 in saphenous veins and internal mammary arteries before coronary artery surgery. The Annals of thoracic surgery 78, 1312-1318 (2004).
35. Rotmans, J.I., et al. Hemodialysis access graft failure: time to revisit an unmet clinical need? Journal of nephrology 18, 9-20 (2005).
36. Aslam, S., Vaida, F., Ritter, M. & Mehta, R.L. Systematic review and meta-analysis on management of hemodialysis catheter-related bacteremia. Journal of the American Society of Nephrology : JASN 25, 2927-2941 (2014).

37. Geelhoed, W.J., Moroni, L. & Rotmans, J.I. Utilizing the Foreign Body Response to Grow Tissue Engineered Blood Vessels in Vivo. Journal of cardiovascular translational research 10, 167-179 (2017).
38. Rothuizen, T.C., et al. Development and evaluation of in vivo tissue engineered blood vessels in a porcine model. Biomaterials 75, 82-90 (2016).
39. Nath, K.A., Kanakiriya, S.K., Grande, J.P., Croatt, A.J. & Katusic, Z.S. Increased venous proinflammatory gene expression and intimal hyperplasia in an aorto-caval fistula model in the rat. The American journal of pathology 162, 2079-2090 (2003).

Chapter 2

Deficiency of TLR4 homologue RP105 aggravates outward remodeling in a murine model of arteriovenous fistula failure.

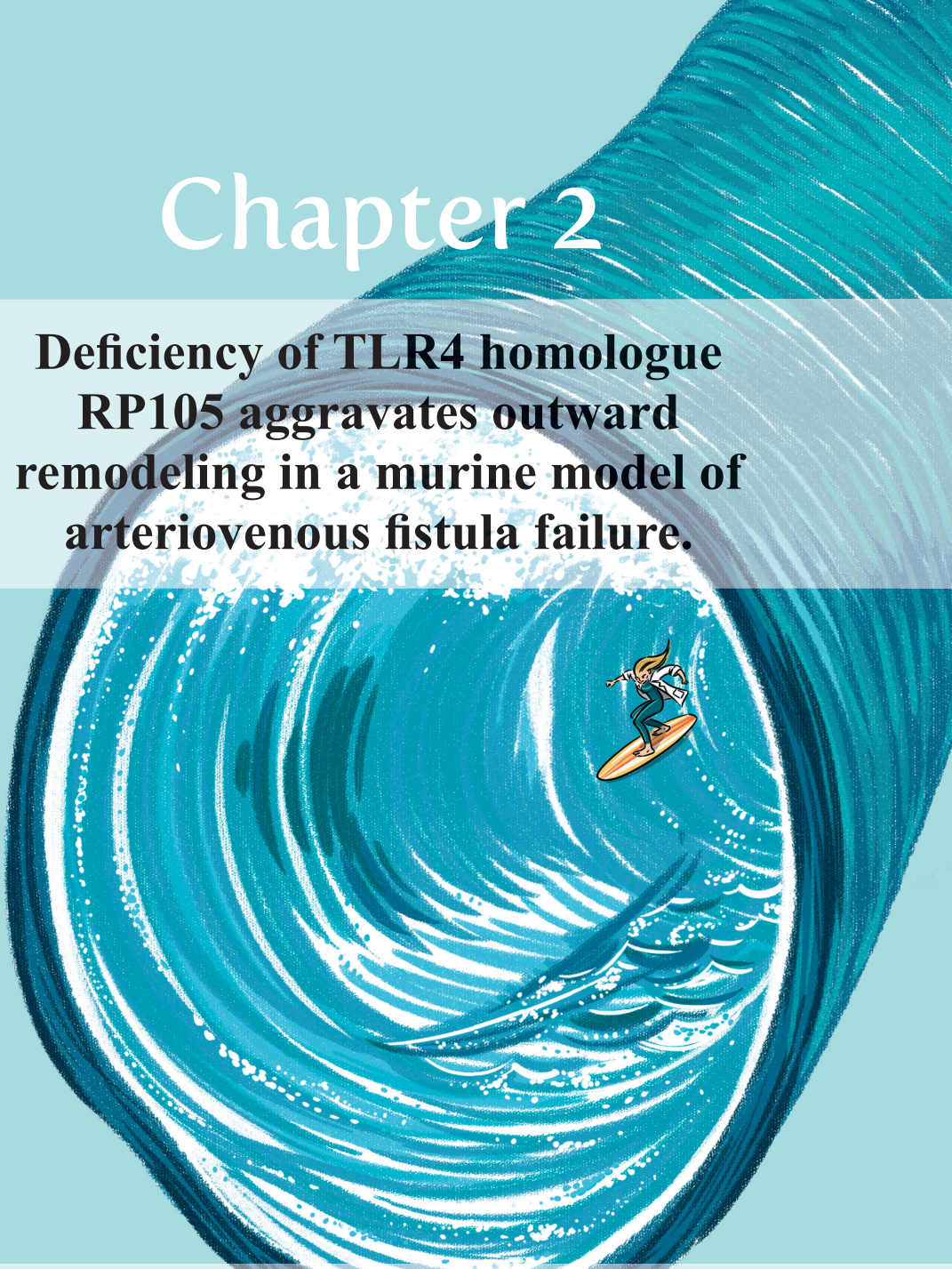

Taisiya Bezhaeva, ChunYu Wong, Margreet R. de Vries, Eric P. van der Veer, Carla M.A. van Alem, Ivo Que, Reshma A. Lalai, Anton Jan van Zonneveld, Joris I. Rotmans and Paul H.A. Quax

Sci Rep. 2017 Aug 31;7(1):10269

Abstract

Arteriovenous access dysfunction is a major cause of morbidity for hemodialysis patients. The pathophysiology of arteriovenous fistula (AVF) maturation failure is associated with inflammation, impaired outward remodeling (OR) and intimal hyperplasia. RP105 is a critical physiologic regulator of TLR4 signaling in numerous cell types. In the present study, we investigated the impact of RP105 on AVF maturation, and defined cell-specific effects of RP105 on macrophages and vascular smooth muscle cells (VSMCs). Overall, $RP105^{-/-}$ mice displayed a 26% decrease in venous OR. The inflammatory response in $RP105^{-/-}$ mice was characterized by accumulation of anti-inflammatory macrophages, a 76% decrease in pro-inflammatory macrophages, a 70% reduction in T-cells and a 50% decrease in MMP-activity. *In vitro*, anti-inflammatory macrophages from $RP105^{-/-}$ mice displayed increased IL10 production, while MCP1 and IL6 levels secreted by pro-inflammatory macrophages were elevated. VSMC content in $RP105^{-/-}$ AVFs was markedly decreased. *In vitro*, $RP105^{-/-}$ venous VSMCs proliferation was 50% lower, whereas arterial VSMCs displayed a 50% decrease in migration, relative to WT.

In conclusion, the impaired venous OR in $RP105^{-/-}$ mice could result from a shift in both macrophages and VSMCs towards a regenerative phenotype, identifying a novel relationship between inflammation and VSMC function in AVF maturation.

Introduction

The placement of an arteriovenous fistula (AVF) is currently regarded as the best available option for permanent vascular access in patients requiring chronic hemodialysis. For proper maturation of the AVFs, both a major increase in blood flow and venous diameter are required to allow adequate hemodialysis treatment. However, several clinical trials have shown that the 1-year primary patency rate of AVFs does not exceed 60%, illustrating the fact that the need for further improvement of this access conduit is vital[1,2]. AVF-related complications are frequently encountered shortly after AVF surgery, as 30-60% of the AVF fail to mature adequately to support dialysis therapy[3]. The exact mechanisms that lead to AVF maturation failure remain unknown, but both impaired outward remodeling (OR) and formation of intimal hyperplasia (IH) are regarded as primary contributors to this pathophysiology[4]. Recent studies have shown that the process of vascular adaptation after AVF creation is associated with an excessive inflammatory response[5-8] and proliferation and migration of arterial and venous vascular smooth muscle cells (VSMCs) towards the intima at the site of anastomosis[9-11]. In view of extensive adverse consequences resulting from AVF failure and the subsequent burden for hemodialysis patients, there is increasing emphasis on pathophysiological studies aimed to unravel the complex mechanisms underlying AVF failure. The latter is pivotal in efforts to identify novel molecular therapeutic targets that could potentially improve AVF patency.

Toll-like receptor 4 (TLR4) is a well-known sentry that induces a pro-inflammatory signaling cascade[12]. Its function is modulated not only by exogenous pathogens in the context of microbial infections[13], but also by several endogenous stimuli in inflammatory conditions such as atherosclerosis[14,15] or during vascular remodeling[16-19]. To initiate the TLR4 signaling cascade, activation of its adaptor molecule MD2 is required which is responsible for the recognition of bacterial lipopolysaccharide (LPS) on the cell surface[20]. Due to the hierarchical importance of TLR4 in the innate immune response and its ubiquitous function, the signaling activity of this protein is firmly regulated by several regulatory molecules. One such regulator is RP105 (radioprotective 105, also known as CD180), a cell surface protein expressed by numerous cell types, including inflammatory cells and VSMCs[21,22]. The structure of RP105 is evolutionarily similar to TLR4 and it associates with MD1, a MD2 homologue which promotes RP105 cell surface expression[23,24]. RP105–MD1 exerts dichotomous regulatory activities on TLR4-mediated LPS responses in a cell type-dependent fashion[25]. On B-cells, RP105-MD1 drives cellular proliferation and enhances B-cell-dependent inflammatory processes[26]. In contrast, in myeloid cells, RP105 acts as a natural antagonist of TLR4 signaling[27], while the functional role in VSMCs remains poorly understood. Previous studies from our group have demonstrated that RP105 deficiency results in decreased atherosclerotic lesion formation via alterations on pro-inflammatory B-cells[28] and a CCR2-dependent decrease in monocyte influx[29]. Strikingly, complete opposite effects were observed in a murine model of vein graft disease, where a 90% increase in graft lesion area was linked to a local increase in macrophage content and lesional

levels of monocyte chemoattractant protein-1 (MCP1), expressed by VSMCs[21]. In a model of post-interventional vascular remodeling, artery cuff placement in RP105$^{-/-}$ mice resulted in increased neointima formation, which coincided with an increase in arterial VSMC proliferation *ex vivo*[22].

In the context of both AVF maturation and failure, numerous cell types are involved including inflammatory cells and VSMCs from both the feeding artery[10,30] and local venous wall[31], making it a unique model to unravel specific functional consequences of RP105 on remodeling in AVF.

In the present study, we aimed to elucidate the role of RP105 on AVF maturation in a murine model of AVF failure by assessing cell type-specific effects of RP105 deficiency, on macrophage polarization and VSMC behavior.

Results

RP105 deficiency influence AVF maturation

To investigate how differential expression of RP105 could influence AVF maturation, we created an AVF by an end-to-side ligation of the jugular vein to the carotid artery of wild-type (WT) and RP105$^{-/-}$. Two weeks after surgery the tissue was processed to paraffin, and 5-μm sections were made perpendicular to the vein at 12 locations with an interval of 150 μm. Because most of the stenotic lesions in human AVFs occur in the venous outflow tract we analyzed first 3 consecutive venous sections downstream from the area closest to the anastomosis. AVF material was evaluated using morphometric and immunohistochemical approaches. RP105$^{-/-}$mice showed a 26% smaller circumference of the external jugular vein compared to WT mice (P=0.03) (Figure 1a), indicating that RP105 deficiency impacts outward remodeling. As shown in Figure 1b, diminished RP105 expression did not influence IH in the venous outflow tract of the AVF. Importantly, immunohistochemical staining revealed that the vast majority of intimal cells are αSMA^{+} in both WT and RP105$^{-/-}$ mice (Figure 1b).

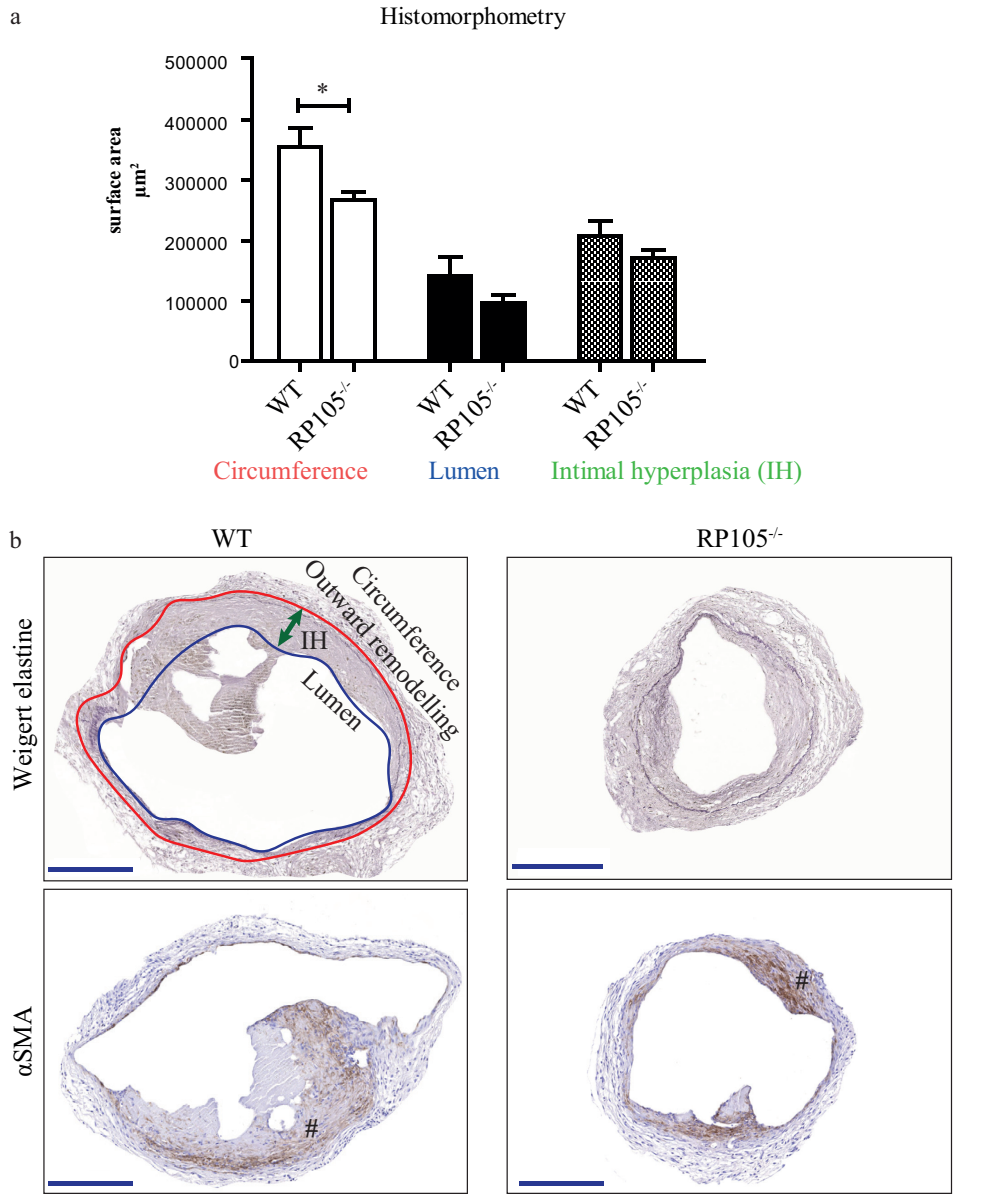

Figure 1. Effect of RP105 deficiency on AVF maturation *in vivo*.
(a) Quantification of morphometric parameters. Decrease in vessel circumference (outward remodeling) in RP105 deficient mice was observed 14 days after AVF creation, as compared to WT. Lumen and intimal hyperplasia did not differ between RP105$^{-/-}$ and WT mice. (b) Histological staining of venous outflow tract 14 days after surgery. Weigert elastin staining was used to determine histomorphometrical parameters of the vessel. Circumference (internal elastic lamina area) was used to quantify outward remodeling (red line). Intimal hyperplasia (green arrow) measured as a difference between luminal area (blue line) and vessel circumference. αSMA staining shows area of intimal hyperplasia 14 days after AVF creation. (#) intimal hyperplasia; *P<0.05; n=11 per group. Bar=200 µm: 100x magnification.

RP105 deficiency leads to reduced VSMC proliferation in AVF lesions

Given this VSMC enrichment in the intimal region of mature AVF, we sought to determine the proliferation capacity of these cells immunohistochemically. For this, we quantitated the amount of proliferating αSMA$^+$/Ki67$^+$ cells in AVF sections. These studies revealed a 31% decrease in αSMA$^+$/Ki67$^+$ VSMCs in RP105$^{-/-}$ mice, as compared to WT mice (Figure 2a).

Since both arterial and venous VSMC might contribute to the portion of proliferating VSMC and we cannot discriminate between arterial and venous VSMCs *in vivo*, this borderline significance in the number of αSMA$^+$/Ki67$^+$ VSMCs (P=0.07) might be relevant (Figure 2b).

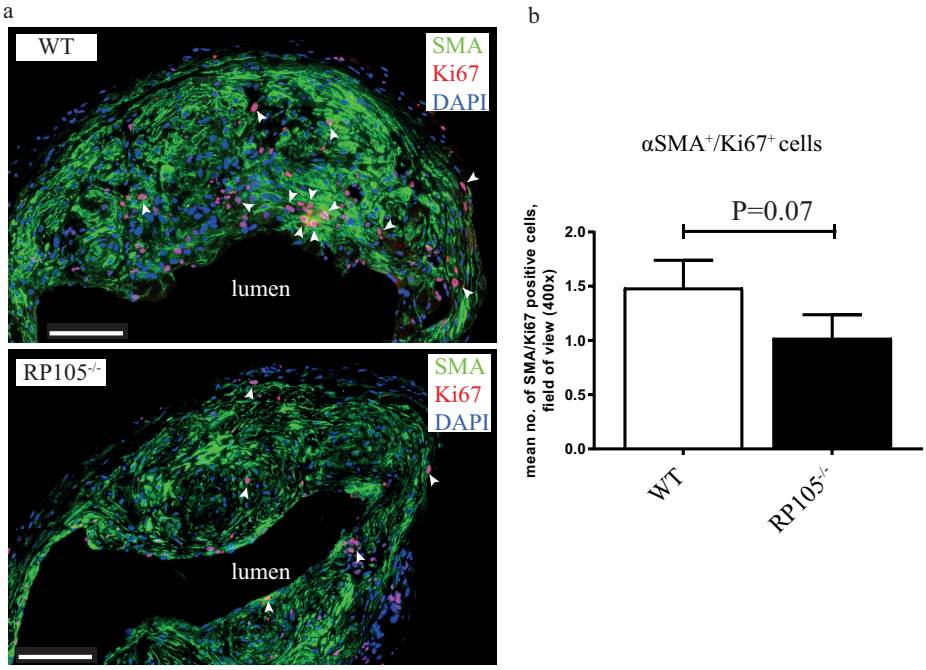

Figure 2. Effect of RP105 deficiency on VSMC proliferation *in vivo*.
Immunofluorescent staining (**a**) and quantification (**b**) of αSMA$^+$/Ki67$^+$ cells (white arrows) revealed reduction in number of proliferating VSMCs in AVF lesions of RP105$^{-/-}$ mice compared to WT 14 days after AVF surgery. n=11 per group. Bar=100 μm.

Diminution of RP105 differently affects arterial and venous VSMC function

To further dissect the contribution of arterial and venous VSMCs to AVF maturation and failure, we elected to study the consequences of differential RP105 expression in arterial and venous VSMCs *ex vivo*. For this, we cultured explant material from the carotid artery and vena cava of WT and RP105$^{-/-}$ mice for 2 weeks. Morphologically, we observed that arterial VSMCs possessed an elongated phenotype, whereas venous cells had a more stellate appearance (Figure 3a). Both arterial and venous VSMCs displayed characteristics of differentiated VSMCs, as confirmed by stable

gene expression of VSMCs markers (smooth muscle α-actin (SMA), myosin heavy chain (MYHC) and calponin) after 2 weeks of culture (Figure 3b). The phenotypic difference and the vascular origin of arterial versus venous VSMCs was confirmed by assessing EphB4 expression levels, an established embryological marker of venous origin[32,33], which was increased in cultured venous VSMCs up to 2 weeks after isolation (Figure 3c).

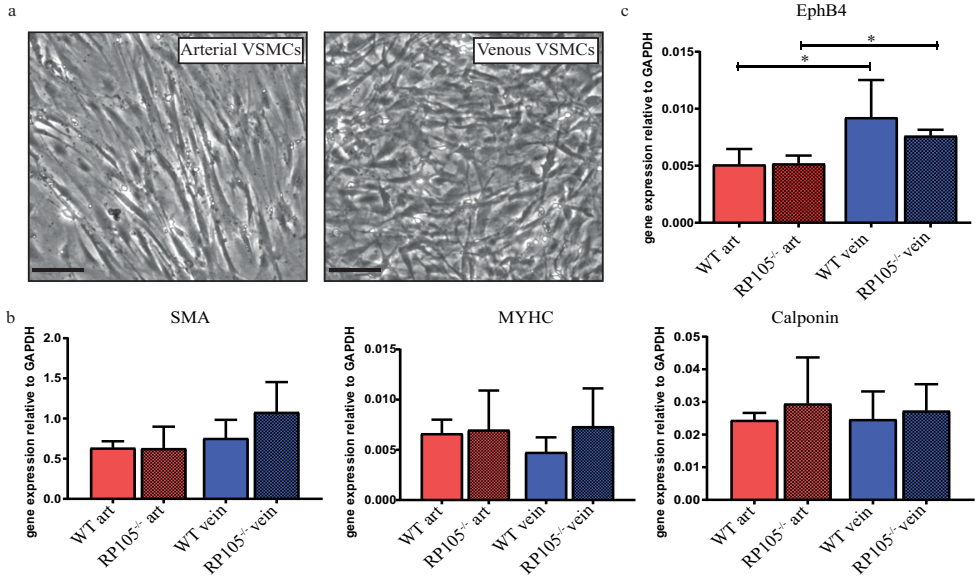

Figure 3. ***In vitro*** **cultured arterial and venous VSMCs.**
(a) Microscopic representation of morphological difference between cultured arterial and venous SMCs. Bar=100μm, x200 magnification. **(b)** VSMCs phenotype after 14 days in culture was confirmed by stable mRNA expression levels of smooth muscle α-actin (SMA), myosin heavy chain (MHC) and calponin. **(c)** Stable increase in EphB4 mRNA levels was detected in venous SMCs isolated from WT and RP105$^{-/-}$ mice. Cells were maintained in culture for 14 days. *P<0.05; n=3.

Next, we further determine expression levels of RP105 associating molecules. Interestingly, RT-PCR analysis of RP105 by WT VSMCs revealed a striking > 100-fold increase in gene expression on venous VSMCs as compared to arterial VSMCs (Figure 4a). Expression of its accessory molecule MD1 was also elevated > 100-fold on venous VSMCs isolated from both WT and RP105$^{-/-}$ mice (Figure 4b). mRNA levels of inflammatory marker TLR4 was elevated by 48% in venous cells, as compared to arterial VSMCs (Figure 4c). Expression of the TLR4 accessory molecule MD2 did not differ between WT and RP105$^{-/-}$ mice arterial and venous VSMCs (Supplementary Figure 1).

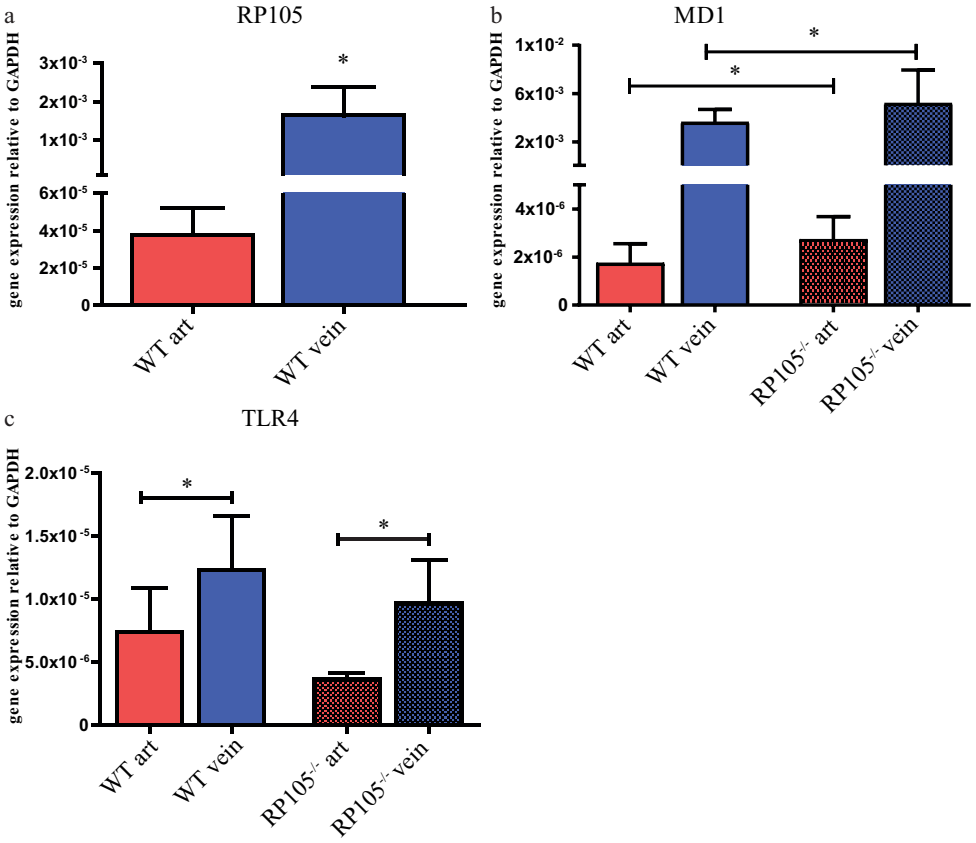

Figure 4. Difference in mRNA expression levels between arterial and venous VSMCs *in vitro*. **(a)** RP105, **(b)** MD1, **(c)** TLR4. The relative expression normalized to GAPDH. *P<0.05; n=3.

Functionally, venous VSMCs derived from RP105$^{-/-}$ mice displayed a 50% reduction in their rate of proliferation, relative to VSMCs derived from WT mice, while arterial VSMCs proliferation was unaltered (Figure 5a). In contrast, migratory capacity was reduced by 50% over a 16h time period in arterial VSMCs derived from RP105$^{-/-}$, venous SMCs showed no difference in migration between WT and RP105$^{-/-}$ mice (Figure 5a). As VSMCs are also potent cytokine producers we measured amount of pro-inflammatory cytokines IL6 and MCP1 secreted by arterial and venous VSMCs from WT and RP105$^{-/-}$ mice. Although there was no difference in IL6 and MCP1 levels between WT and RP105$^{-/-}$, venous VSMCs isolated from both WT and RP105$^{-/-}$ mice exhibited higher inflammatory state characterized by 70% and 84% increase in IL6 secretion by WT and RP105$^{-/-}$ VSMCs respectively when compared to arterial VSMC and 57% and 61% upregulation in MCP1 levels produced by WT and RP105$^{-/-}$ VSMCs respectively when compared to arterial VSMCs (Figure 5b). There was no difference in the amount of anti-inflammatory cytokine IL10 produced either by arterial or venous VSCMs from WT and RP105$^{-/-}$ VSMCs (Supplementary Figure 2).

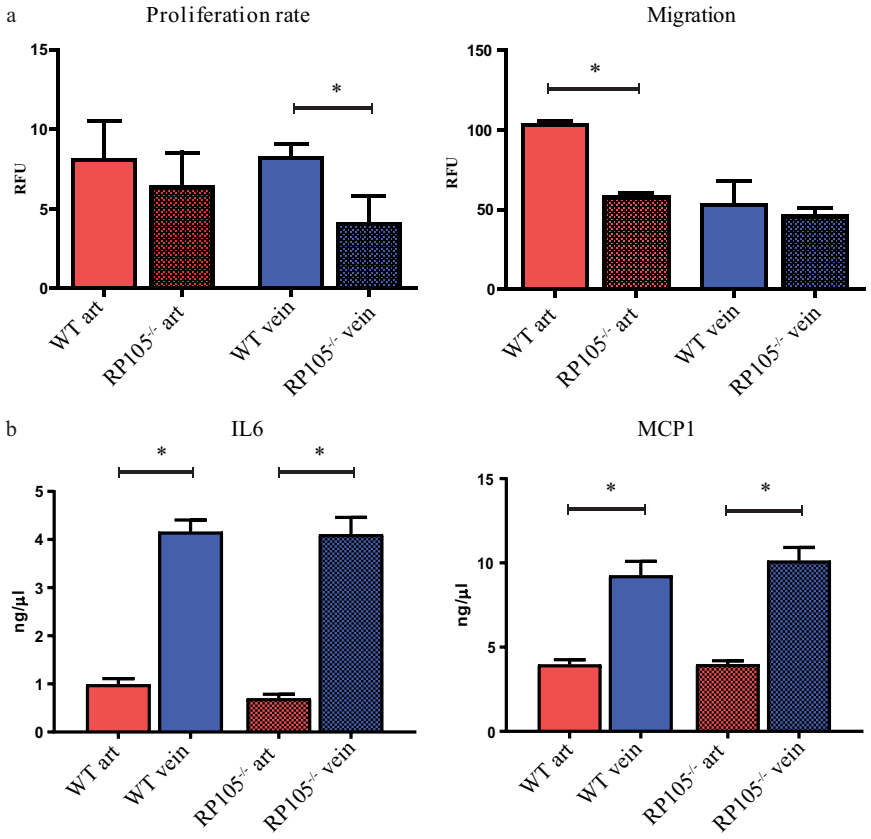

Figure 5. Functional difference between arterial and venous VSMCs *in vitro*.
(a) Reduction in proliferative rate was limited to VSMCs isolated from RP105$^{-/-}$ veins. Decrease in migration of VSMCs isolated from RP105$^{-/-}$ mice was restricted to arterial cells only. Proliferation rate and migration were measured over 16h time period. (b) Venous VSMCs isolated from WT and RP105$^{-/-}$ mice produce significantly higher amounts of inflammatory cytokines IL6 and MCP1. Cells were maintain in culture for 14 days. (*) P<0.05; n=3.

RP105 deficiency impacts the inflammatory status of AVF infiltrating cells

To gain insight into the consequences of differential expression of RP105 on the inflammatory response to injury *in vivo*, we evaluated the inflammatory cell composition of AVFs in RP105$^{-/-}$ and WT mice. Analysis of AVF material 2 weeks after surgery revealed a 76% reduction in MAC3^{+}/CCR2^{+} pro-inflammatory macrophages cell number in the venous lesions of RP105$^{-/-}$ mice. Furthermore, the number of infiltrating MAC3^{+}/CD206^{+} anti-inflammatory macrophages was increased by 35%, as compared to WT mice (Figure 6a). The number of CD3^{+} T-lymphocytes in RP105$^{-/-}$ mice was decreased by 70% (Figure 6b). Interestingly, we observed an enrichment of these inflammatory cells in the adventitial layer of the vessel (Figure 6a, b). No changes between RP105$^{-/-}$ and WT mice were found in the number of MCP1^{+} cells in the AVF lesions at 2 weeks after surgery (Supplementary Figure 3). Notably, the distribution of the total population of macrophages in RP105$^{-/-}$ 2 weeks after AVF

creation was skewed towards a tissue repair, or regenerative state. More than 90% of all MAC3^{+} cells were CD206^{+}, a cell surface protein that defines the anti-inflammatory repair associated macrophage phenotype, whereas but 6% of these MAC3^{+} macrophages were found to express CCR2, the pro-inflammatory macrophage marker.

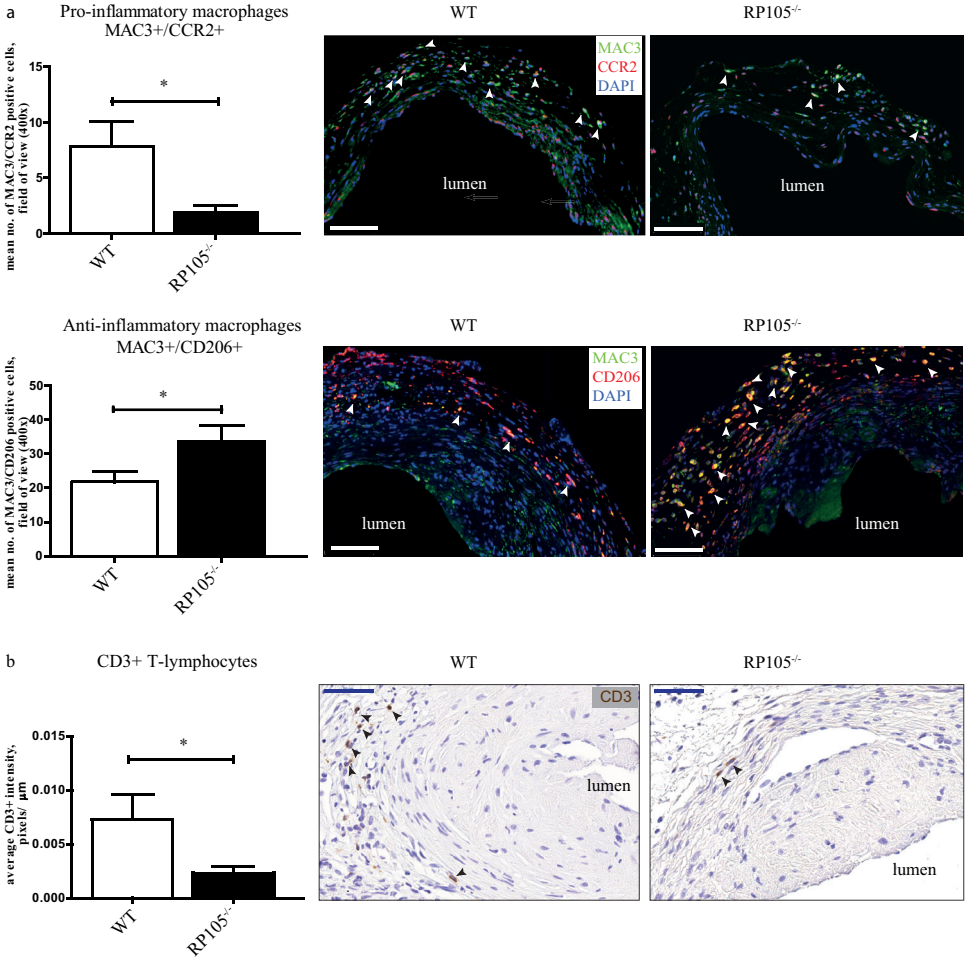

Figure 6. Effects of RP105 deficiency on inflammatory response *in vivo*.
Quantification and immunohistochemical staining of (a) MAC3^{+}/CCR2^{+} macrophages and MAC3^{+}/CD206^{+} macrophages (white arrows) and (b) CD3^{+} T-lymphocytes (black arrows) in AVF lesions 14 days after surgery. Decrease in cell number of pro-inflammatory macrophages and upregulation of anti-inflammatory macrophages upon RP105 deletion was observed. Bar=100 µm. Number of CD3^{+} T-lymphocytes was reduced in RP105$^{-/-}$ as compared to WT. Bar=50 µm: 400x magnification. (*) P<0.05; n=11 per group.

Macrophage-mediated cytokine production is affected by RP105 expression levels

Having identified that AVFs in RP105$^{-/-}$ mice are enriched for anti-inflammatory macrophages, we subsequently isolated bone marrow from WT and RP105$^{-/-}$ mice and polarized bone marrow-derived macrophages towards either pro- or anti-inflammatory phenotypes with LPS/IFN-gamma or IL4/IL13 treatment for 24h, respectively. We observed an augmented inflammatory response by pro-inflammatory macrophages derived from RP105$^{-/-}$ mice as evidenced by a 40% increase in MCP1 secretion and a 73% up regulation in IL6 production, as compared to macrophages obtained from WT mice (Figure 7a).

Macrophages that were isolated from RP105$^{-/-}$ mice and driven towards the anti-inflammatory phenotype exhibited a 72% increase in anti-inflammatory cytokine IL10 production as compared to WT macrophages (Figure 7b).

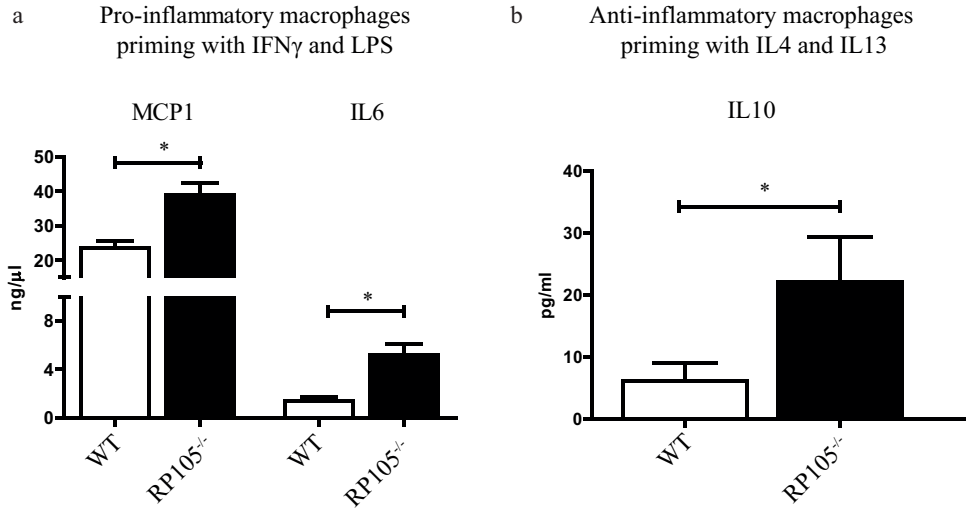

Figure 7. Effect of RP105 deficiency on macrophage function.
(a) Bone marrow-derived macrophages from RP105$^{-/-}$ primed towards pro-inflammatory phenotype secrete increased levels of MCP1 and IL6 as compared to WT control mice. **(b)** Anti-inflammatory macrophages from RP105$^{-/-}$ secrete increased levels of repair assicoated cytokine IL10. *P<0.05; n=3.

MMP activity is decreased in AVF lesions of RP105 deficient mice

Matrix metalloproteinases (MMPs) are known for the role they play in extracellular matrix (ECM) remodeling, such as collagen and elastin. MMP-mediated degradation of the ECM is critically involved in vascular remodeling following AVF placement and during AVF maturation[34]. We assessed MMP activity in the lesions using *in vivo* near-infrared fluorescent imaging. We observed a two-fold reduction (6.3±1.6 WT vs. 2.9±0.2 RP105$^{-/-}$ AU) in fluorescence intensity indicating reduced *in vivo* MMP activity in RP105$^{-/-}$ mice as compared to WT (Figure 8).

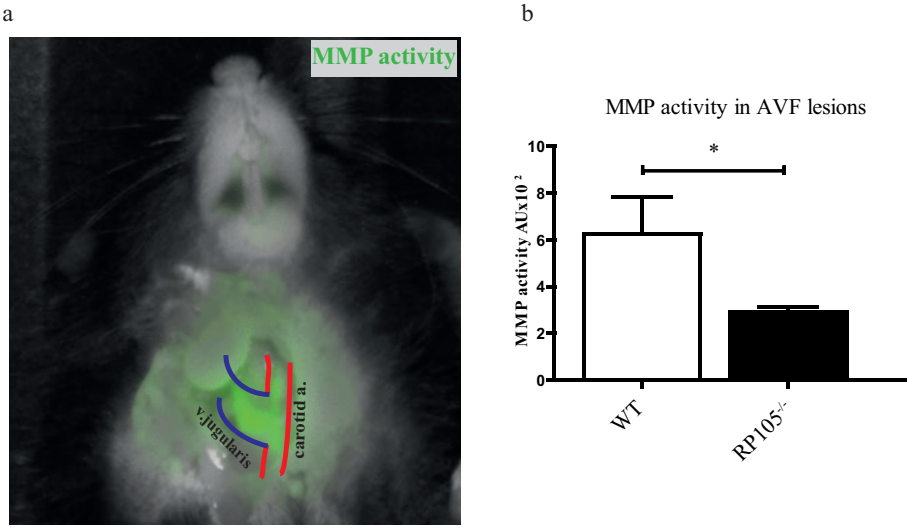

Figure 8. ***In vivo*** **near-infrared biofluorescent imaging and quantitative analysis of MMP activity.**
(a) Visual representation of near-infrared signal from active MMPs. Accumulation of green color can be seen in the anastomotic region 24h after injection of MMPSense™ 680 probe. *P<0.05; n=4 per group. **(b)** Quantitative analysis of fluorescent intensity showed decrease in MMP activity in RP105$^{-/-}$ mice, as compared to WT.

RP105 is present in the venous wall of human AVF

Human AVF was obtained in the operating room during AVF correction surgery and processed in the same manner as mouse samples. Immunohistochemical staining of human AVF sections showed an impressive accumulation of RP105 expression within the venous wall. Cells positive for RP105 were mainly located in the neointima (Figure 9).

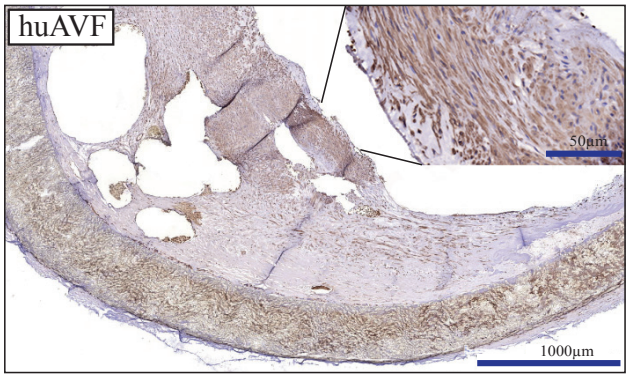

Figure 9. RP105 expression in human AVF.
RP105 is highly expressed within the venous neointimal lesions of human AVF; n=4.

Discussion

In this study, we addressed the specific role of TLR4 homologue RP105 in vascular remodeling, inflammation and VSMCs function in a murine model of AVF failure. The process of AVF maturation is complex and integrates several cellular responses, including the infiltration of inflammatory cells shortly after AVF surgery[5,35]. In addition, VSMCs play a pivotal role in AVF maturation as they contribute to thickening of the venous vessel wall and the concurrent outward remodeling. Here, we clearly show that RP105 deficiency affects the inflammatory and VSMC-mediated response to injury during the course of AVF maturation, accumulating in an impaired outward remodeling 14 days after the placement of an AVF.

A vital aspect of AVF maturation involves the outward remodeling response, a vessel widening process that is tightly coupled with VSMC proliferation. While VSMC proliferation in IH is generally considered to be detrimental, the process is beneficial for vascular adaptation in AVF, especially in the early phase of AVF maturation. To this end, the reduction in venous outward remodeling in RP105$^{-/-}$ mice, coupled with a reduction in proliferating venous VSMC within AVFs and *ex vivo*, suggests that inhibiting VSMCs proliferation (and migration) could be detrimental for long-term AVF maturation.

A striking observation in our studies was that RP105 diminution differentially affected arterial and venous VSMCs, as evidenced by RP105-specific effects on proliferation and inflammatory cytokine production by venous cells as well as impact on arterial migration. The endogenous expression levels of RP105 in arterial and venous VSMCs support this finding, along with differential expression profiles of associating TLR4-family members (including TLR4 and MD1). Collectively, these findings suggest that the susceptibility for inflammatory stimuli could potentially differ between arterial and venous VSMCs. Importantly, our studies support the notion that numerous cell sources are involved in venous IH in AVF (including resident venous cells, infiltrating arterial cells, and circulating bone marrow-derived cells[7,36-39]). Furthermore, our studies illustrate the need for continued investigation of the phenotypic properties and functional characteristics of VSMCs in AVFs, in particular due to the contrasting lineage tracing studies detailing a predominance of arterial VSMCs[10] versus venous VSMCs[31] in venous IH following AVF placement.

Increased expression of the pro-inflammatory mediators IL6, TNF and MCP1 are associated with AVF failure[8,40,41], while the reduction of anti-inflammatory molecule heme oxygenase-1 (HO-1) is linked to AVF failure[42-44]. In our study, we demonstrated that the polarization of macrophages isolated from the bone marrow of RP105$^{-/-}$ mice towards the pro- or anti-inflammatory phenotypes appears to remove a regulatory repressor, as both phenotypes displayed an up regulation of signature cytokines being produced. The augmentation of pro-inflammatory cytokine production in RP105$^{-/-}$ macrophages is in keeping with RP105 being an antagonist of pro-inflammatory TLR4 signaling[25,27,45], while the spike in IL10 production is supported by recent reports that low grade inflammation triggers bone marrow-derived macrophages to generate anti-inflammatory cytokines in a TLR4 dependent fashion[46].

AVF placement in RP105$^{-/-}$ mice yielded decreased MAC3^{+}/CCR2^{+} macrophages and CD3^{+} T-lymphocytes. Our previous study performed by Wezel *et al.* on the role of RP105 in atherosclerosis showed the same difference which was linked to decrease in CCR2^{+} monocytes in RP105$^{-/-}$ mice hampering process of monocyte infiltration into the lesions. After additional *in vitro* stimulation with LPS the dose dependent decrease in CCR2 expression on CCR2^{+} monocytes isolated from RP105$^{-/-}$ mice was observed which may point onto increased signaling via TLR4 route[29]. A noteworthy observation two weeks after AVF placement in RP105$^{-/-}$ mice was the attenuation of vessel wall MMP activity. While the type of vascular injury impacts the degree by which MMPs remodel the vascular wall, these factors also play a role in determining which MMPs are activated[47], and could differ between arterial and venous segments. Castier *et al.* reported that increased MMP-9 activity coincided with increased OR in the arterial segment of the AVF[48], while Nieves Torres *et al.* demonstrated that MMP inhibition enhanced venous OR in AVF[49]. Our studies contradict this finding, and suggest instead that decreased MMP limits venous OR in maturating AVFs.

During the process of vascular remodeling the initial pro-inflammatory reaction is gradually changing towards resolution of inflammation characterized by accumulation of anti-inflammatory cells[50-53]. The specific dynamics with regard to pro-/anti-inflammatory response in the context of AVF maturation is still unknown. In our murine model, RP105 deficiency caused significant increase in MAC3^{+}/CD206^{+} anti-inflammatory macrophages in the venous lesions of AVF, compared to controls. Overall prevalence in anti-inflammatory population (93.7%), compared to 6.3% of pro-inflammatory macrophages at 2 weeks after AVF creation might suggest either that in the current model pro-inflammatory response is completed at earlier time points or that anti-inflammatory macrophages play a dominant role in the tissue response in murine AVF. Thus, despite the increased production of both pro- and anti-inflammatory cytokines by macrophages *in vitro*, the effect of RP105 deletion on anti-inflammatory macrophages was dominant in the venous lesions of murine AVF.

Finally, to our knowledge it is the first study to demonstrate expression of RP105 in human AVF, which is an important observation supporting further research related to RP105 as a potential therapeutic target to improve AVF maturation.

Study limitations

Current study is performed in mice, which do not precisely mimic the human inflammatory response to injury; however this model remains highly useful for studying the vital pathophysiological aspects of AVF maturation and failure. Another limitation is the absence of uremia, given that a recent *in vivo* study by Kang *et al.* demonstrated that fistula maturation in mice is affected by CKD[44]. Here, the chronic accumulation of waste products and uremic toxins in the blood impacted AVF flow, resulting in increased venous wall thickness and thrombus formation. Also, future studies should include flow measurements, as the rate of blood flow is critical functional parameter of AVF.

In conclusion, our study demonstrates the complex role of RP105 in VSMCs and macrophages in a murine model of AVF. The design and implementation of therapeutic strategies targeting the TLR4/RP105 axis to prevent AVF failure must include cell specific targeting approaches and be temporally controlled.

Material and Methods

Animals

Murine model of AVF failure

This study was performed in compliance with Dutch government guidelines and the Directive 2010/63/EU of the European Parliament. All animal experiments were approved by the Institutional Committee for Animal Welfare of Leiden University Medical Center. RP105$^{-/-}$ mice (C57BL/6 background) were obtained from the local animal breeding facility, WT C57BL/6 mice were obtained from Charles River. Adult male mice aged 10-11 weeks were used for the experiments. AVFs were created in an end-to-side manner between the dorsomedial branch of the external jugular vein and the common carotid artery as previously described[5,54] (Supplementary Methods S1). The mice were euthanized at 2 weeks after AVF surgery.

In vivo near-infrared MMPs assay

In vivo MMP activity of endogenous MMP-2, -3, -9, -12 and -13 was assessed by injecting fluorescent imaging agent MMPSense^{TM} 680 from PerkinElmer's (Waltham, MA, USA) which is activated in the presence of active MMPs[55]. First, AVF was created as described above (n=4 per group). 14 days later mice were anesthetized under isoflurane and 4 nmol of MMPSense^{TM} 680 probe were injected into the tail vein. 24 hours later, mice were placed under anesthesia, AVF was dissected and mice were scanned using the Optix MX2 optical imaging system. Excitation was performed with a 670-nm pulsing laser, and emission was detected with a 693-nm long-pass filter. Lifetime analysis was used to confirm the specificity of MMP-activated probes. Fluorescence intensities and fluorescence lifetime were expressed in pseudo colors and projected on the bright field grayscale image of the mouse. Quantification of the fluorescent intensity was performed using the Optiview 2.2 software as described previously[56].

Tissue harvesting and processing

14 days after surgery, the mice were anesthetized using isoflurane whereupon the AVF was dissected. After a thoracotomy, the inferior vena cava was transsected followed by a mild pressure perfusion fixation with 4% formalin through an intracardiac perfusion. The tissue was embedded in paraffin and 5 μm-thick sections of the venous outflow tract were made perpendicular to the vein with an interval of 150 μm.

Morphometric and histological analysis

Morphometric analysis was performed on Weigert's elastin stained sections using ImageJ software. Vessel circumference as a parameter displaying the process of outward remodeling was determined by measuring the length of the internal elastic lamina (IEL). The intimal

hyperplasia was calculated by subtracting the luminal area from the area within the IEL. Immunohistochemical staining was performed for macrophages (MAC3, 1:200, BD-Pharmingen, SanDiego, USA) in a combination with CCR2 for pro-inflammatory phenotype (1:400, Abcam, Cambridge, UK) or CD206 (1:1000, Abcam) for anti-inflammatory phenotype, T-lymphocytes (CD3, 1:300, Abcam) and VSMCs (αSMA, 1:1000, Dako, Glostrup, Denmark) in a combination with Ki67 (1:200, Abcam) to detect proliferating cells. For the immunohistochemical analysis of the MAC3/CD206, MAC3/CCR2 and αSMA/Ki67 staining, the number of positive cells was counted in 3 random fields of view using a 400x magnification from which the mean was calculated. Quantification of $CD3^+$ cells was performed with ImageJ software by calculating % DAB positive area from the total vessel area. All immunohistochemical quantifications were performed on the first 3 venous sections starting from the anastomosis per AVF. Slides were digitized using an automated microscopic scanner (Panoramic digital MIDI, 3DHISTECH, Hungary). Results are expressed as mean±standard error of the mean.

Cell culture

Vascular smooth muscle cells

Primary arterial and venous vascular smooth muscle cells were isolated from murine carotid artery and vena cava of C57Bl/6 and $RP105^{-/-}$ mice (n=3 per group) respectively. Connective tissues were removed and vessels cut open. Endothelial monolayer was detached by gentle scraping with sterile surgical forceps. The carotid artery and caval vein were dissected into small pieces and plated onto petri dish 100 mm or 60 mm diameter coated with 0.1 mg/ml fibronectine. After 14 days of culture with DMEM medium supplemented with 20% FCS, 2 mmol/l l-glutamine, 100 U/ml penicillin and 100 μg/ml streptomycin, cells were trypsinized and re-plated onto 6 or 12 well plates and left for 7 days in culture. Upon enrichment in 80-90% confluence VSMCs were trypsinized and seeded at required density for further functional assays.

Macrophages

Macrophages were derived from bone marrow by flushing tibia and femur of healthy C57Bl/6 or $RP105^{-/-}$ mice (n=3 per group) and seeded at a density of 500.000 cells/well in 6-wells plates. Cells were cultured for 7 days in RPMI GlutaMax (Gibco) supplemented with 100 U/ml penicillin/streptavidin, 25% Fetal Calf Serum (FCS) and 20 mg/ml M-CSF (Myltec Biotechnologies) as described previously[6]. On day 7, cells were stimulated either with LPS (100 ng/ml) and IFN-gamma (10 ng/ml) to differentiate them towards pro-inflammatory phenotype or with IL4 (10 ng/ml) and IL13 (10 ng/ml) (all from Preprotech) for anti-inflammatory phenotype. After 24 hours the supernatants were collected for ELISA assays and cells were lysed with Trizol reagent (Invitrogen, Carlsbad, CA, USA) for RNA isolation.

VSMC proliferation assay

Murine VSMCs, explanted from aortas and veins of control or $RP105^{-/-}$ mice, were subsequently cultured as described above, and proliferation was measured using neutral red cell proliferation and cytotoxicity assay kit from Boster Bio (Pleasanton, CA, USA)

according to the manufacturer protocol (Supplementary Methods S2).

VSMC migration assay

Primary arterial and venous VSMCs from control and RP105$^{-/-}$ mice were grown to confluence and then made quiescent in cultured medium supplemented with 1% FCS for 24 hours. Cells were detached from the surface using Accutase Cell Detachement Solution (Innovative Cell Technologies, Inc., San Diego, CA, USA) and suspended at a concentration of 100.000 cells/ml in culture medium supplemented with 1% FCS. Migration was assayed with a polycarbonate membrane inserts having 8 μm-pores in 24-well chemotaxis chambers using commercial CytoSelect Cell Migration Assay Kit (Cell Biolabs, Inc., San Diego, CA, USA) over 16 hours towards the 20% FCS gradient. All migratory cells were lysed and labeled with fluorescent dye (CyQuant GR). Quantification was performed on a fluorescence plate reader at 480 nm/520 nm.

ELISA assays

ELISA assays for MCP1, IL6 and IL10 production were performed with cell free supernatant collected from bone marrow-derived macrophages after 24 hours polarization towards pro- or anti-inflammatory phenotype or *ex vivo* cultured arterial and venous VSMCs using commercial available kits following the instructions of the manufacturer (BD Biosciences, San Jose, CA, USA: MCP1- Catalog No 555260; IL6- Catalog No 555240, IL10- Catalog No 555252).

RT-PCR

Total RNA was extracted from the macrophages and VSMCs using Trizol reagent (Invitrogen) according to the manufacturer's protocol. RNA was reverse transcribed using a 5-minute 65°C incubation of 1 μg total RNA with deoxyribonucleotide triphosphates (Invitrogen) and random primers (Invitrogen). c-DNA was synthesized using an M-MLV First-Strand Synthesis system (Invitrogen), and used for quantitative analysis of mouse genes (Supplementary Table 1) with an SYBR Green Master Mix (Applied Biosystems, Foster City, CA, USA). The relative mRNA expression levels were determined by normalization to murine glyceraldehyde 3-phosphate dehydrogenase (GAPDH) using $2[-\Delta\Delta C(T)]$ method.

Statistical analysis

Results are expressed as mean±SEM and considered statistically significant for $p<0.05$; T-tests and Mann-Whitney tests for parametric and nonparametric data, respectively, were used as appropriate. All *in vitro* experiments were performed in biological n=3 in experimental triplicates.

Acknowledgements

This study was supported by a grant from the Dutch Kidney Foundation (KJPB 08.0003).

References

1. Tordoir, J.H., *et al.* Prospective evaluation of failure modes in autogenous radiocephalic wrist access for haemodialysis. *Nephrology, dialysis, transplantation : official publication of the European Dialysis and Transplant Association - European Renal Association* **18**, 378-383 (2003).
2. Dember, L.M., *et al.* Effect of clopidogrel on early failure of arteriovenous fistulas for hemodialysis: a randomized controlled trial. *JAMA : the journal of the American Medical Association* **299**, 2164-2171 (2008).
3. Lazarides, M.K., Georgiadis, G.S., Antoniou, G.A. & Staramos, D.N. A meta-analysis of dialysis access outcome in elderly patients. *Journal of vascular surgery* **45**, 420-426 (2007).
4. Rothuizen, T.C., *et al.* Arteriovenous access failure: more than just intimal hyperplasia? *Nephrology, dialysis, transplantation : official publication of the European Dialysis and Transplant Association - European Renal Association* **28**, 1085-1092 (2013).
5. Wong, C.Y., *et al.* Vascular remodeling and intimal hyperplasia in a novel murine model of arteriovenous fistula failure. *Journal of vascular surgery* (2013).
6. Wong, C., *et al.* Liposomal prednisolone inhibits vascular inflammation and enhances venous outward remodeling in a murine arteriovenous fistula model. *Scientific reports* **6**, 30439 (2016).
7. Wang, Y., *et al.* Venous stenosis in a pig arteriovenous fistula model--anatomy, mechanisms and cellular phenotypes. *Nephrology, dialysis, transplantation : official publication of the European Dialysis and Transplant Association - European Renal Association* **23**, 525-533 (2008).
8. Nath, K.A., Kanakiriya, S.K., Grande, J.P., Croatt, A.J. & Katusic, Z.S. Increased venous proinflammatory gene expression and intimal hyperplasia in an aorto-caval fistula model in the rat. *The American journal of pathology* **162**, 2079-2090 (2003).
9. Lee, T. & Haq, N.U. New Developments in Our Understanding of Neointimal Hyperplasia. *Advances in chronic kidney disease* **22**, 431-437 (2015).
10. Liang, M., *et al.* Migration of smooth muscle cells from the arterial anastomosis of arteriovenous fistulas requires Notch activation to form neointima. *Kidney international* **88**, 490-502 (2015).
11. Roy-Chaudhury, P., *et al.* Neointimal hyperplasia in early arteriovenous fistula failure. *American journal of kidney diseases : the official journal of the National Kidney Foundation* **50**, 782-790 (2007).
12. Akira, S., Takeda, K. & Kaisho, T. Toll-like receptors: critical proteins linking innate and acquired immunity. *Nature immunology* **2**, 675-680 (2001).
13. Kawai, T. & Akira, S. The role of pattern-recognition receptors in innate immunity: update on Toll-like receptors. *Nature immunology* **11**, 373-384 (2010).
14. Ding, Y., *et al.* Toll-like receptor 4 deficiency decreases atherosclerosis but does not protect against inflammation in obese low-density lipoprotein receptor-deficient mice. *Arteriosclerosis, thrombosis, and vascular biology* **32**, 1596-1604 (2012).
15. Lu, Z., Zhang, X., Li, Y., Jin, J. & Huang, Y. TLR4 antagonist reduces early-stage atherosclerosis in diabetic apolipoprotein E-deficient mice. *The Journal of endocrinology* **216**, 61-71 (2013).
16. Hollestelle, S.C., *et al.* Toll-like receptor 4 is involved in outward arterial remodeling. *Circulation* **109**, 393-398 (2004).
17. Karper, J.C., *et al.* Toll-like receptor 4 is involved in human and mouse vein graft remodeling, and local gene silencing reduces vein graft disease in hypercholesterolemic APOE*3Leiden mice. *Arteriosclerosis, thrombosis, and vascular biology* **31**, 1033-1040 (2011).
18. Karper, J.C., *et al.* Blocking toll-like receptors 7 and 9 reduces postinterventional remodeling via reduced macrophage activation, foam cell formation, and migration. *Arteriosclerosis, thrombosis, and vascular biology* **32**, e72-80 (2012).

19. Vink, A. In Vivo Evidence for a Role of Toll-Like Receptor 4 in the Development of Intimal Lesions. *Circulation* **106**, 1985-1990 (2002).
20. Akashi-Takamura, S. & Miyake, K. TLR accessory molecules. *Current opinion in immunology* **20**, 420-425 (2008).
21. Wezel, A.*, et al.* Deficiency of the TLR4 analogue RP105 aggravates vein graft disease by inducing a pro-inflammatory response. *Scientific reports* **6**, 24248 (2016).
22. Karper, J.C.*, et al.* TLR accessory molecule RP105 (CD180) is involved in post-interventional vascular remodeling and soluble RP105 modulates neointima formation. *PloS one* **8**, e67923 (2013).
23. Divanovic, S.*, et al.* Inhibition of TLR-4/MD-2 signaling by RP105/MD-1. *Journal of endotoxin research* **11**, 363-368 (2005).
24. Ohto, U., Miyake, K. & Shimizu, T. Crystal structures of mouse and human RP105/MD-1 complexes reveal unique dimer organization of the toll-like receptor family. *Journal of molecular biology* **413**, 815-825 (2011).
25. Schultz, T.E. & Blumenthal, A. The RP105/MD-1 complex: molecular signaling mechanisms and pathophysiological implications. *Journal of leukocyte biology* (2016).
26. Divanovic, S.*, et al.* Regulation of TLR4 signaling and the host interface with pathogens and danger: the role of RP105. *Journal of leukocyte biology* **82**, 265-271 (2007).
27. Divanovic, S.*, et al.* Negative regulation of Toll-like receptor 4 signaling by the Toll-like receptor homolog RP105. *Nature immunology* **6**, 571-578 (2005).
28. Karper, J.C.*, et al.* An Unexpected Intriguing Effect of Toll-Like Receptor Regulator RP105 (CD180) on Atherosclerosis Formation With Alterations on B-Cell Activation. *Arteriosclerosis, thrombosis, and vascular biology* **33**, 2810-2817 (2013).
29. Wezel, A.*, et al.* RP105 deficiency attenuates early atherosclerosis via decreased monocyte influx in a CCR2 dependent manner. *Atherosclerosis* **238**, 132-139 (2015).
30. Rotmans, J.I. & Bezhaeva, T. The battlefield at arteriovenous crossroads: invading arterial smooth muscle cells occupy the outflow tract of fistulas. *Kidney international* **88**, 431-433 (2015).
31. Skartsis, N.*, et al.* Origin of neointimal cells in arteriovenous fistulae: bone marrow, artery, or the vein itself? *Seminars in dialysis* **24**, 242-248 (2011).
32. Wang, H.U., Chen, Z.F. & Anderson, D.J. Molecular distinction and angiogenic interaction between embryonic arteries and veins revealed by ephrin-B2 and its receptor Eph-B4. *Cell* **93**, 741-753 (1998).
33. Gerety, S.S., Wang, H.U., Chen, Z.F. & Anderson, D.J. Symmetrical mutant phenotypes of the receptor EphB4 and its specific transmembrane ligand ephrin-B2 in cardiovascular development. *Molecular cell* **4**, 403-414 (1999).
34. Wong, C.Y.*, et al.* Elastin is a key regulator of outward remodeling in arteriovenous fistulas. *European journal of vascular and endovascular surgery : the official journal of the European Society for Vascular Surgery* **49**, 480-486 (2015).
35. Roy-Chaudhury, P.*, et al.* Pathogenetic role for early focal macrophage infiltration in a pig model of arteriovenous fistula (AVF) stenosis. *The journal of vascular access* **15**, 25-28 (2014).
36. Caplice, N.M.*, et al.* Neoangiogenesis and the presence of progenitor cells in the venous limb of an arteriovenous fistula in the rat. *American journal of physiology. Renal physiology* **293**, F470-475 (2007).
37. Tanaka, K.*, et al.* Circulating progenitor cells contribute to neointimal formation in nonirradiated chimeric mice. *FASEB journal : official publication of the Federation of American Societies for Experimental Biology* **22**, 428-436 (2008).
38. Misra, S.*, et al.* Adventitial remodeling with increased matrix metalloproteinase-2 activity in a porcine arteriovenous polytetrafluoroethylene grafts. *Kidney international* **68**, 2890-2900 (2005).

39. Li, L., *et al.* Cellular and morphological changes during neointimal hyperplasia development in a porcine arteriovenous graft model. *Nephrology, dialysis, transplantation : official publication of the European Dialysis and Transplant Association - European Renal Association* **22**, 3139-3146 (2007).
40. Croatt, A.J., *et al.* Characterization of a model of an arteriovenous fistula in the rat: the effect of L-NAME. *The American journal of pathology* **176**, 2530-2541 (2010).
41. Juncos, J.P., *et al.* MCP-1 contributes to arteriovenous fistula failure. *Journal of the American Society of Nephrology : JASN* **22**, 43-48 (2011).
42. Tsapenko, M.V., *et al.* Increased production of superoxide anion contributes to dysfunction of the arteriovenous fistula. *American journal of physiology. Renal physiology* **303**, F1601- 1607 (2012).
43. Lin, C.C., *et al.* Length polymorphism in heme oxygenase-1 is associated with arteriovenous fistula patency in hemodialysis patients. *Kidney international* **69**, 165-172 (2006).
44. Kang, L., *et al.* A new model of an arteriovenous fistula in chronic kidney disease in the mouse: beneficial effects of upregulated heme oxygenase-1. *American journal of physiology. Renal physiology* **310**, F466-476 (2016).
45. Liew, F.Y., Xu, D., Brint, E.K. & O'Neill, L.A.J. Negative regulation of Toll-like receptor- mediated immune responses. *Nat Rev Immunol* **5**, 446-458 (2005).
46. Sanin, D.E., Prendergast, C.T. & Mountford, A.P. IL-10 production in macrophages is regulated by a TLR-driven CREB-mediated mechanism that is linked to genes involved in cell metabolism(). *Journal of immunology (Baltimore, Md. : 1950)* **195**, 1218-1232 (2015).
47. Galis, Z.S. & Khatri, J.J. Matrix metalloproteinases in vascular remodeling and atherogenesis: the good, the bad, and the ugly. *Circulation research* **90**, 251-262 (2002).
48. Castier, Y., Ramkhelawon, B., Riou, S., Tedgui, A. & Lehoux, S. Role of NF-kappaB in flow- induced vascular remodeling. *Antioxidants & redox signaling* **11**, 1641-1649 (2009).
49. Nieves Torres, E.C., *et al.* Adventitial Delivery of Lentivirus-shRNA-ADAMTS-1 Reduces Venous Stenosis Formation in Arteriovenous Fistula. *PloS one* **9**, e94510 (2014).
50. Mantovani, A., Biswas, S.K., Galdiero, M.R., Sica, A. & Locati, M. Macrophage plasticity and polarization in tissue repair and remodelling. *The Journal of pathology* **229**, 176-185 (2013).
51. Jetten, N., *et al.* Anti-inflammatory M2, but not pro-inflammatory M1 macrophages promote angiogenesis in vivo. *Angiogenesis* **17**, 109-118 (2014).
52. Lichtnekert, J., Kawakami, T., Parks, W.C. & Duffield, J.S. Changes in macrophage phenotype as the immune response evolves. *Current opinion in pharmacology* **13**, 555-564 (2013).
53. Perdiguero, E.G. & Geissmann, F. The development and maintenance of resident macrophages. *Nature immunology* **17**, 2-8 (2015).
54. Wong, C.Y., *et al.* A Novel Murine Model of Arteriovenous Fistula Failure: The Surgical Procedure in Detail. *Journal of visualized experiments : JoVE*, e53294 (2016).
55. de Vries, M.R., *et al.* Plaque rupture complications in murine atherosclerotic vein grafts can be prevented by TIMP-1 overexpression. *PloS one* **7**, e47134 (2012).
56. Kaijzel, E.L., *et al.* Multimodality imaging reveals a gradual increase in matrix metalloproteinase activity at aneurysmal lesions in live fibulin-4 mice. *Circulation. Cardiovascular imaging* **3**, 567-577 (2010).

Supplementary material

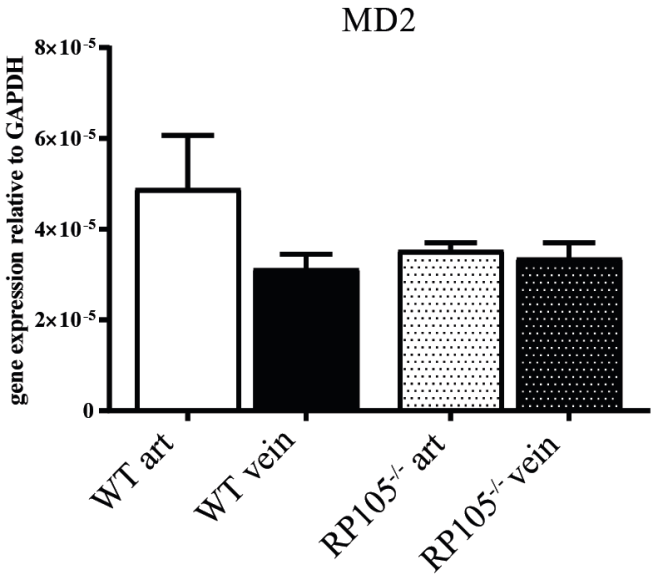

Supplementary Figure 1. MD2 mRNA expression levels.
The relative expression normalized to GAPDH. n=3 per group.

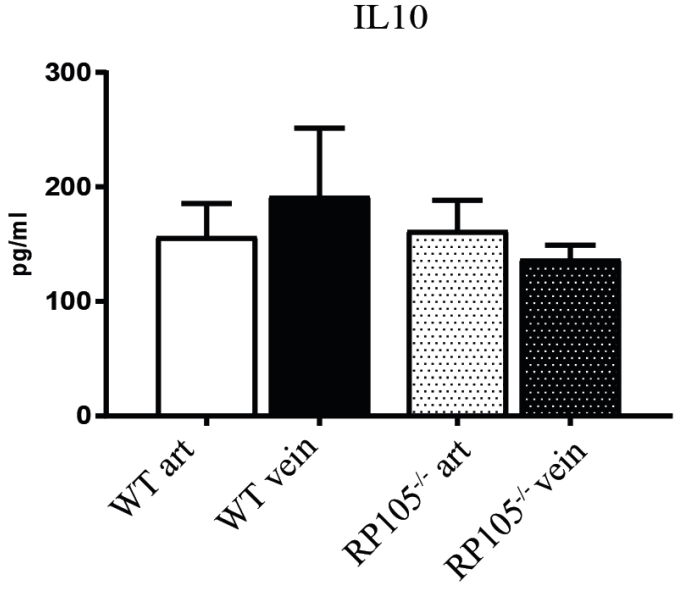

Supplementary Figure 2. IL10 production by SMCs *in vitro*.
Quantification of anti-inflammatory cytokine IL10 production by in vitro cultured SMCs isolated from WT and RP105$^{-/-}$. No difference in IL10 levels was detected between RP105$^{-/-}$ and WT mice. n=3 per group.

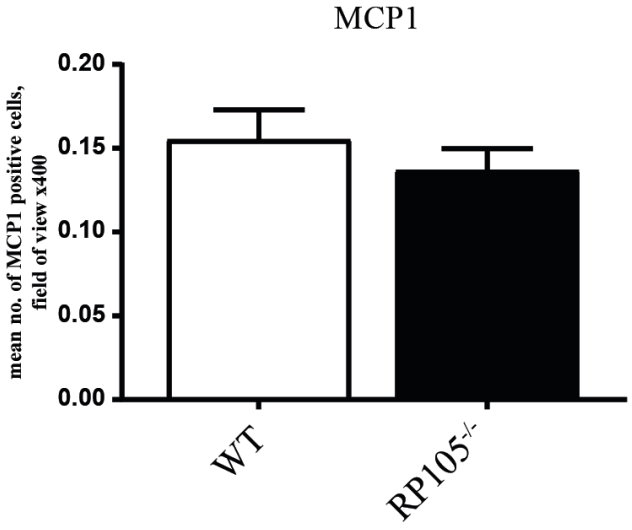

Supplementary Figure 3. Effects of RP105 deficiency on MCP1 expression *in vivo*.
Quantification of MCP^{+} cells in AVF lesions 14 days after surgery. No difference in MCP1^{+} cell number was detected between RP105$^{-/-}$ and WT mice. n=11 per group.

MATHERIAL AND METHODS

S1. Surgical procedure

The animal was anesthetized using isoflurane followed by shaving and disinfection of the skin in the ventral neck area and fixed in a supine position on a heating blanket. The mouse was then injected with buprenorphin (0.1 mg/kg) (MSD, Whitehouse Station, NJ, USA) and 0.5 mL saline. Under a dissecting microscope (Leica, Wetzlar, Germany), an incision in the ventral midline of the neck area was made, followed by a dissection of the right dorsomedial branch of the external jugular vein and ipsilateral common carotid artery after the excision of the sternocleidomastoid muscle using a heat cauterizer. Next, after applying a vascular clamp (S&T, Neuhausen, Switzerland) on the proximal and distal artery an approximate 1 mm incision was made using a microscissor (Fine Science Tools, Heidelberg, Germany) and the lumen was rinsed with a heparin solution (100 IU/ml) (LEO Pharma, Ballerup, LLDenmark). The vein was then clamped proximally and ligated distally, followed by a transection just proximal to the ligation. After rinsing the vein with a heparin solution, an end-to-side anastomosis was created using 10.0 interrupted sutures (BBraun, Melsungen, Germany). Halfway during the suturing procedure, heparin (0.2 IU/gram bodyweight) together with 200 µL of either L-Pred (10 mg/kg bodyweight), Pred (10 mg/kg bodyweight), L-PBS or PBS was injected intravenously. After completion of the anastomosis, the remaining clamps were removed and patency was assessed. The skin was closed with a 6.0 running suture (BBraun, Melsungen, Germany). Following completion of the surgery 0.5 mL of saline was injected subcutaneously and the mice were kept warm until recovery.

S2. VSMC proliferation assay

$5x10^4$ cells per well were seeded in 96 well plates. Next, cells were synchronized overnight in culture medium supplemented with 1% FCS followed by stimulation with 1ng/µl LPS in completed medium supplemented with 20% FCS. Absorbance of neutral red (C15H17IN4) by the cells over a 16 hours period was measured by an ELISA plate reader at A540. Absorbance was compared between the control and knock-out animals with or without stimulation with LPS. All experiments were performed in biological triplicates.

Table 1 Primers used for *in vitro* experiments

Gene	Forward primer	Reversed primer
SMA	CTGACAGAGGCACCACTGAA	CATCTCCAGAGTCCAGCACA
MYHC	TGGCTAGCAGCTTGTCAGGAA	GCCTTGCGTACTCTATCACTCATG
Calponin	GAAGGCAGGAACATCATTGGA	CCTGCTGACTGGCAAACTTG
EphB4	AGTGGCTTCGAGCCATCAAGA	CTCCTGGCTTAGCTTGGGACTTC
RP105	CTTTGAATGCCTCCGTCTTG	GCCCTCTCCACCTTAGACCT
TLR4	TGCCGTTTCTTGTTCTTCC	GAGCTCGGTACTGGCTGTTT
MD1	CTTGGTTATCAGTGGTTCTTGC	AGCGGGATCGAGCCCTC
MD2	CTTACGCTTCGGCAACTCTA	CCTATCCCCTTTGTGAGGAG
GAPDH	ACTCCCACTCTTCCACCTTC	CACCACCCTGTTGCTGTAG

Chapter 3

Liposomal prednisolone inhibits vascular inflammation and enhances venous outward remodeling in a murine arteriovenous fistula model

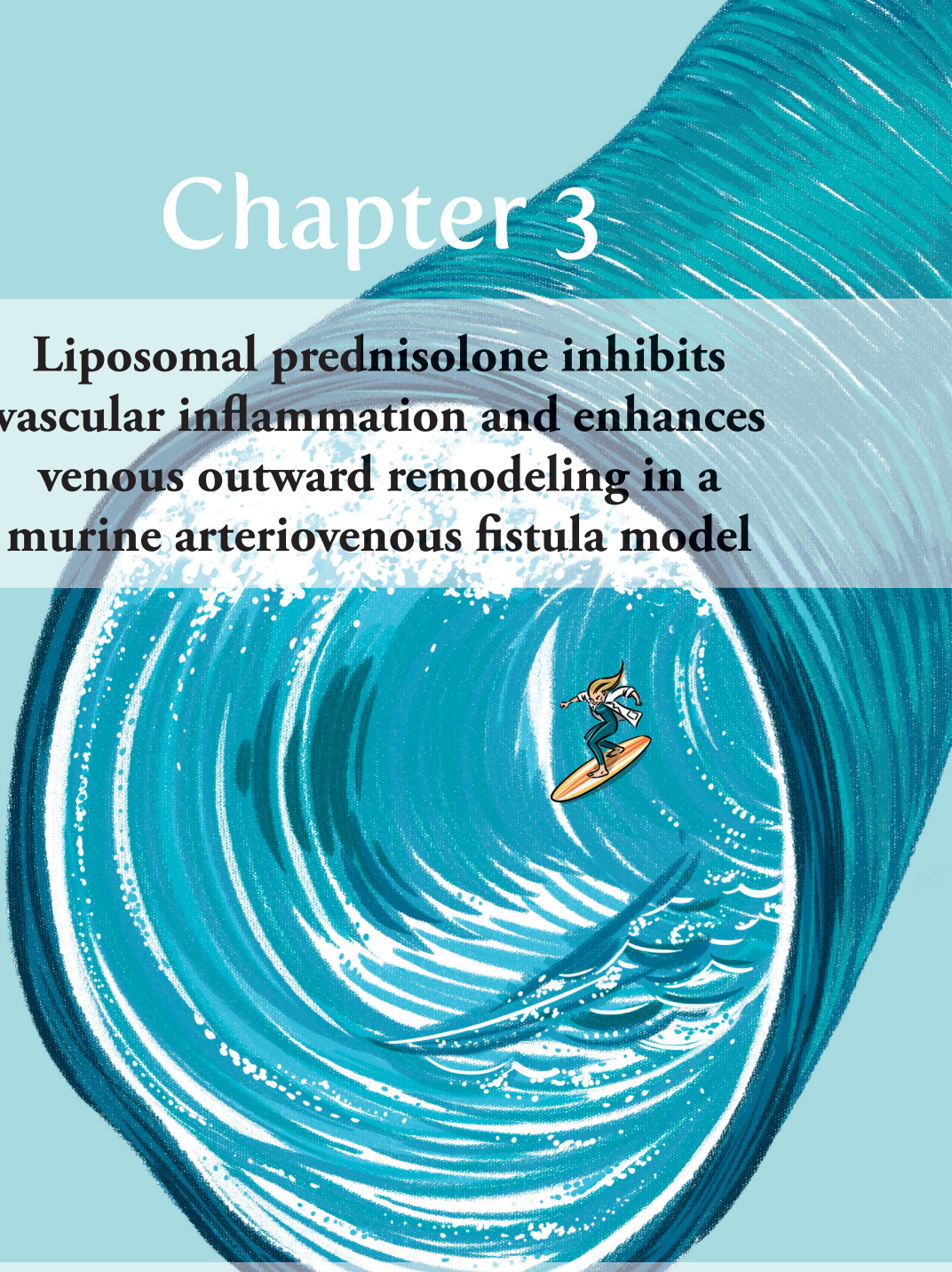

ChunYu Wong, Taisiya Bezhaeva, Tonia C. Rothuizen, Josbert M. Metselaar, Margreet R. de Vries, Floris P.R. Verbeek, Alexander L. Vahrmeijer, Anouk Wezel, Anton Jan van Zonneveld, Ton. J. Rabelink, Paul H.A. Quax and Joris I. Rotmans

Sci Rep. 2016 Jul 27; 6:30439

Abstract

Arteriovenous fistulas (AVFs) for hemodialysis access have a 1-year primary patency rate of only 60%, mainly as a result of maturation failure that is caused by insufficient outward remodeling and intimal hyperplasia. The exact pathophysiology remains unknown, but the inflammatory vascular response is thought to play an important role. In the present study we demonstrate that targeted liposomal delivery of prednisolone increases outward remodeling of the AVF in a murine model. Liposomes accumulate in the post-anastomotic area of the venous outflow tract in which the vascular pathology is most prominent in failed AVFs. On a histological level, we observed a reduction of lymphocytes and granulocytes in the vascular wall. In addition, a strong anti-inflammatory effect of liposomal prednisolone on macrophages was demonstrated *in vitro*. Therefore, treatment with liposomal prednisolone might be a valuable strategy to improve AVF maturation.

Introduction

Arteriovenous fistulas (AVFs) are the preferred type of permanent vascular access for hemodialysis in view of their superior patency and lower rate of infectious complications, when compared to prosthetic arteriovenous grafts. However, the durability of AVFs is far from optimal with a 1-year primary patency of only 60%[1]. AVF maturation refers to the process of enlargement of the lumen of the access conduit and the concomitant increase in blood flow, both needed to allow safe cannulation and adequate hemodialysis treatment. The exact mechanisms underlying maturation failure are unknown, but impaired outward remodeling (OR) as well as intimal hyperplasia (IH) are both considered to contribute[2]. Animal studies have shown that the adaptive response that occurs upon AVF creation, is characterized by marked vascular inflammation as illustrated by the infiltration of macrophages and lymphocytes[3,4] as well as the up regulation of pro-inflammatory cytokines[5]. In addition, recent clinical studies suggest that this inflammatory response is harmful for AVF maturation, by showing that plasma levels of C-reactive protein are inversely correlated with successful AVF maturation[6].

Glucocorticoids (GCs) are well-known anti-inflammatory drugs that are widely used for the treatment of numerous inflammatory diseases[7]. Despite their excellent anti-inflammatory efficacy, the therapeutic use of systemic GCs is hampered by the high risk of occurrence of adverse side effects. Nanoparticle therapeutics such as liposomes have shown to facilitate selective delivery of drugs to inflamed tissues with a highly permeable microvasculature[8], where liposomes are being phagocytized by macrophages[9].

In the present study, we evaluated the feasibility and efficacy of liposomal prednisolone (L-Pred) to target the inflamed peri-anastomotic region of murine AVFs and assessed its effect on the morphometry and composition of the venous outflow tract. Subsequently, we assessed the efficacy of L-Pred to reduce the inflammatory profile of cultured macrophages and evaluated its effect on vascular smooth muscle cell (VSMC) proliferation *in vitro*.

Results

Surgical outcome

In total, 54 mice received an AVF (PBS; n=10, L-PBS; n=8 Pred; n=9, L-Pred; n=10, gold-containing PEG-liposomes; n=3), of which 14 mice (26%) did not survive the surgical procedure. The number of deaths did not differ significantly between the different intervention groups when compared to the PBS treated group. In 6 of the 14 mice (43%), the cause of death was clearly due to postoperative bleeding in the surgical area. In the rest of the cases, the cause of death was unclear. The surviving mice showed normal behavior after recovering from the surgery until time to sacrifice. Figure 1, A-B and video 1-2 illustrate the AVF directly after surgery as well as circulating liposomes shortly after intravenous administration.

With regard to adverse effects of systemic prednisolone phosphate therapy, animals

that received either liposomal prednisolone phosphate or free prednisolone phosphate both showed disturbed wound healing in the ears that was caused by the placement of earmarks at the start of the surgical procedure. However, we did not observe any disturbance in the wound healing of the skin incisions located in the neck and upper leg. Apart from this adverse effect, the general condition of all the animals remained normal during the study.

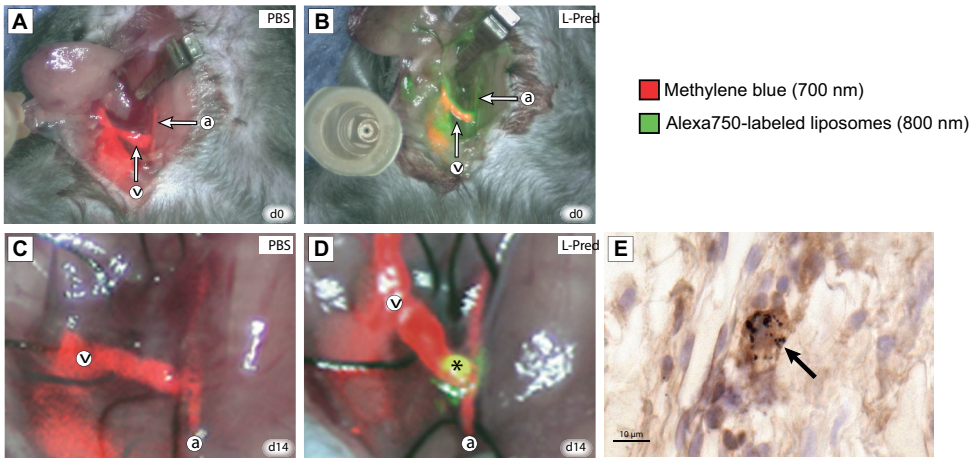

Figure 1. Localization of liposomes using near infrared fluoroscopy and immunohistochemistry. (A,B)

In vivo imaging using NIRF of the AVF directly after creation (day 0) in mice that were injected with PBS (**A**) or L-Pred. (**B**) Red color overlay corresponds to the intravenously administered methylene blue visualized on the 700 nm channel. Green color overlay corresponds to the intravenously administered liposomes that are labeled with the Alexa-750 fluorochrome visualized on the 800 nm channel. (**C,D**) ***In vivo*** imaging using NIRF of the AVF at time of sacrifice (day 14) in mice that were injected with either PBS (**C**) or L-Pred (**D**) at day 0, 2, 5 and 10.(*) Extravasation of liposomes in the anastomotic area of the AVF. (**E**) Double staining against F4/80 and gold particles showing accumulation of gold-labeled liposomes in macrophages in the venous outflow tract (black arrows). (a) Artery, (v) Vein. Bar =10 µm.

Patency

Using near infrared fluorescence (NIRF) (Figure 1, C-D and video 3-4), we observed a 100% patency in all the groups except for the mice treated with prednisolone in which 2 out of the 9 (22%) AVFs were occluded at time of sacrifice. This difference in patency was not significant when compared to PBS (P=0.15). These two occluded AVFs were excluded from further analysis.

Distribution of liposomes in murine AVF

At 14 days after surgery, liposomes accumulated in the peri-anastomotic area of the AVF as assessed, by NIRF imaging (Figure 1D and video 4). At this time, 4 days after the last injection, no circulating liposomes were detected. Histological analysis of the venous outflow tract in mice that were injected with the gold-labeled liposomes, showed marked accumulation of gold in F4/80(+) macrophages (Figure 1E).

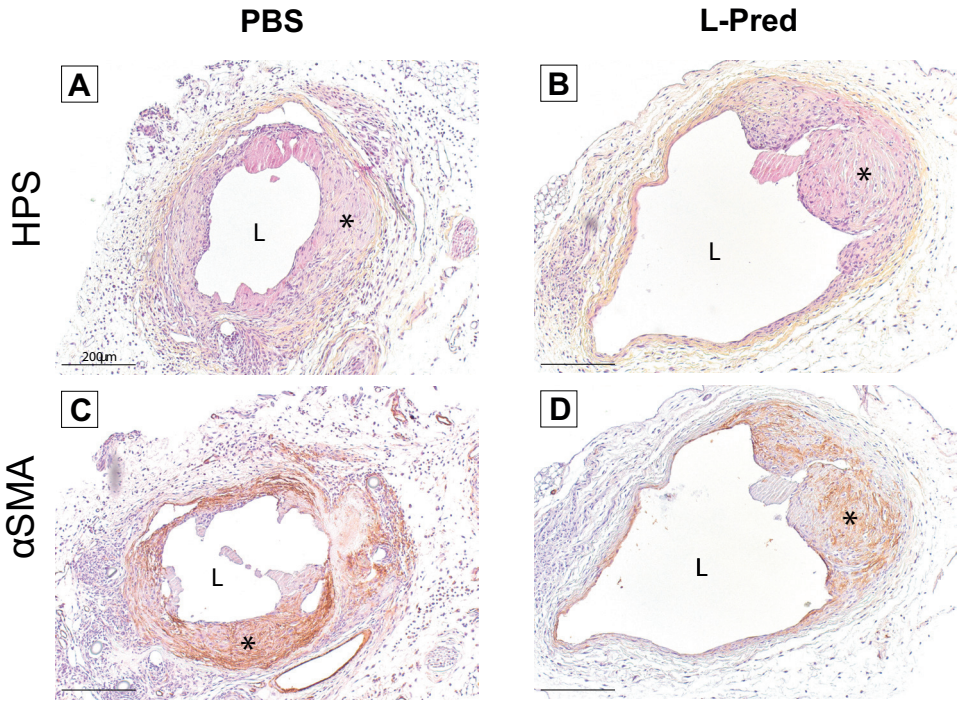

Figure 2. Histological stainings of the venous outflow tract of the AVF at day 14 after surgery. (**A,B**) Hematoxylin, phloxin and saffron staining (HPS). (**C,D**) Immunohistological staining against α -smooth muscle actin. (*) Intimal hyperplasia, (L) Lumen, Original magnification 100x. Bar = 200 µ m.

Morphometric analysis

Representative sections from the venous outflow tract of the AVF are shown in figure 2A-B. At day 14 after surgery, the mice that were treated with L-Pred showed a 27% larger circumference of the external jugular vein when compared to the PBS-treated group (P=0.004), whereas no significant differences were observed in the Pred-treated mice (P= 0.195) or L-PBS treated mice (P=0.396) (Figure 3A).

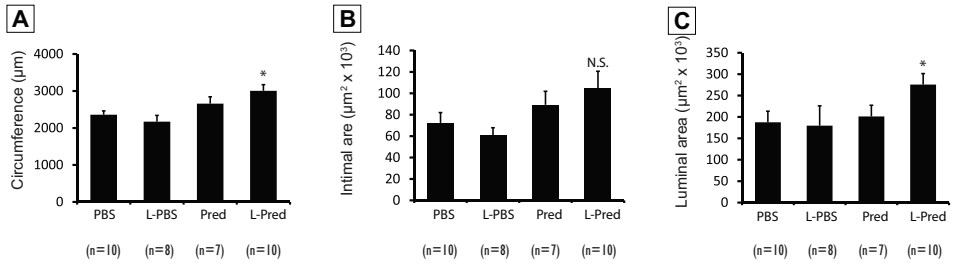

Figure 3. Histomorphometric parameters 14 days after AVF surgery.
(**A**) Venous circumference. (**B**) Intimal area at the venous outflow tract. (**C**) Luminal area at the venous outflow tract. (*)$P < 0.05$ compared to PBS,(N.S) not significant compared to PBS.

No significant differences were observed in intimal area in the experimental groups (L-Pred: P=0.052, Pred: P=0.350, L-PBS: P=0.494) when compared to PBS-treated mice (Figure 3B). Immunohistochemical staining revealed that the vast majority of the cells in the intima stained positive for αSMA in all the groups (Figure 2, C-D).
The luminal area in the L-pred treated mice showed a 47% increase compared to the PBS treated mice (P=0.042), whereas the mice treated with Pred (P=0.766) or L-PBS (P=0.861) did not show a significant difference when compared to the PBS-treated mice (Figure 3C).

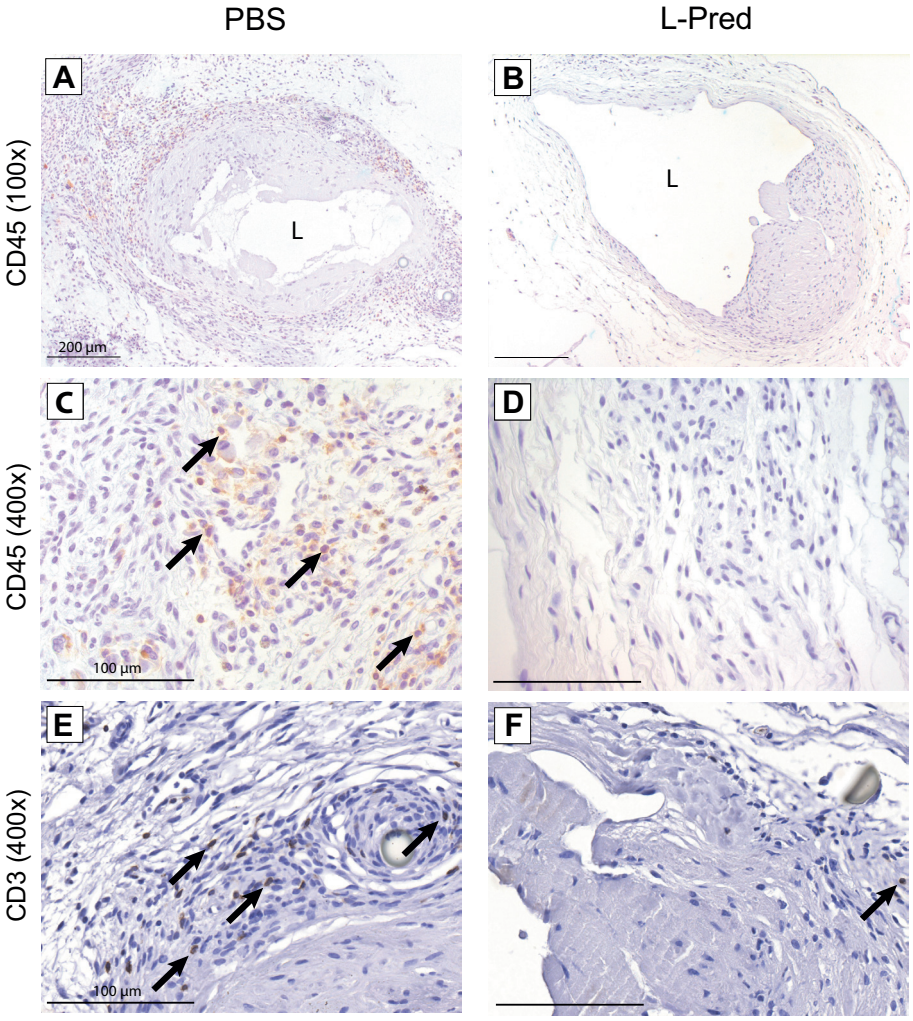

Figure 4. Representative sections of immunohistochemical stainings against CD45 and CD3 at 14 days after AVF surgery.
(**A–D**) CD45(+) cells (black arrow) in the venous outflow tract of the AVF. (**E,F**) CD3(+) cells (black arrow) in the venous outflow tract of AVF. Original magnification (**A,B**): 100x. Bar = 200 µm,(**C–F**): 400x, Bar = 100 µm (L) Lumen.

Inflammatory response in the AVF

Representative sections of the immunohistochemical staining against CD45 and CD3 are shown in figure 4, A-F. Immunohistochemical analysis of sections obtained from the venous outflow tract revealed that the mean number of CD45(+) cells present in the venous outflow tract of the L-Pred treated mice was reduced by 83%, when compared to the mice treated with PBS (P<0.001). A trend towards reduction of CD45-positive cells in the venous vascular wall was observed in the Pred-treated mice, when compared to PBS (P=0.069) (Figure 5A). Additional immunohistochemical stainings for subsets of inflammatory cells revealed a 86% decrease in CD3(+) T-cells (P<0.001) and a 51% decrease in GR1(+) granulocytes (P=0.008) in the L-Pred treated group when compared to the PBS treated group (Figure 5, B-D).

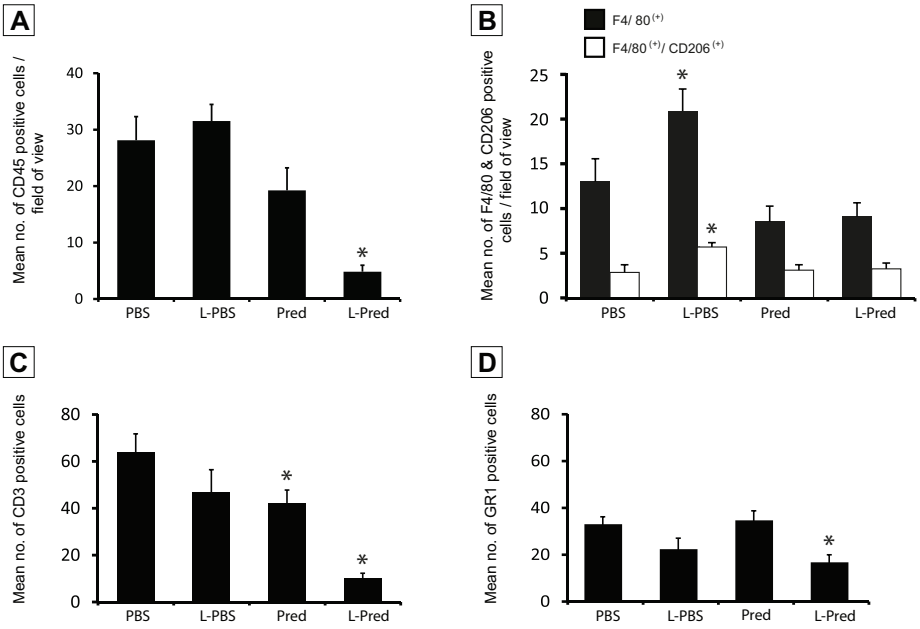

Figure 5. Quantification of immunohistological staining against different inflammatory cells at day 14.

(**A**) CD45(+) leukocytes. (**B**) F4/80(+) macrophages and F4/80(+)CD206(+) M2 macrophages. (**C**) CD3(+) granulocytes. (**D**) GR1(+) granulocytes in the venous outflow tract of AVF at day 14. (*)$P < 0.05$ compared to PBS.

Inflammatory effect of L-Pred in cultured macrophages

To study the inflammatory effects on a mRNA level, we exposed murine M1 and M2 macrophages to L-Pred, L-PBS, Pred and PBS. Upon incubation with L-Pred and Pred, a strong reduction was observed in the expression of pro-inflammatory genes including TNF-α, MCP-1 and IL-6 (all P<0.01) by M1 polarized macrophages, whereas M2 macrophages showed a significant increase in the expression of the anti-inflammatory cytokine IL-10 after addition of L-Pred and L-PBS (both P<0.01) when compared to the incubation with PBS (Figure 6, A-D).

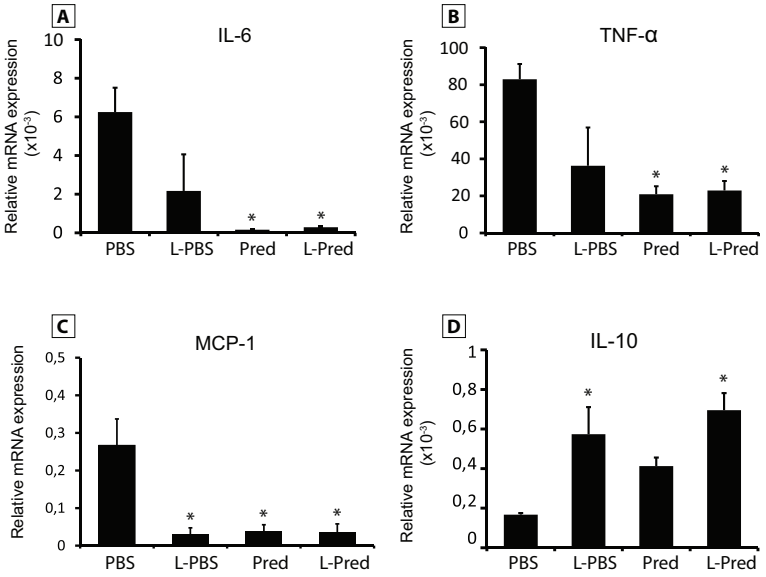

Figure 6. mRNA expression levels of pro- and anti-inflammatory cytokines in macrophages *in vitro* after incubation with PBS (control medium), L-PBS, Pred and L-Pred.
(**A–C**) Relative mRNA expression of proinflammatory cytokines (IL-6, TNF-α and MCP-1) in M1 macrophages and (**D**) the anti-inflammatory cytokine IL-10 in M2 macrophages. The relative expression is normalized against GAPDH. (*)$P < 0.05$ compared to PBS.

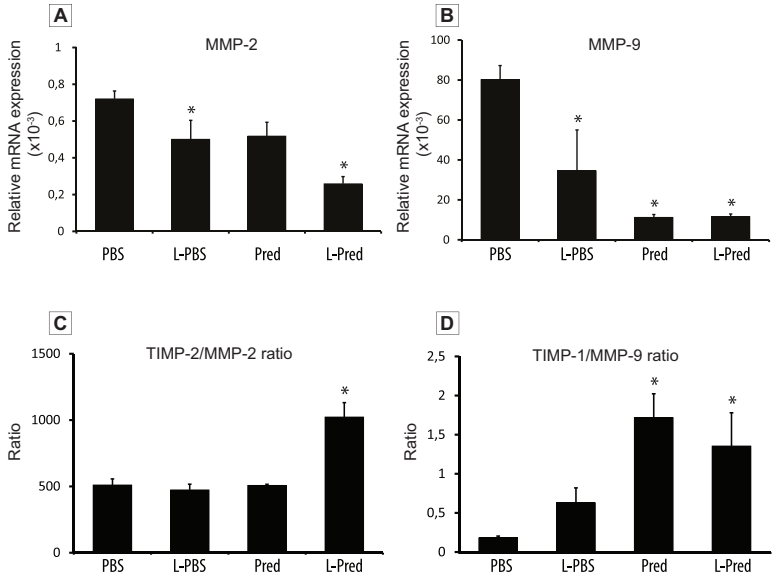

Figure 7. mRNA expression levels of MMP-2, MMP-9 and the ratios of TIMP-2/MMP-2 and TIMP-1/MMP-9 in macrophages after incubation with PBS (control medium), L-PBS, Pred and L-Pred. (A,B)
Relative mRNA expression of MMP-2 and MMP-9. (C,D) Ratios of TIMP-2/MMP-2 and TIMP-1/MMP-9. Expression was normalized against GAPDH. (*)P < 0.05 compared to PBS.

Effect of liposomal prednisolone on the expression of MMPs and TIMP.
We measured the expression of matrix metalloproteinases (MMP-2 and MMP-9) and their endogenous inhibitors (TIMP-2 and TIMP-1, respectively) on RNA level in M1 macrophages. Upon incubation with L-Pred, both MMP-2 and MMP-9 expression decreased when compared to PBS incubation. In addition, both the TIMP1/MMP-9 and the TIMP2/ MMP-2 ratio increased upon incubation with L-Pred when compared to PBS incubation (Figure 7, A-D).

Discussion

In the present study, we demonstrate that intravenously administered liposomes selectively target the anastomotic region and can effectively improve venous outward remodeling of murine AVF when prednisolone is encapsulated in the liposomes.

Liposomes are one the most prominent drug carrier systems currently available, due to their relative easy preparation using biocompatible components and the high drug payload[10]. Moreover, liposomes can hold their payload while circulating in the vasculature until they extravasate and accumulate at sites of inflammation as a result of enhanced vascular permeability in inflamed tissues, thereby reducing possible systemic adverse side effects[11]. The PEG-coating of liposomes is designed to improve their bioavailability in inflamed tissues as it serves as a steric barrier that minimizes liposomal uptake by circulating mononuclear cells[12]. Once extravasated, the liposomes are recognized as foreign particles and phagocytized by macrophages[10]. Using NIRF and immunohistochemistry, we demonstrated that liposomes indeed accumulate in macrophages in the anastomotic area of murine AVF. These results are consistent with previous studies in rabbits[13] and humans[14] which revealed marked accumulation of liposomes in macrophages within inflammatory atherosclerotic plaques.

GCs are powerful anti-inflammatory drugs that act through binding to cytosolic glucocorticoid receptors in target cells, leading to a reduction in the expression of pro-inflammatory cytokines and diminished recruitment of inflammatory cells[15,16]. Despite these potent anti-inflammatory effects, chronic and systemic therapeutic use of GCs is limited by the high incidence of serious adverse effects[16]. Moreover, as a result of rapid clearance from the circulation, systemic administration of GCs results in low efficacy of drug delivery at the target location. Therefore, encapsulation of GCs in liposomal nanoparticles has great potential to enhance the therapeutic effect of GCs in inflamed tissues. Previous studies on L-Pred in murine model of arthritis[17] have underscored this potential, as complete remission of the inflammatory response was shown upon a single injection, which was superior to the effect of unencapsulated prednisolone.

Preclinical studies have shown that GCs reduce the formation of both arterial and venous stenotic lesions[18-20]. However, the role of inflammation in vascular remodeling upon AVF surgery has not been elucidated yet. Although various animal studies[3-5, 21] revealed infiltration of inflammatory cells in the venous outflow tract in the early phase after AVF surgery, it is unclear whether this inflammatory response directly contributes to maturation failure. Our experiments revealed that L-Pred resulted in inhibition of vascular

inflammation in the AVF, as illustrated by a significant reduction of lymphocytes and granulocytes in the venous outflow tract. Interestingly, treatment with unencapsulated prednisolone resulted solely in a modest reduction in inflammatory cells , suggesting that liposomal encapsulation indeed resulted in a higher concentration of prednisolone in the venous outflow tract. As shown *in vitro,* L-Pred induced a conversion towards an anti-inflammatory profile of macrophages, as demonstrated previously[22]. Moreover, liposomes themselves contribute to the reduction of the pro-inflammatory profile of macrophages, as illustrated by the reduction of pro-inflammatory cytokines in M1 macrophages upon stimulation with L-PBS. This shift towards an anti-inflammatory profile of macrophages might have inhibited the recruitment of lymphocytes and granulocytes to the injured vessels of the AVF. Alternatively, prednisolone might have had a direct effect on lymphocytes and granulocytes as GCs can easily pass the cellular membrane of macrophages in both directions.

While previous studies evaluated the therapeutic effect of GCs to inhibit IH in various vascular injury models[18-20], none of these studies focused on its effect on vascular remodeling. The question arises how treatment with L-Pred resulted in enhanced outward remodeling in the venous outflow tract of AVF. In order to investigate whether L-Pred influenced VSMC proliferation and collagen production, we directly stimulated cultured murine VSMCs with L-Pred. However, no significant effect on VSMC proliferation and collagen synthesis was observed (data not shown).

MMPs are a group of proteolytic enzymes involved in vascular remodeling by facilitating the turnover of extracellular matrix components such as collagen and elastin[23]. The effect of MMPs on the vascular remodeling depend on the specific MMPs that are activated and the type of vascular injury[24]. Previous studies in a porcine balloon angioplasty model in peripheral arteries revealed that treatment with the MMP-inhibitor marimastatin resulted in reduced constrictive arterial remodeling in favor of expansive remodeling[25]. The exact contribution of MMPs in vascular remodeling in AVF still remains to be elucidated. Previous studies suggest that the effect of MMP activation on vascular remodeling in AVF might differ between the arterial and venous segment. Indeed, Castier *et al.* observed that enhanced MMP-9 activity coincided with increased outward remodeling in the arterial segment of murine AVF, whereas studies by Nieves Torres *et al.*[27] revealed that MMP inhibition enhanced venous outward remodeling in AVF. In the latter study, adventitial delivery of a small hairpin RNA against the MMP ADAMTS-1, resulted in reduced macrophage infiltration, decreased MMP-9 activity and enhanced venous outward remodeling in murine AVF. Although we have not been able to quantify MMP activity *in vivo*, we speculate that the enhanced venous outward remodeling in murine AVF that occurred upon treatment with L-Pred is mediated by the dampened inflammatory response and decreased MMP activity in macrophages. In addition, a recent clinical trial evaluating the efficacy of the MMP-inhibitor doxycycline to inhibit growth of abdominal aortic aneurysms resulted in an unexpected acceleration of the aneurysmal growth[26]. These data suggest that in certain vascular disease conditions, inhibition of MMPs could enhance outward remodeling. Interestingly, elegant studies by Nieves Torres and coworkers[27] suggest a similar effect of MMP inhibiton on venous outward remodeling in AVF. Indeed, adventitial delivery of a small hairpin RNA against

the MMP ADAMTS-1, resulted in reduced macrophage infiltration, decreased MMP-9 activity and enhanced outward remodeling in murine AVF. Although we have not been able to quantify MMP activity *in vivo*, we speculate that the enhanced outward remodeling in murine AVF that occurred upon treatment with L-Pred is mediated by the dampened inflammatory response and decreased MMP activity in macrophages.

In contrast to its effect on outward remodeling, no inhibitory effect of L-Pred on IH in the venous outflow tract was observed. These results deviate from other preclinical studies that evaluated the therapeutic effect of GCs in other vascular injury models, that have reported a strong inhibitory effect of dexamethasone on IH[18-20]. This discrepancy may result from a difference in potency between prednisolone and dexamethasone to inhibit VSMC proliferation[28]. Alternatively, it may relate to the difference in pathophysiological stimuli that contribute to IH after arterial injury, when compared to venous IH in AVF. While hemodynamic stimuli are considered to be of vital importance for IH[29,30], the contribution of inflammation to IH in AVF might be limited, as suggested by our results. Interestingly, our study showed an increase in OR that was accompanied by a trend towards an increase in IH, which could potentially reduce the luminal area and therefore blood flow. Although the exact explanation for this phenomenon is not fully elucidated, we believe that this is due to the fact that both OR and IH are processes that involves VSMC proliferation. As a consequence, interventions that facilitate OR might therefore also result in a (modest) stimulation of IH. Of note, a stimulatory effect of an intervention on OR is more important for the ultimate luminal surface area than the coinciding effect on IH, as there is a quadratic relationship between radius and surface area of the vessel.

Preclinical studies in pigs[4] revealed that the inflammatory response in the venous outflow tract of AVF is temporal, peaking in the early weeks after surgery. This acute, localized inflammatory response makes the application of L-Pred particularly appealing as a short-term treatment in the first weeks after surgery.

In conclusion, liposomal prednisolone reduces the local inflammatory response and stimulates venous outward remodeling in murine AVF. Therefore, treatment with liposomal prednisolone might be valuable strategy to reduce AVF non-maturation. The efficacy of liposomal prednisolone to enhance AVF maturation in ESRD patients will be evaluated in the LIPMAT trial (clinicaltrial.gov ID NCT0249566), a double-blind, randomized, placebo-controlled trial that will commence in Q4 of 2015.

Methods

Liposomes

Prednisolone polyethylene glycol-coated (PEG)-liposomes were prepared as described in the supplemental data and contained 2 mg prednisolone phosphate per ml. The PEG-liposomes were labeled with Alexa 750 succinimidyl (Invitrogen, Carlsbad, CA, USA) and contained either prednisolone phosphate (Fagron, Capelle aan den IJssel, The Netherlands) or PBS. In order to trace the liposomes microscopically, additional PEG liposomes were coupled to gold particles (Nanoprobes, Yaphank, NY, USA).

Animal experiment

The Institutional Committee for Animal Welfare at the Leiden University Medical Center approved all animal experiments that were performed in accordance with the relevant guidelines and regulations. Adult male C57bl6 mice aged 10-11 weeks were used for the experiments and received an unilateral AVF between the dorsomedial branch of the external jugular vein and the common carotid artery in an end-to-side manner as previously described[3]. At the end of the procedure, either L-Pred (10 mg/kg bodyweight), Pred (10 mg/kg bodyweight) (Fagron), L-PBS or PBS was injected intravenously. The dose was determined according to the guidelines of the Food and Drugs Administration, in which the safe starting dose level of prednisolone was set at 1 mg/kg. The injection volume of L-PBS and PBS was equal to the injected volume of the L-Pred and Pred (200 µL). Due to a positive additive effect of multiple injections as compared to a single injection[31], we injected the mice intravenously at day 2, 5 and 10. In addition, 3 separate mice received a single bolus injection intravenously of gold-labeled empty liposomes (130 µL) at day 2 to evaluate liposomal accumulation in the AVF microscopically. All mice were sacrificed 14 days after the surgical procedure.

Near-infrared fluorescence imaging

To assess the accumulation of the liposomes macroscopically, we used the near infrared fluorescence (NIRF) imaging technique[3] directly after surgery and at time of sacrifice. After positioning of the Fluorescence Assisted Resection and Exploration (FLARE) imaging system (Center for Molecular Imaging, Boston, MA, USA) approximately 46 cm above the AVF, 200 µl 1% methylene blue (Sterop, Belgium) dissolved in saline was injected in the left femoral vein to assess the patency of the AVF. Video images were captured with 30-frames-per-second. Multiple video channels (color video, 700 nm and 800 nm) were obtained simultaneously with 60 milliseconds exposure times. After computer-controlled image acquisition, color video and NIRF images were displayed individually and merged in real-time. The 800 nm and 700 nm channel were used for imaging the liposomes and methylene blue, respectively.

Tissue harvesting and processing

Fourteen days after surgery, the mice were anesthetized (supplemental data) whereupon the AVF was dissected and assessed using NIRF as described above. Next, the inferior vena cava was transsected followed by mild pressure perfusion fixation with 4% formalin through an intracardiac perfusion. The tissue was processed to paraffin and 5 µm-thick sections of the venous outflow tract were made perpendicular to the vein with an interval of 150 µm.

Morphometric analysis

Morphometric analysis was performed on Weigert's elastin stained sections using quantitative imaging software (Qwin, Leica, Wetzlar, Germany). The intimal area was calculated by subtracting the luminal area from the area within the internal elastic lamina (IEL). The circumference of the vessel was determined by measuring the length of the IEL. Results are expressed as mean ± SEM.

Immunohistochemical staining and analysis

All immunohistochemical quantifications were performed on the first 3 venous sections starting from the anastomosis per AVF. Slides were digitized using an automated microscopic scanner (Pannoramic digital MIDI slice scanner, 3DHISTECH, Hungary). Detailed protocols of the immunohistochemical stainings are listed in supplemental data.

Serial sections from each AVF were stained with the following antibodies: anti-α-smooth muscle actin (αSMA) for vascular smooth muscle cells and myofibroblasts (Dako, Glostrup, Denmark); anti-CD45 for leukocytes (BD Pharmingen, San Diego, California, USA); anti-F4/80 for macrophages (Abcam, Cambridge, UK); anti-CD-206 for anti-inflammatory (M2) macrophages (Abcam); anti-CD-3 for T-lymphocytes (Abcam) and GR-1 for granulocytes (from G. Kraal, VUMC, Amsterdam, The Netherlands). To distinguish anti-inflammatory (M2) macrophages from the whole macrophage population anti-F4/80 and anti-CD-206 antibodies were combined in a double immunofluorescence staining.

For the immunohistochemical analysis of the CD206-F4/80 and CD45 staining, the number of positive cells was counted in two random fields of view using a 400x magnification from which the mean was calculated. In view of the limited presence of CD3+ and GR1+ cells, quantification of these cells was performed by counting all positive cells that were present in the venous segment of the AVF. Gold-labeled liposomes were visualized using the LI Silver enhancement kit (Nanoprobes) and combined with the F4/80 staining.

Generation and stimulation of bone marrow derived macrophages

To generate bone marrow-derived macrophages (BMDM) femurs of healthy C57Bl/6 male mice (n=3) were flushed with sterile PBS. Total bone marrow progenitor cells (BMPCs) were centrifuged at 300 g at 4 °C for 10 min and incubated for 5 min on ice with erythrocyte lysis buffer (Sigma-Aldrich R7757, St. Louis, MO, USA). After erythrocytes were depleted, remaining cells were washed three times with PBS, centrifuged at 300 g at 4 °C for 10 min, and resuspended in RPMI medium supplemented with 20% fetal calf serum (FCS), 2 mmol/L l-glutamine, 100 U/ml penicillin, 100 µg/ml streptomycin (all from PAA, Colbe, Germany). To promote differentiation of BMPCs towards macrophages, cultured medium was supplemented with 10 ng/ml of macrophage colony-stimulating factor (M-CSF) (Peprotech, Rocky Hill, NJ, USA). Cells were seeded at a density of $1.0*10^6$ cells per well, and the medium was replaced on day 3 and 5.

On day 7, cells were stimulated either with LPS (100 ng/ml) and IFN-gamma (10 ng/ml) to differentiate them towards pro-inflammatory (M1) phenotype or with IL-4 (10 ng/ml) and IL-13 (10 ng/ml) (all from Preprotech) for anti-inflammatory (M2) phenotype. On the same day Pred (10 µg/ml), L-Pred (10 µg/ml), L-PBS or control medium was added to the cells (n=3). After 24 hours the supernatant was collected and cells were lysed for RNA isolation.

RNA isolation, cDNA synthesis and qPCR

Total RNA was extracted from the macrophages cells using Trizol reagent (Invitrogen, Carlsbad, CA, USA). RNA was reverse transcribed using a 5-minute 65°C incubation of 1 μg total RNA with deoxyribonucleotide triphosphates (Invitrogen) and random primers (Invitrogen). c-DNA was synthesized using an M-MLV First-Strand Synthesis system (Invitrogen), and used for quantitative analysis of mouse genes (supplemental data) with an SYBR Green Master Mix (Applied Biosystems, Foster City, CA, USA). Levels of gene expression were determined by normalization to murine glyceraldehyde 3-phosphate dehydrogenase (GAPDH).

Statistical analysis

All data except the patency outcome were expressed as mean ± SEM. SPSS 20.0 was used for all statistical calculations. Except for the data on AVF patency and animal survival, all measurements were analyzed statistically using One-way ANOVA with Dunett post-hoc test with the PBS group as the reference category. A Fisher's exact test was used for the data on AVF patency and animal survival. A P-value < 0.05 was considered statistically significant.

Acknowledgements

We thank Enceladus Pharmaceuticals BV for generously manufacturing and supplying the liposomes.

Reference List

1. Tordoir,J.H. *et al.* Prospective evaluation of failure modes in autogenous radiocephalic wrist access for haemodialysis. *Nephrol. Dial. Transplant.* **18**, 378-383 (2003).
2. Rothuizen,T.C. *et al.* Arteriovenous access failure: more than just intimal hyperplasia? *Nephrol. Dial. Transplant.* **28**, 1085-1092 (2013).
3. Wong,C.Y. *et al.* Vascular remodeling and intimal hyperplasia in a novel murine model of arteriovenous fistula failure. *J. Vasc. Surg.* **59**, 192-201 (2014).
4. Wang,Y. *et al.* Venous stenosis in a pig arteriovenous fistula model--anatomy, mechanisms and cellular phenotypes. *Nephrol. Dial. Transplant.* **23**, 525-533 (2008).
5. Nath,K.A., Kanakiriya,S.K., Grande,J.P., Croatt,A.J., & Katusic,Z.S. Increased venous proinflammatory gene expression and intimal hyperplasia in an aorto-caval fistula model in the rat. *Am. J. Pathol.* **162**, 2079-2090 (2003).
6. Kaygin,M.A. *et al.* The relationship between arteriovenous fistula success and inflammation. *Ren Fail.* **35**, 1085-1088 (2013).
7. Vandevyver,S., Dejager,L., Tuckermann,J., & Libert,C. New insights into the anti-inflammatory mechanisms of glucocorticoids: an emerging role for glucocorticoid-receptor-mediated transactivation. *Endocrinology* **154**, 993-1007 (2013).
8. Farokhzad,O.C. & Langer,R. Impact of nanotechnology on drug delivery. *ACS Nano.* **3**, 16-20 (2009).
9. Schmidt,J. *et al.* Drug targeting by long-circulating liposomal glucocorticosteroids increases therapeutic efficacy in a model of multiple sclerosis. *Brain* **126**, 1895-1904 (2003).
10. Lasic,D.D. & Papahadjopoulos,D. Liposomes revisited. *Science* **267**, 1275-1276 (1995).
11. Lasic,D.D. Novel applications of liposomes. *Trends Biotechnol.* **16**, 307-321 (1998).
12. Schiffelers,R.M., Banciu,M., Metselaar,J.M., & Storm,G. Therapeutic application of long-circulating liposomal glucocorticoids in auto-immune diseases and cancer. *J. Liposome Res.* **16**, 185-194 (2006).
13. Lobatto,M.E. *et al.* Multimodal clinical imaging to longitudinally assess a nanomedical anti-inflammatory treatment in experimental atherosclerosis. *Mol. Pharm.* **7**, 2020-2029 (2010).
14. van der Valk,F.M. *et al.* Prednisolone-containing liposomes accumulate in human atherosclerotic macrophages upon intravenous administration. *Nanomedicine.* **11**, 1039-1046 (2015).
15. Cronstein,B.N., Kimmel,S.C., Levin,R.I., Martiniuk,F., & Weissmann,G. A mechanism for the antiinflammatory effects of corticosteroids: the glucocorticoid receptor regulates leukocyte adhesion to endothelial cells and expression of endothelial-leukocyte adhesion molecule 1 and intercellular adhesion molecule 1. *Proc. Natl. Acad. Sci. U. S. A* **89**, 9991-9995 (1992).
16. Rhen,T. & Cidlowski,J.A. Antiinflammatory action of glucocorticoids--new mechanisms for old drugs. *N. Engl. J. Med.* **353**, 1711-1723 (2005).
17. Metselaar,J.M., Wauben,M.H., Wagenaar-Hilbers,J.P., Boerman,O.C., & Storm,G. Complete remission of experimental arthritis by joint targeting of glucocorticoids with long-circulating liposomes. *Arthritis Rheum.* **48**, 2059-2066 (2003).
18. Pires,N.M. *et al.* Histopathologic alterations following local delivery of dexamethasone to inhibit restenosis in murine arteries. *Cardiovasc. Res.* **68**, 415-424 (2005).
19. Schepers,A. *et al.* Short-term dexamethasone treatment inhibits vein graft thickening in hypercholesterolemic ApoE3Leiden transgenic mice. *J. Vasc. Surg.* **43**, 809-815 (2006).
20. Villa,A.E. *et al.* Local delivery of dexamethasone for prevention of neointimal proliferation in a rat model of balloon angioplasty. *J. Clin. Invest* **93**, 1243-1249 (1994).

21. Manning,E. *et al.* A new arteriovenous fistula model to study the development of neointimal hyperplasia. *J. Vasc. Res.* **49**, 123-131 (2012).
22. Hofkens,W., Schelbergen,R., Storm,G., van den Berg,W.B., & van Lent,P.L. Liposomal targeting of prednisolone phosphate to synovial lining macrophages during experimental arthritis inhibits M1 activation but does not favor M2 differentiation. *PLoS. One.* **8**, e54016 (2013).
23. Wang,M., Kim,S.H., Monticone,R.E., & Lakatta,E.G. Matrix metalloproteinases promote arterial remodeling in aging, hypertension, and atherosclerosis. *Hypertension* **65**, 698-703 (2015).
24. Galis,Z.S. & Khatri,J.J. Matrix metalloproteinases in vascular remodeling and atherogenesis: the good, the bad, and the ugly. *Circ. Res.* **90**, 251-262 (2002).
25. Sierevogel,M.J. *et al.* Oral matrix metalloproteinase inhibition and arterial remodeling after balloon dilation: an intravascular ultrasound study in the pig. *Circulation* **103**, 302-307 (2001).
26. Meijer,C.A. *et al.* Doxycycline for stabilization of abdominal aortic aneurysms: a randomized trial. *Ann. Intern. Med.* **159**, 815-823 (2013).
27. Nieves Torres,E.C. *et al.* Adventitial delivery of lentivirus-shRNA-ADAMTS-1 reduces venous stenosis formation in arteriovenous fistula. *PLoS. One.* **9**, e94510 (2014).
28. Reil,T.D., Sarkar,R., Kashyap,V.S., Sarkar,M., & Gelabert,H.A. Dexamethasone suppresses vascular smooth muscle cell proliferation. *J. Surg. Res.* **85**, 109-114 (1999).
29. Roy-Chaudhury,P., Spergel,L.M., Besarab,A., Asif,A., & Ravani,P. Biology of arteriovenous fistula failure. *J. Nephrol.* **20**, 150-163 (2007).
30. Asif,A., Roy-Chaudhury,P., & Beathard,G.A. Early arteriovenous fistula failure: a logical proposal for when and how to intervene. *Clin. J. Am. Soc. Nephrol.* **1**, 332-339 (2006).
31. van den Hoven,J.M. *et al.* Optimizing the therapeutic index of liposomal glucocorticoids in experimental arthritis. *Int. J. Pharm.* **416**, 471-477 (2011).

Supplementary data

METHODS

Liposomal prednisolone preparation

Prednisolone phosphate polyethylene glycol-coated (PEG)-liposomes were prepared by injecting 1 mL of an alcoholic lipid solution of 1 Molar (containing dipalmitoyl phosphatidyl choline and dipalmitoyl phosphatidyl glycerol, both from Lipoid GmbH, Germany, and cholesterol (Sigma Aldrich, saint Louis, MO, USA)) in a molar percentage of 62%, 5%, and 33% of total lipid content, respectively), in 9 mL of an aqueous solution of 100 mg/ml prednisolone phosphate disodium salt (Fagron, Capelle aan den IJssel,The Netherlands). Subsequently the 10 ml crude liposome dispersion was sized by multiple extrusion at 60 degrees C using a medium pressure extruder (Lipex) equipped with two stacked polycarbonate membrane filters with 100 nm pores. Alcohol and free prednisolone phosphate (not incorporated in liposomes) were removed by ultrafiltration and replacement of the filtrate with clean phosphate buffered 0.9% saline (pH 7.4). The resulting formulation consisted of liposomes of approximately 105 nm in diameter as measured by dynamic light scattering, with a polydispersity index of 0.05 and a zeta-potential of approximately -30 mV. Content determination was done by extraction using the organic phase for lipid determination (HPLC followed by evaporative light scattering detection) and the aqueous phase to assess the prednisolone phosphate content (UV spectrophotometry at 254 nm). The liposomes contained approximately 2 mg prednisolone phosphate/mL and 70 μmol total lipid/ml. "Empty" liposomes (L-PBS) were prepared in the same manner using phosphate buffered saline instead of the aqueous prednisolone phosphate solution.

The liposomes were labeled with Alexa 750 by first mixing PEG(2000)-DSPE-NH2 and PEG(2000)-DSPE (Avanti Polar Lipids, Birmingham, AL, USA) in a 1:1 molar ratio in 0.1 M sodium bicarbonate solution at pH 8.3. This mixture was then heated at 60°C and Alexa 750 succinimidyl (Invitrogen, Carlsbad, CA, USA) was added, which led to coupling of Alexa 750 to the NH2-PEGylated lipid. This mixture was subsequently added to the liposomes and mixed under repeated temperature cycling between 60°C and room temperature, allowing the PEGylated and Alexa-conjugated lipid to insert in the liposome bilayer. In order to trace the liposomes at a microscopic level, gold-containing PEG-liposomes were prepared by adding to the PEG-liposome lipid mixture described above 0.1mol% dipalmitoyl phosphatidyl ethanolamine coupled to 1.4 nm gold particles (Nanoprobes, Yaphank NY, USA). After formation of the crude liposome dispersion multiple extrusion was performed using the same method as with prednisolone phosphate PEG-liposomes and identical size characteristics were obtained (103 nm, polydispersity index 0.08). The final formulation contained 10 μmol lipid/ml.

Surgical procedure

The animal was anesthetized using isoflurane followed by shaving and disinfection of the skin in the ventral neck area and fixed in a supine position on a heating blanket. The mouse was then injected with buprenorphin (0.1 mg/kg) (MSD, Whitehouse Station, NJ, USA) and 0.5 mL saline. Under a dissecting microscope (Leica, Wetzlar,

Germany), an incision in the ventral midline of the neck area was made, followed by a dissection of the right dorsomedial branch of the external jugular vein and ipsilateral common carotid artery after the excision of the sternocleidomastoid muscle using a heat cauterizer. Next, after applying a vascular clamp (S&T, Neuhausen, Switzerland) on the proximal and distal artery an approximate 1 mm incision was made using a microscissor (Fine Science Tools, Heidelberg, Germany) and the lumen was rinsed with a heparin solution (100 IU/ml) (LEO Pharma, Ballerup, LLDenmark). The vein was then clamped proximally and ligated distally, followed by a transection just proximal to the ligation. After rinsing the vein with a heparin solution, an end-to-side anastomosis was created using 10.0 interrupted sutures (BBraun, Melsungen, Germany). Halfway during the suturing procedure, heparin (0.2 IU/gram bodyweight) together with 200 µL of either L-Pred (10 mg/kg bodyweight), Pred (10 mg/kg bodyweight), L-PBS or PBS was injected intravenously. After completion of the anastomosis, the remaining clamps were removed and patency was assessed. The skin was closed with a 6.0 running suture (BBraun, Melsungen, Germany). Following completion of the surgery 0.5 mL of saline was injected subcutaneously and the mice were kept warm until recovery.

Sacrification and tissue harvesting

Upon sacrifice, mice received an intraperitoneal injection with an anesthetic-mixture containing midazolam (5 mg/kg) (Roche, Basel, Switzerland), medetomidine (0.5 mg/kg) (Orion, Espoo, Finland) and fentanyl (0.05 mg/kg) (Janssen, High Wycombe, UK) whereupon a reincision was made over the scar. The AVF was dissected and assessed using NIRF as described above. After a thoracotomy, the inferior vena cava was transsected followed by a mild pressure perfusion fixation with 4% formalin through an intracardiac perfusion.

Immunohistochemistry and Immunofluorescence

For immunohistochemical stainings, deparaffinization and hydration was followed by a treatment with 1% hydrogen peroxide and 5% bovine serum albumin in order to block the endogenous peroxidase and aspecific binding sites respectively. To unmask the antigens and epitopes antigen retrieval with Citrate Buffer (pH6) at 95-100 °C for 1 hour was done for CD-3, CD-206 and F4/80 antibodies. After 15 min blocking with 3% BSA (Sigma-Aldrich, , St. Louis, MO, USA) in PBS sections were incubated overnight at room temperature with specific antibodies to goat anti-mouse F4/80 (Abcam, Cambridge, UK), rabbit anti-mouse CD-206 (Abcam, Cambridge, UK), rabbit anti-mouse CD-3 (Abcam, Cambridge, UK) and goat anti-mouse GR-1 (from G. Kraal, VUMC, Amsterdam, The Netherlands). Control sections were incubated with rabbit IgG at 1:200 or 1:1000 dilution for CD-3 or CD-206 respectively or goat IgG at 1:100 or 1:300 dilution for F4/80 or GR-1 respectively. On the next day sections were briefly rinsed in 1% BSA (Sigma-aldrich) in PBS and incubated for 1 hour at room temperature with appropriate secondary antibodies that were goat anti-rabbit IgG labeled with Alexa-488 or goat anti-rat IgG labelled with Alexa-568 (Molecular Probes) for F4/80, CD-206 double immunofluorescence staining or horseradish peroxidase conjugated (Jackson ImmunoResearc bh,Westgrove, PA) goat anti-rat IgG at 1:200 dilution or peroxidase-based EnVision kit (DAKO, Glostrup, Denmark) for GR-1

or CD-3 respectively. For horseradish peroxidase-based stainings (CD-3 and GR-1) immunoreactive tissue was then developed by using a 3.3′-diaminobenzidine peroxidase substrate kit (Dako) and counterstained with hematoxylin. For immunofluorescence F4/80+/CD-206+ double staining sections were coverslipped with ProLong® Gold Antifade with DAPI (Life technologies, California, US) to counterstain nuclei. All slides were further digitized by an automated microscopic scanner (Panoramic digital MIDI slice scanner, 3DHISTECH, Hungary). All histologic evaluations were performed in a blinded manner on the first three venous sections upstream from anastomotic area. Venous part was chosen because most of the stenotic lesions in human AVFs occur in the venous outflow tract. For CD-3 and GR-1 immunohistochemistry the total number of positive cells per section was counted. F4/80 single or CD-206 double positive immunofluorescence staining were quantified as total number of positive cells per field of view in x400 magnification.

Table 1. Primers used for *in vitro* experiments

Gene	Forward primer	Reversed primer
IL-6	CTGCAAGAGACTTCCATCCAG	AGTGGTATAGACAGGTCTGTTGG
TNF	CCCTCACACTCAGATCATCTTCT	GCTACGACGTGGGCTACAG
IL-10	GCTGGACAACATACTGCTAACC	CCCAAGTAACCCTTAAAGTCCTG
MCP-1	GCACCAGCCAACTCTCAC	CTTCTTGGGGTCAGCACAG
MMP2	CCGAGGACTATGACCGGGATA	GGGCACCTTCTGAATTTCCA
MMP9	CTGGCGTGTGAGTTTCCAAAAT	TGCACGGTTGAAGCAAAGAA
TIMP1	ACACCCCAGTCATGGAAAGC	CTTAGGCGGCCCGTGAT
TIMP2	GTTTATCTACACGGCCCCCTCTT	ATCTTGCCATCTCCTTCTGCCTT
GAPDH	ACTCCCACTCTTCCACCTTC	CACCACCCTGTTGCTGTAG

SUPPLEMENTAL VIDEOS

Video 1-4. *In vivo* NIRF imaging of the AVF at day 0 and day 14 in mice treated with intravenously administered PBS or Alexa-750 labeled L-Pred. The red color overlay corresponds to the intravenously administered methylene blue visualized on the 700 nm channel. Green color overlay corresponds to the intravenously administered liposomes that are labeled with the Alexa-750 fluorochrome visualized on the 800 nm channel. The animal was oriented in such a fashion that the top of the screen resembles the cranioventral side.

Video 1. *In vivo* NIRF imaging of the AVF directly after creation (day 0) in an animal that was injected with PBS. Using methylene blue, we confirmed the patency of the AVF.

Video 2. *In vivo* NIRF imaging of the AVF directly after creation (day 0) in an animal that was injected with L-Pred. Intravascular circulating liposomes was confirmed together with AVF patency.

Video 3. *In vivo* NIRF imaging of the AVF at time of sacrification in an animal that was injected intravenously with PBS at day 0, 2, 5 and 10. The neck was dissected bilaterally in order to expose the contralateral side. Suture threads were placed around the venous outflow tract, proximal and distal common carotid artery of the AVF and around the contralateral branch of the external jugular vein. AVF patency was confirmed after administration of intravascular methylene blue.

Video 4. *In vivo* NIRF imaging of the AVF at time of sacrification in an animal that was injected intravenously with L-Pred at day 0, 2, 5 and 10. Suture threads were placed around the venous outflow tract, proximal and distal common carotid artery of the AVF and around the contralateral branch of the external jugular vein. At day 14, liposomal extravasation was observed around the anastomosis of the AVF and in the wound edges. No circulating liposomes were observed.

Chapter 4

Relaxin receptor deficiency promotes vascular inflammation and impairs outward remodeling in arteriovenous fistulas

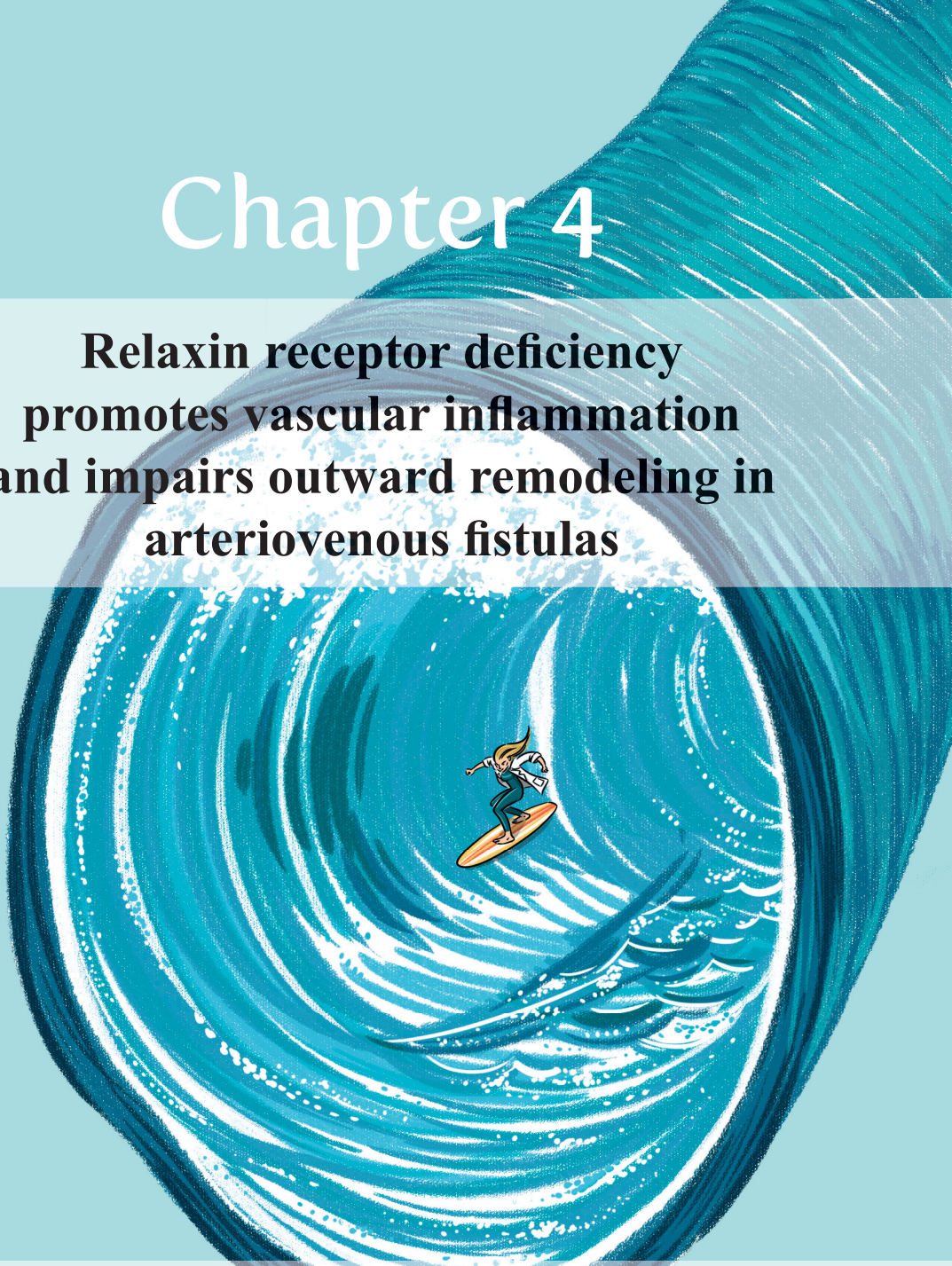

Taisiya Bezhaeva, Margreet R. de Vries, Wouter J. Geelhoed, Eric P. van der Veer, Sabine Versteeg Carla M.A. van Alem, Bram M. Voorzaat, Niels Eijkelkamp, Koen E. van der Bogt, Alexander I. Agoulnik, Anton Jan van Zonneveld, Paul H.A.Quax and Joris I. Rotmans

FASEB. 2018 Nov Vol.32

Abstract

The pathophysiology of arteriovenous fistula (AVF) maturation failure is incompletely understood but impaired outward remodeling and intimal hyperplasia are considered to contribute. This adverse vascular response upon AVF surgery results from an interplay between vascular smooth muscle cells (VSMCs), extracellular matrix (ECM) and inflammatory cells. Relaxin (RLN) is a hormone exhibiting its action on the vasculature via interaction with its receptor (RXFP1), resulting in vasodilatation, ECM remodeling and decreased inflammation. In the present study, we evaluated the consequences of RXFP1 knockout (*Rxfp1*$^{-/-}$) on AVF maturation in a murine model of AVF failure. At 14 days after AVF surgery, *Rxfp1*$^{-/-}$ mice showed a 22% decrease in vessel size at the venous outflow tract. Furthermore, a 43% increase in elastin content was observed in the lesions of *Rxfp1*$^{-/-}$ mice which coincided with a 41% reduction in elastase activity. In addition, *Rxfp1*$^{-/-}$ mice displayed a 6-fold increase in CD45^{+} leukocytes, along with a 2-fold increase in MCP1 levels, when compared to WT mice. *In vitro*, VSMCs from *Rxfp1*$^{-/-}$ mice exhibited a synthetic phenotype, as illustrated by augmentation of collagen, fibronectin, TGFβ and PDGF mRNA. In addition, VSMCs derived from *Rxfp1*$^{-/-}$ mice showed a 5-fold increase in cell migration. Finally, RXFP1 and RLN expression levels were increased in human AVFs, as compared to unoperated cephalic veins. In conclusion, RXFP1 deficiency hampers elastin degradation and results in induced vascular inflammation after AVF surgery. These processes impair outward remodeling in murine AVF, suggesting that the relaxin-axis could be a potential therapeutic target to promote AVF maturation.

Introduction

A proper functioning vascular access site is a lifeline for a lifetime for patients required hemodialysis. While an arteriovenous fistula (AVF) remains the vascular access of choice, the frequency of primary AVF failure is approximately 40%[1]. Moreover, the primary patency rates at 1 year after creation do not exceed 60%[2], making vascular access related complications one of the most common causes of hospitalization and morbidity in hemodialysis patients.

While the pathophysiology of arteriovenous fistula maturation failure is incompletely understood, it is well established that both intimal hyperplasia (IH) and outward remodeling (OR) of the arteriovenous conduit ultimately determine luminal dimensions, fistula flow and patency[3]. Several studies have shown that vascular adaptation of the arteriovenous conduit is characterized by an inflammatory response that coincides with flow-mediated remodeling of the extracellular matrix (ECM) and proliferation and migration of vascular smooth muscle cells (VSMCs)[4-11].

Relaxin (RLN) is a 6-kDa peptide hormone, originally known for its role in the growth and differentiation of the reproductive tract, and systemic hemodynamic adaptations during pregnancy, in particular vasodilatation[12-15]. Three relaxin genes, namely relaxin-1, -2, and -3 (*RLN1*, *2* and *3*) exist in humans, whereas rats and mice have two (*Rln1* and *3*), with *Rln1* in rats and mice corresponding to human RLN2 and representing the major source of circulating relaxin[16]. In the last 20 years, relaxin has emerged as a pleotropic hormone that serves critical functions irrespective of gender. The systemic effects mediated by RLN2 on arterial mechanical properties include increasing arterial compliance, reducing systemic vascular resistance, and myogenic reactivity as demonstrated in rats and mice[12,17-20].
Furthermore, administration of recombinant RLN2 ameliorates renal and cardiac fibrosis, stimulates ECM turnover, and moderates inflammation by reducing inflammatory cytokines[21-27].

In the context of AVF maturation, it is important to emphasize that RLN2 is expressed in the vessel wall[28,29] and that the observed vascular effects of RLN2 are mediated though an interaction with RXFP1 (relaxin/insulin-like peptide family receptor 1, original abbreviation LGR7), a G-protein-coupled receptor. RXFP1 is primarily expressed on VSMCs and to a lesser extent on the cell surface of macrophages and endothelial cells of arteries and veins[30-32].

In view of the emerging role of the RLN2-RXFP1 axis in vascular remodeling and inflammation, we examined the consequences of disturbing this hormone-receptor balance in AVF maturation. For this purpose, we used the well-established murine AVF model in which we studied the effect of RXFP1 deficiency on fistula remodeling. Furthermore, we determined the effects of RXFP1 deficiency on the phenotype and function of VSMCs *in vitro.*

Material and Methods

Animals

Murine model of AVF failure

This study was performed in agreement with Dutch government guidelines and the Directive 2010/63/EU of the European Parliament. All animal experiments were approved by the Institutional Committee for Animal Welfare of Leiden University Medical Center and University Medical Center Utrecht. The phenotype of *Rxfp1*$^{-/-}$ mice was described previously[33]. Male wild type (WT, C57BL/6, n=10) and *Rxfp1*$^{-/-}$ mice (C57BL/6 background, n=10), were bred in the animal facility at the University Medical Center Utrecht. All animals were given water and chow ad libitum. Adult male mice aged 10-13 weeks were used for the experiments. AVF were created in an end-to-side manner between the dorsomedial branch of the external jugular vein and the common carotid artery as previously described[5,34]. In short, the animal was anesthetized using isoflurane followed by shaving and disinfection of the skin in the ventral neck area and fixed in a supine position on a heating blanket. The mouse was then injected with buprenorphin (0.1 mg/kg) (MSD, USA) and 0.5 mL saline. Under a dissecting microscope (Leica, Germany), an incision in the ventral midline of the neck area was made, followed by a dissection of the right dorsomedial branch of the external jugular vein and ipsilateral common carotid artery after the excision of the sternocleidomastoid muscle using a heat cauterizer. Next, after applying a vascular clamp (S&T, Switzerland) on the proximal and distal artery an approximate 1 mm incision was made using a microscissor (Fine Science Tools, Germany) and the lumen was rinsed with a heparin solution (100 IU/ml) (LEO Pharma, Denmark). The vein was then clamped proximally and ligated distally, followed by a transection just proximal to the ligation. After rinsing the vein with a heparin solution, an end-to-side anastomosis was created using 10.0 interrupted sutures (BBraun, Germany). After completion of the anastomosis, the remaining clamps were removed and patency was assessed. The skin was closed with a 6.0 running suture (BBraun, Germany). Following completion of the surgery 0.5 mL of saline was injected subcutaneously and the mice were kept warm until recovery. The animals were sacrificed 14 days following the surgical procedure.

Blood pressure

Systolic blood pressure was assessed with the non-invasive tail cuff system in conscious mice before the AVF surgery and at day 7 and 14 after an AVF was created using the CODA system (Kent Scientific, CT, USA). Animals were acclimated to the restrainer before measurements. Following the acclimation period, telemetry blood pressure measurements were acquired. Ten seconds data segments were collected throughout the duration of each noninvasive measurement session (10 acclimation cycles followed by 20 measurement cycles).

Arterial compliance

Aortas from *Rxfp1*$^{-/-}$ (n=3) and WT (n=5) mice were cannulated from the distal side at the base of the heart and proximal at the abdominal area (1 cm of length) and placed immediately in ice-cold HEPES buffered physiological saline solution. Consequently, the vessels were placed in an *ex vivo* vessel perfusion system containing 37^0C 10^{-4} M

papaverine in calcium-free HEPES buffered physiologic saline solution. The vessel segments were tensioned to a longitudinal strain of 30 g and left to acclimatize for 15 minutes. The vessel segment was then exposed to a pressurized flow in a cyclic fashion at 60 BPM ± 5 BPM, where the systolic pressure was gradually increased to 120 mmHg. Papavarin (10^{-4}M) in calcium-free HEPES buffered PBS was used as perfusate. The systolic and diastolic pressures throughout the test were recorded using a pressure sensor (700 G Precision Pressure Test Gauge, Fluke, Singapore). To measure the vessel diameter a microscope camera (Digital microscope DSCO-P03, Frederiksen Scientific, Denmark) capable of measuring with an accuracy of ± 0.02 mm was placed above the perfused vessels. Recordings of each test was calibrated to the pressure and saved. To calculate arterial compliance, the vessel diameter during the systolic and diastolic phase of the pressure cycles, were measured. The dynamic compliance is provided as % compliance per 100 mmHg.

Tissue harvesting and processing

Fourteen days after AVF surgery, the animals were anesthetized using isoflurane. The venous and arterial limb of the AVF was dissected and a thoracotomy was performed whereupon the inferior vena cava was transsected followed by a fixation with 4% formalin through an intracardiac perfusion. The tissue was embedded in paraffin and 5 µm-thick sections of the venous outflow tract were made perpendicular to the vein at 150 µm interval.

Morphometric and histological analysis

All (immuno)-histochemical stainings and measurements were performed on the first 3 venous cross-sections downstream from the area of anastomosis. Weigert's elastin staining was used for the morphometric measurements. The area of the internal elastic lamina (IEL) was measured to assess the degree of the outward remodeling (Figure 1a). Intimal hyperplasia was calculated by subtracting the luminal area from the area within the IEL. Composition of the AVF lesions was further evaluated by staining for total leukocytes (CD45, 1:200; BD- Pharmingen 550539, CA, USA), macrophages (MAC3, 1:200, BD-Pharmingen 550292, CA, USA) in a combination with CCR2 for pro-inflammatory phenotype (1:400, Abcam ab32144, Cambridge, UK) or CD206 (1:1000, Abcam ab64693, Cambridge, UK) for anti-inflammatory phenotype, neutrophils (GR1, 1:300, from G. Kraal, VUMC, The Netherlands), T-lymphocytes (CD3, 1:300, Abcam ab32144, Cambridge, UK) and MCP1 (MCP1, 1:300, Santa Cruz sc-1784, Texas, USA) vascular smooth muscle cells (SM-α-actin, 1:1000, Dako M0851, CA, USA) was stained in a combination with Ki67 (1:200, BD-Pharmigen 550609, CA, USA) to detect proliferating VSMCs.

All slides were digitized using an automated microscopic scanner (Pannoramic digital MIDI, 3DHISTECH, Budapest, Hungary). For the immunohistochemical analysis of the MAC3/CD206, MAC3/CCR2 and αSMA/Ki67 staining, the number of positive cells was counted in 3 random fields of view using a 400x magnification from which the mean was calculated. Quantification of $CD45^+$, $GR1^+$, $CD3^+$ and MCP1 staining was performed with ImageJ software by calculating % DAB positive area from the total vessel area.

Cell culture

Vascular smooth muscle cells

Primary arterial and venous vascular smooth muscle cells were isolated from murine carotid artery and vena cava of C57BL/6 and *Rxfp1*$^{-/-}$ mice (n=4 per group), respectively. Connective tissues were removed and vessels cut open. The endothelial monolayer was detached by gentle scraping using sterile surgical forceps. The carotid artery and caval vein were dissected into small pieces and plated onto fibronectin pre-coated petri dishes (0.1 mg/mL) of 100 or 60 mm diameter. After 14 days of culture with DMEM medium supplemented with 20% fetal calf serum (FCS), 2 mM L-glutamine, 100 U/ml penicillin and 100 μg/ml streptomycin, cells were trypsinized and re-plated onto 6- or 12-well plates and cultured for 7 days. At 80-90% confluence, VSMCs were trypsinized and seeded at required density for further functional assays.

Western Blotting

Proteins from tissue lysates were harvested in RIPA buffer and subjected to polyacrylamide gel electrophoresis. Protein determinations (BCA) were performed to ensure equal loading of protein on a per-sample basis. RXFP1 was detected using primary antibodies (1:500, Acris AP23446SU-S, MD, USA). GAPDH (1:5000, Cell signaling 5174S, MA, USA) was used as a loading control. All gels were run and blotted with Bio-Rad TGX pre-cast gels and blotted on nitrocellulose 0.2 μm using the Bio-Rad TurboBlot system (Bio-Rad Laboratories, CA, USA).

RNA isolation, cDNA synthesis and qPCR

Total RNA was extracted from VSMCs using Trizol reagent (Invitrogen, CA, USA) according to the manufacturer's protocol. RNA was reverse transcribed by M-MLV First-Strand Synthesis system (Invitrogen, CA, USA), and used for quantitative analysis of mouse genes (Supplementary Table 1) with an SYBR Green Master Mix (Applied Biosystems, CA, USA). Murine β-actin was used as standard housekeeping gene. The relative mRNA expression levels were determined using 2[–ΔΔC(T)] method.

VSMC migration and haptotaxis assays

Primary arterial and venous VSMCs from control and *Rxfp1*$^{-/-}$ mice were grown to confluence and made quiescent in cultured medium supplemented with 1% FCS for 24 hours. Cells were detached from the surface and suspended at a concentration of 100.000 cells/mL in culture medium supplemented with 1% FCS. Migration was assayed with inserts having 8 μm-pores in 24-well chemotaxis chambers using commercial CytoSelect Cell Migration Assay Kit. Haptotaxis was assayed by plating cells into Transwell inserts with collagen I-coated inserts (CytoSelect Cell Haptotaxis Assay, Cell Biolabs, CA, USA). After 16 hours, migratory VSMCs were lysed and labeled with fluorescent dye according to the manufacturer's instructions. 20% FCS was used as gradient. Quantification was performed by reading fluorescence at 480 nm/520 nm.

VSMC proliferation assay

Murine VSMCs, explanted from aortas and veins of control or *Rxfp1*$^{-/-}$ mice, were cultured as described above and aliquoted into a 96-well plate. All cell numbers were subsequently determined 24 hours later using the CyQuant Direct Cell Proliferation

Assay as per the manufacturer's instructions (Life Technologies, CA, USA).

Elastase activity assay
Elastase activity was measured on total tissue lysates isolated from *Rxfp1*$^{-/-}$ and WT mice (n=10 per group) using the EnzChek Assay Kit (Thermo Fisher Scientific, MA, USA) according to the manufacturer's instructions. Briefly, 10 μm sections of AVF were lysed in RIPA buffer and protein determinations (BCA) was performed to ensure equal loading of protein on a per-sample basis. DQ™ elastin , a soluble bovine neck ligament elastin labeled with BODIPY® FL dye, was used as a substrate such that the conjugate's fluorescence is quenched. In the presence of elastase, the non-fluorescent substrate is digested yielding highly fluorescent fragments which is measured with a microplate reader at ex/em = 480 ± 20 nm/528 ± 20 nm.

Collagen assay
Collagen was analyzed in formaldehyde-fixed paraffin-embedded venous tissues isolated from *Rxfp1*$^{-/-}$ and WT mice (n=10 per group) using QuickZyme Total Collagen Assay Kit (QuickZyme Biosciences, the Netherlands). In brief, five to ten 10 μm tissue sections were hydrolyzed by o/n incubation at 95°C in a heat block. Upon hydrolysis, without any pretreatment, 35 μl was used for collagen quantification using the QuickZyme total collagen assay (assay time 90 min). The assay measured the total amount of hydroxyproline present in the sample, which represents all collagen-types present in the sample. The assay results in a chromogen with an absorbance maximum at 570 nm.

Human tissue specimens
Human cephalic veins before AVF surgery (n=3) and during surgical revisions of AVF (n=3) were obtained at the Leiden University Medical Center in accordance with guidelines set out by the 'Code for Proper Secondary Use of Human Tissue' of the Dutch Federation of Biomedical Scientific Societies (Federa) and conform with the principles outlined in the Declaration of Helsinki. Specimens were formalin fixed, embedded in paraffin and sectioned. The human AVF sections were stained with SM-α-actin (1:1000, DAKO M0851, CA, USA), RLX2 (RLN2, 1:1000, Abcam ab183505, Cambridge, UK) and RXFP1 (1:4000, Acris AP23446SU-S, MD, USA).

For RXFP1 antibody validation 3 human fistula samples were incubated with the primary antibody or isotype control both at 1:4000 dilution. Human endometrium was used as a positive control. Briefly, after deparaffinization step endogenous peroxidase was suppressed by incubation in 1% H_2O_2 for 15 min at room temperature (RT). Sections were then blocked with 5% PBSA ($NaPO_4$, NaCl, NaAz and 1% bovine serum albumin) and 5% NHS (normal human serum) for 30min. Next, sections were incubated with the primary antibody or isotype control, diluted at 1:4000 in 1% PBSA buffer together with 5% NHS, overnight at RT. After rinsing 3 × 5 min in PBS, sections were then incubated with rabbit Evision (Agilent Dako, CA, USA) and 5% NHS for 30min at RT. Specific signals were detected using DAB (Sigma-Aldrich, MO, USA) as chromogen, stopping the reaction by rapidly rinsing in tap water, followed by conventional haemalaun counterstaining.

For immunofluorescent staining of double positive αSMA^{+}, RXFP1^{+} cells, after primary antibody sections were counterstained with Alexa 568 conjugated goat anti mouse IgG2a (1:250; Molecular probes A21134, MA, USA), for SM-α-actin and Alexa 488 conjugated secondary goat anti rabbit IgG (1:250; Molecular probes A11008, MA, USA) for RXFP1. Secondary antibody were diluted in 1% PBSA and 5% NHS was added to prevent nonspecific binding. Nuclei were visualized with ProLong™ Gold Antifade Mountant with DAPI (Thermo Fisher P369, MA, USA) (Supplemental Figure 6).

Statistical analysis

Results are expressed as mean±SEM and considered statistically significant for $P<0.05$. T-tests and Mann-Whitney tests for parametric and nonparametric data, respectively, were used as appropriate. All *in vitro* experiments were performed in biological n=4 in experimental triplicates.

Results

Surgical outcome and patency

In total, 23 mice were successfully operated and received an AVF (WT; n=12, *Rxfp1*$^{-/-}$; n=11), of which two (17%) from the wild-type (WT) group and one (9%) from the *Rxfp1*$^{-/-}$group were occluded 14 days after surgery. The occluded AVFs were excluded from morphometric analysis, yielding 10 animals per group. The body weight of the mice was similar in both groups (29±3 gram) and remained stable until the end of experiment.

Effect of RXFP1 deficiency on AVF maturation

To study the effect of RXFP1 deficiency on AVF maturation, we created AVFs in WT and *Rxfp1*$^{-/-}$ mice in an end-to-side fashion between the jugular vein and carotid artery as described previously[34]. Given that most of the stenotic lesions in human AVF occur in the venous outflow tract, we harvested the first three consecutive venous sections downstream of the anastomotic area for morphometric analysis. The impact of RXFP1 deficiency on vessel morphometry was evaluated by assessing both intimal and luminal area as well as the area within the internal elastic lamina (IEL), reflecting the degree of outward remodeling of the venous outflow tract (Figure 1a). The absence of the RXFP1 protein in *Rxfp1*$^{-/-}$ mice was confirmed by analyzing total tissue lysates isolated from jugular veins by Western blotting (Figure 1b). Mice deficient for RXFP1 showed a 22% decrease of the IEL area at the venous outflow tract when compared to WT mice ($P=0.002$). The luminal area of the venous outflow tract in *Rxfp1*$^{-/-}$ mice was 31% smaller when compared to control mice, although this difference was not significant ($P=0.14$). The intimal area did not differ between groups (Figure 1c). Arterial blood pressure and compliance did not significantly differ between *Rxfp1*$^{-/-}$ and WT mice (Supplemental Figure 1).

In terms of ECM remodeling, we observed a 43% increase in elastin content in *Rxfp1*$^{-/-}$ mice as compared to WT mice ($P=0.04$) (Figure 1d), while collagen production was similar between the groups (Supplemental Figure 2). In both WT and *Rxfp1*$^{-/-}$ mice, the majority of intimal cells expressed SM-α-actin, indicating that these cells are primarily of VSMC or fibroblastic origin (Figure 1e).

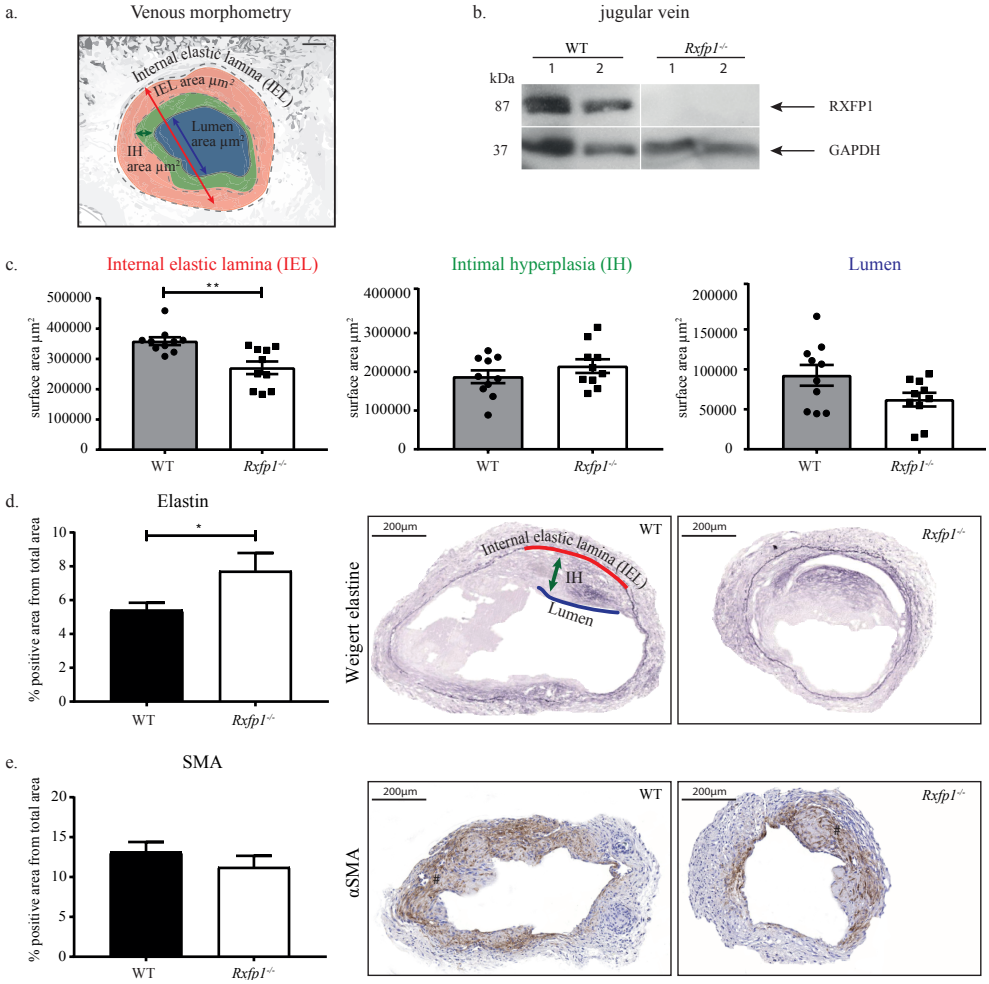

Figure 1. Morphometry and histology of the venous outflow tract of the AVF in *Rxfp1*$^{-/-}$ and WT mice 14 days after surgery.

(a) The area within the internal elastic lamina (IEL) (red), reflects the degree of outward remodeling of the venous outflow tract. Intimal hyperplasia (green) was calculated by subtracting the luminal area (blue) from the area within the IEL. (b) Western blotting of the jugular vein confirms the absence of RXFP1 protein in RXFP1 deficient mice, GAPDH was used as a loading control. (c) Quantification of histomorphometry. RXFP1 deficient mice displayed decrease in the area of IEL (22%, P=0.002) and lumen (31%, P=0.14), whereas intimal hyperplasia was comparable to WT mice. (d) Increase in elastin deposition in the AVF lesions from *Rxfp1*$^{-/-}$ mice. (e) SM-α-actin (αSMA) staining shows area of intimal hyperplasia which did not differ between the groups. Weigert elastine staining was used to determine histomorphometrical parameters of the vessel. (#) intimal hyperplasia; (*) P<0.05; (**)P<0.005 n=10 per group.

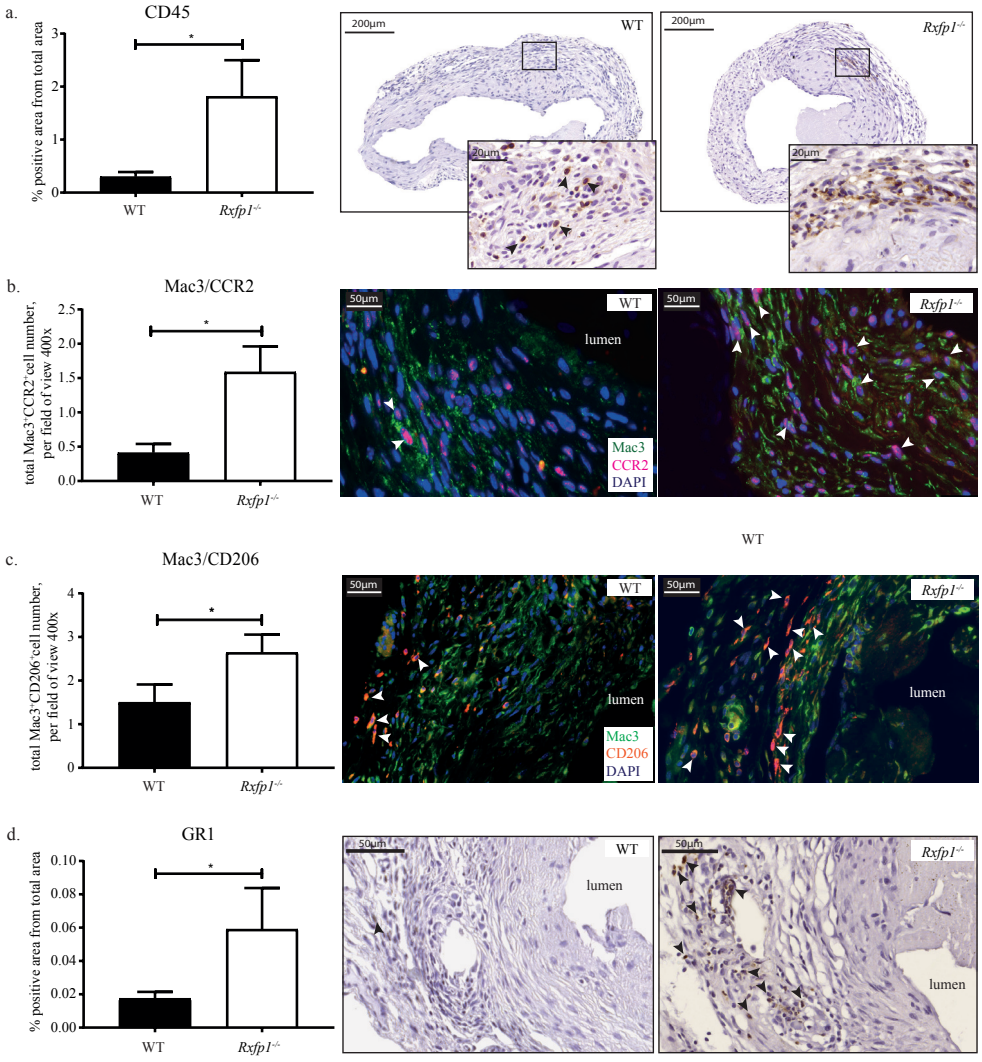

Figure 2. Effects of RXFP1 deficiency on inflammatory status *in vivo*.
Quantification and immunohistochemical staining of (a) CD45⁺ leukocytes (black arrows); (b) MAC3⁺/CCR2⁺ macrophages, (c) MAC3⁺/CD206⁺ macrophages (white arrows), and (d) GR1⁺ neutrophils (black arrows) in the AVF lesions 14 days after surgery. All cell populations were increased in the lesions from *Rxfp1*$^{-/-}$ mice as compared to WT. (*) P<0.05; n=10 per group.

RXFP1 deficiency resulted in increased inflammation of AVF lesions

Immunohistochemical analysis of sections obtained from the venous outflow tract showed a 6-fold increase in the amount of CD45⁺ leukocytes in lesions of *Rxfp1*$^{-/-}$ mice as compared to WT mice (P=0.02) (Figure 2a). As shown in Figure 2b-c, further characterization of the leukocyte subpopulations revealed a 4-fold increase in the number of pro-inflammatory Mac3⁺/CCR2⁺ macrophages (P=0.02) and a 43% increase

in the Mac3^{+}/CD206^{+} anti-inflammatory macrophages in the lesions from *Rxfp1*$^{-/-}$ mice (P=0.04). The number of GR1^{+} neutrophils was 3-fold higher in *Rxfp1*$^{-/-}$ mice as compared to WT mice (P=0.05) (Figure 2d). The number of CD3^{+} T-lymphocytes in the venous outflow tract was not affected by RXFP1 deficiency (Supplemental Figure 3). At the level of cytokine production within the lesions, a 2-fold increase of MCP1 expression was observed in *Rxfp1*$^{-/-}$ mice as compared to WT mice (P=0.01) (Figure 3). *In vitro*, activated macrophages differentiated from monocytes derived from *Rxfp1*$^{-/-}$ mice produced similar amounts of cytokines as compared to WT mice, as ELISA analysis demonstrated comparable expression of MCP1, IL12 and IL10 proteins (data not shown).

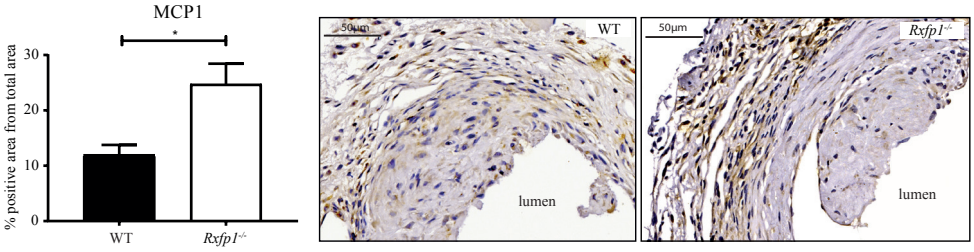

Figure 3. Accumulation of MCP1 in the AVF lesions from *Rxfp1*$^{-/-}$ and WT mice 14 days after surgery.
RXFP1 deficiency resulted in increased MCP1 expression (brown DAB signal) as compared to WT mice. (*) P<0.05; n=10 per group.

Phenotypic switch of arterial and venous VSMCs upon RXFP1 deletion

The impact of RXFP1 deficiency on VSMCs phenotype was studied *in vitro* using primary arterial and venous VSMCs, isolated from the aorta and caval vein of *Rxfp1*$^{-/-}$ or WT mice. Phenotypic difference of arterial and venous VSMCs was confirmed by mRNA levels of ephrin B2, an established embryological marker of arterial origin[35]. EphrinB2 was increased in arterial VSMCs from both WT and *Rxfp1*$^{-/-}$ mice following two weeks of culture as compared to venous VSMCs (Figure 4a). Further characterization of these VSMCs confirmed that the cells maintained a highly differentiated state, as evidenced by the maintenance of myosin heavy chain (MHC), calponin and caldesmon expression at two weeks of culture (Figure 4b).

As vascular injury and remodeling trigger the phenotypic switch of VSMCs from a contractile toward a synthetic state, mRNA expression levels of several genes associated with this switch were measured[36,37]. Arterial VSMCs from *Rxfp1*$^{-/-}$ mice expressed markedly higher levels of the synthetic VSMC markers type I collagen[38] and fibronectin[39] as compared to VSMCs derived from WT mice (5-fold, P=0.03; 10-fold, P=0.04; respectively). Similarly, type I collagen and fibronectin mRNA expression was augmented in venous VSMCs harvested from *Rxfp1*$^{-/-}$ mice (3-fold; P=0.05, and 4-fold; P=0.04, respectively). Furthermore, genes linked with cellular proliferation, such as transforming growth factor beta (TGFβ1)[40] and platelet derived growth factor (PDGF)[41], displayed on average 3-fold higher expression levels in both arterial and venous VSMCs isolated from *Rxfp1*$^{-/-}$ mice as compared to WT mice (Figure 4c).

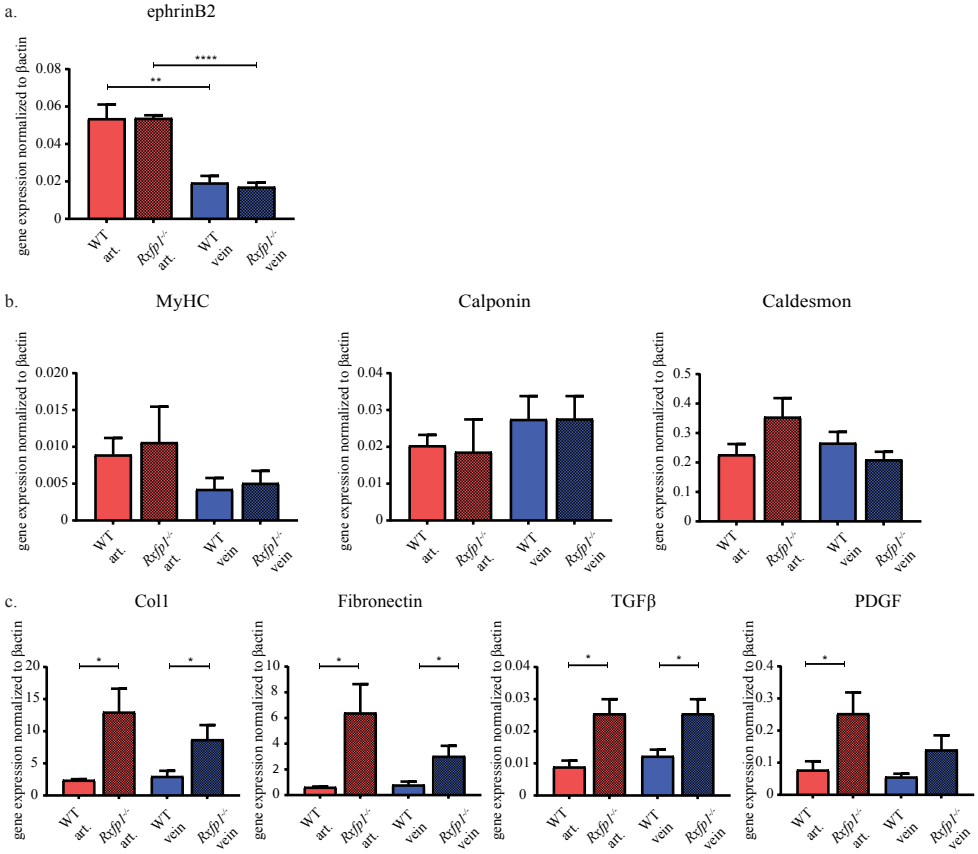

Figure 4. ***In vitro*** **phenotypic difference between primary arterial and venous VSMCs isolated from** ***Rxfp1*** $^{-/-}$ **and WT mice.**

(a) Stable increase in ephrinB2 gene expression was detected in arterial VSMCs isolated from WT and *Rxfp1* $^{-/-}$ mice. (b) Both arterial and venous VSMCs isolated from *Rxfp1* $^{-/-}$ and WT displayed characteristics of mature VSMCs as confirmed by a stable expression of myosin heavy chain (MYHC), calponin and caldesmon genes. (c) RXFP1 deficiency resulted in a switch of arterial and venous VSMCs towards synthetic phenotype as confirmed by increased collagen I (Col1), fibronectine, TGFβ and PDGF mRNA expression levels. VSMCs were maintained in culture for14 days. (*) P<0.05; (**) P<0.005; (****) P<0.0001; n=4.

To further examine whether relaxin deficiency impacts VSMC function, we performed cellular migration assays. These studies revealed that arterial VSMCs derived from *Rxfp1* $^{-/-}$ display a significantly higher migratory capacity relative to VSMCs derived from WT mice, while migration of venous VSMCs was unaltered (Figure 5a). To mimic VSMC migration within the ECM of a blood vessel, a haptotaxis assay was performed in which cellular migration was evaluated in a matrix of type I collagen. As shown in Figure 5b, we observed enhanced migration of arterial and venous VSMCs derived from *Rxfp1* $^{-/-}$ mice as compared to WT (5-fold, P=0.05; 5-fold; P=0.03; respectively). In contrast, cellular proliferation was not affected by relaxin deficiency in either arterial or venous VSMCs (Figure 5c). *In vivo*, the number of proliferating cells in the venous outflow tract of AVF did not differ significantly between groups (Supplemental Figure 4).

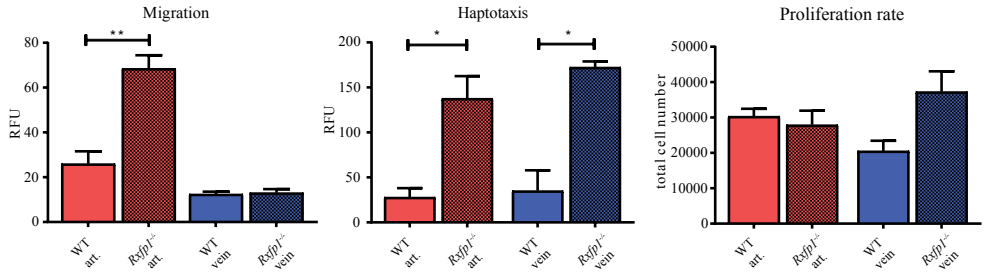

Figure 5. Effect of RXFP1 deficiency on VSMCs function *in vitro*.
(a) Increase in migration of VSMCs isolated from *Rxfp1*$^{-/-}$ mice was restricted to arterial cells only, whereas (b) cellular haptotaxis or migration through the layer of collagen was increased on both arterial and venous cells isolated from *Rxfp1*$^{-/-}$ mice. (c) Proliferation rate did not differ between *Rxfp1*$^{-/-}$ and WT mice. Cells were cultured for 14 days. Migration, haptotaxis and proliferation were measured over 16h time period. (*) P<0.05; (**) P<0.005; n=4.

Elastin metabolism in AVF lesions of RXFP1 deficient mice

Having observed higher elastin content in the venous outflow tract of AVF in *Rxfp1*$^{-/-}$ mice, we next assessed elastase activity in sections obtained from the venous outflow tract of the AVF. We employed the EnzChek assay, which measures fluorescence of the substrate (bovine elastin) digested by elastase. Elastase activity in AVFs from *Rxfp1*$^{-/-}$ mice was significantly reduced as compared to AVFs derived from WT mice (P=0.0001) (Figure 6).

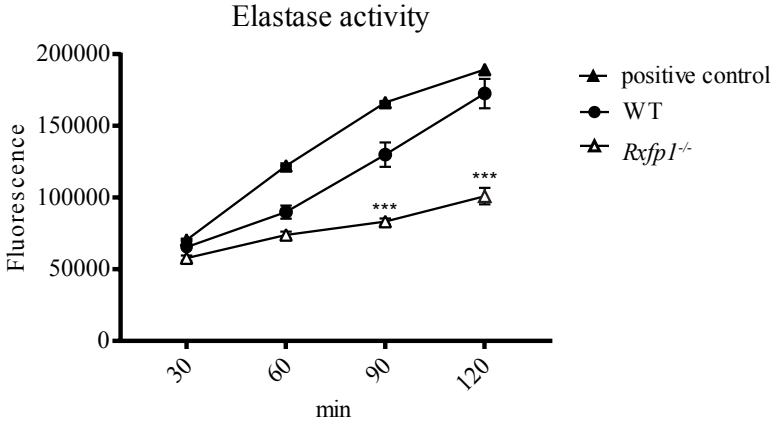

Figure 6. Kinetics of the elastase activity in the lesions of *Rxfp1*$^{-/-}$ and WT mice 14 days after surgery.
AVF tissue lysates from WT and *Rxfp1*$^{-/-}$ mice were incubated with DQ elastin at final concentrations of 25 µg/mL for the indicated time periods. Elastase activity in AVFs from *Rxfp1*$^{-/-}$ mice (empty triangles) was significantly reduced after 90 and 120 min incubation time as compared to AVFs derived from WT mice (full circles). Fluorescence was measured in a fluorescence multi-well plate reader set for excitation at 485 ± 10 nm and emission detection at 530 ± 15 nm. Porcine pancreatic elastase 0.2 U/mL was used as positive control (full triangles). Background fluorescence, determined for a no-enzyme control reaction, has been subtracted from each value. (***) P=0.0002; n=10 per group.

Ex vivo, elastin synthesis in cultured arterial and venous VSMCs isolated from *Rxfp1*$^{-/-}$ or WT mice did not differ, as mRNA expression levels of tropoelastin were similar between the groups (Supplemental Figure 5).

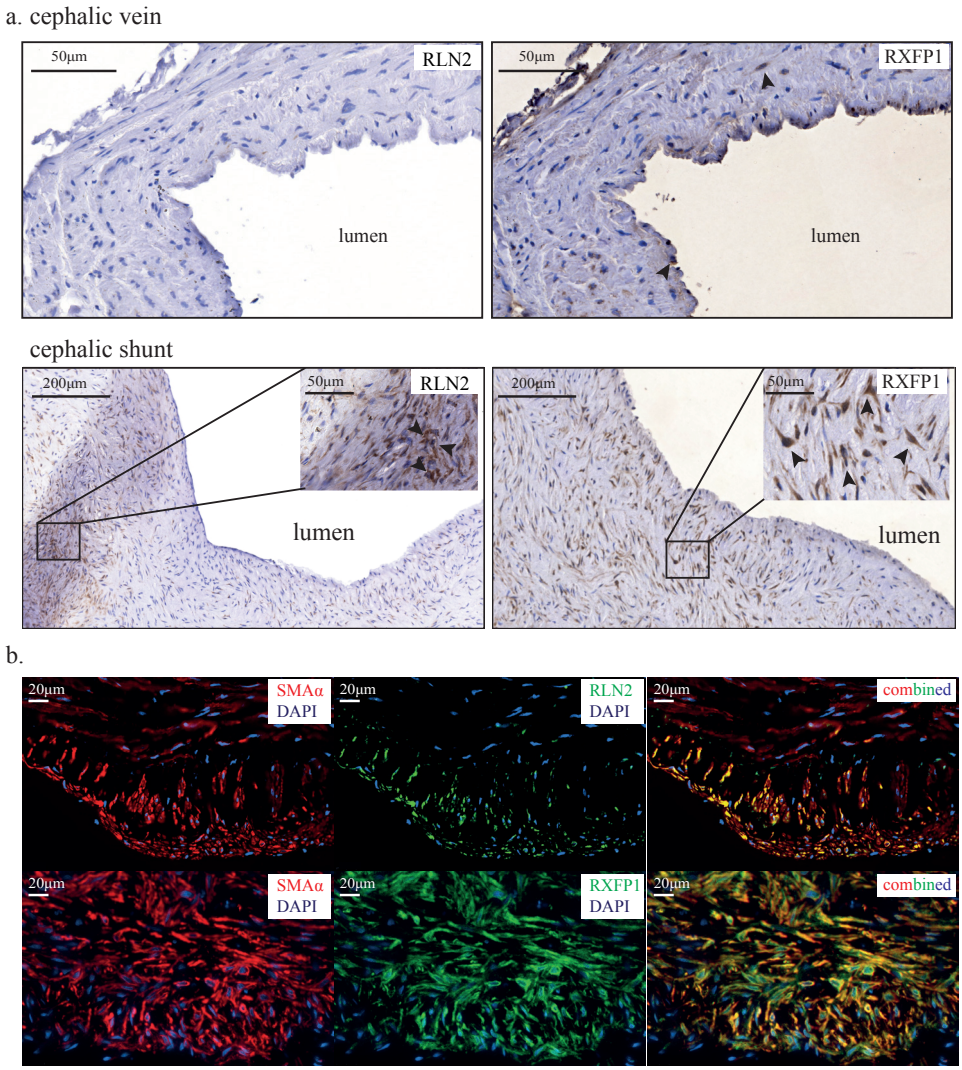

Figure 7. Expression of RLN2 and RXFP1 proteins by αSMA⁺ cells in dialysis patients.
(a) Representative images of RLN2 and RXFP1 proteins (black arrows) in human cephalic veins prior to AVF surgery and cephalic venous outflow tract from AVF. (b) Cells positive for RLN2 and RXFP1 (green color) were mainly located in the intimal region and were co-expressing SM-α-actin (αSMA, red color); n=3.

In humans RXFP1 expression increases during AVF maturation

To explore the relevance of our observations for dialysis patients, we examined three specimens of cephalic vein before AVF surgery and during surgical revisions of AVF. Immunohistochemical analysis revealed increased RLN2 and RXFP1 expression in the cephalic outflow tract of AVF, when compared to segments of cephalic veins from patients with end-stage renal failure during primary AVF surgery (Figure 7a). Cells that expressed RLN2 and RXFP1 were enriched in the intimal region of the outflow tract, and were found to co-express SM-α-actin (Figure 7b). These results strongly suggest that RLN2 and RXFP1 expression is elevated in the venous outflow tract of human AVFs, which underscores the relevance of these proteins in the process of AVF maturation in humans.

Discussion

Here, we show that RXFP1 deficiency substantially impairs outward remodeling in a murine model of AVF, while no effect on intimal hyperplasia is observed. Our findings pinpoint an increase in elastin content in the venous outflow tract in RXFP1 deficient mice linked with attenuated elastase activity as potentially being responsible for this phenotype. As such, impaired elastin degradation, in combination with enhanced vascular inflammation upon AVF surgery, likely triggers adverse vascular response in humans following the placement of an AVF.

Impaired elastin degradation and vascular remodeling in RXFP1 deficient mice

Expansion of the venous lumen and an initial vasodilatory response are prerequisites for successful AVF maturation and patency. Particularly, the process of outward remodeling plays a pivotal role in this process. While past research focused mainly on the development of strategies that aimed to reduce intimal hyperplasia, current view on AVF maturation underscores the link between impaired outward remodeling and AVF failure[42,43]. To promote outward remodeling, matrix metalloproteinases (MMPs) expression must be augmented to degrade and restructure the vascular matrix[44], of which elastic fibers are a major component. Interestingly, peri-adventitial application of recombinant elastase has been shown to stimulate outward remodeling in a rabbit-model of AVF[45]. Interestingly, this concept of pharmacological elastin degradation to promote AVF maturation is now being evaluated in phase III clinical trials[46].

Enhanced expression of relaxin is critical for ECM remodeling in the cervix and myometrium during pregnancy[47,48]. Administration of recombinant relaxin increases the activity of elastase in human myometrial cells[26]. Our discovery that RXFP1 deficiency significantly reduced elastase activity, resulting in elastic fiber accumulation in AVF lesions suggests that RXFP1 is an important regulator of elastin degradation during AVF maturation. Furthermore, it supports the concept that venous outward remodeling requires relaxin axis-mediated augmentation of elastase activity.

RXFP1 deficiency enhances vascular inflammation upon AVF surgery

Successful AVF maturation is severely hampered by excessive inflammation post-surgery. Numerous animal studies have shown that drivers of inflammatory responses, such as heme oxygenase-1 and -2 (HO-1 and HO-2) and MCP1, are linked to AVF failure[49-51]. Within the AVF, MCP1 has been found to enhance monocyte recruitment and macrophage differentiation, activate endothelial cells and stimulate VSMC proliferation[51]. In one of our previous studies, local administration of liposomal prednisolone resulted in a reduction of the inflammatory response that resulted in a sharp increase in venous outward remodeling in a murine-model of AVF[4]. Interestingly, relaxin-relaxin receptor interactions are known to mitigate vascular inflammation, by inhibiting the upregulation of pro-inflammatory cytokines[27]. In keeping with these findings, we here found that RXFP1 deficiency augments vascular inflammation in AVFs, as illustrated by a significant increase in macrophage and neutrophil numbers, as well as accumulation of MCP1 in the venous outflow tract.

Phenotypic switch of VSMCs from RXFP1$^{-/-}$ in vitro does not influence intimal hyperplasia *in vivo*.

Despite elevated levels of MCP1 in AVF lesions of *Rxfp1*$^{-/-}$ mice we unexpectedly did not observe effects on venous intimal hyperplasia. To unravel this observation, *in vitro* studies on VSMCs were performed as they play a key role in intimal hyperplasia formation and AVF maturation. We observed that RXFP1 ablation caused a phenotypic switch of both arterial and venous VSMCs from a contractile towards a synthetic phenotype. The switch from the contractile phenotype to the synthetic, is associated with increased migratory and proliferative capacity. Indeed, functional studies revealed an increase in migration of arterial cells from *Rxfp1*$^{-/-}$ mice while migration of venous cells was not altered. Surprisingly, when cells had to migrate through a layer of collagen, both arterial and venous VSMCs isolated form *Rxfp1*$^{-/-}$ mice displayed elevated migration. Collectively, these findings suggest that the surrounding and ECM architecture will ultimately determine VSMCs behavior and could potentially differ between arterial and venous VSMCs. The question arises why RXFP1 deficiency *in vivo* resulted in decreased outward remodeling and had no effect on intimal hyperplasia, whereas *in vitro* functional studies clearly show impact of RXFP1 deficiency on VSMCs migration. In this respect, it is important to notice that the efficacy of cell migration *in vivo* strongly depends on the balance between cell deformability and ECM density, of which the latter is governed by the capacity of proteolytic enzymes to degrade matrix components[52]. Interestingly, RXFP1 deficiency resulted in a significant increase in elastin content as a result of decreased elastase activity. This preserved elastin density most likely explains why the increased migratory capacity of RXFP1 deficient VSMCs *in vitro*, did not translate into enhanced intima hyperplasia in the venous outflow tract of AVF in *Rxfp1*$^{-/-}$ mice.

Alongside the well-established role for the relaxin-axis in pregnancy, the evolutionally conserved expression of RXFP1 within blood vessels of several mammals in a gender-independent fashion underscores the importance of this protein-receptor interaction in the vasculature. Our data indicate that the RLN2 and RXFP1 proteins are highly expressed in human AVF lesions, strongly suggesting that therapeutic targeting of this

pathway in the context of AVF maturation could be beneficial. In this respect, it is encouraging that clinical trials with serelaxin, a recombinant form of relaxin, have displayed promising effects in the treatment of heart failure[53]. In parallel, small-molecule agonists of RXFP1 are currently being developed[54].

Despite these advances, some aspects of our study require further discussion. Our studies were performed in healthy mice, and given that response in animals does not necessarily mimic human pathology, it is critical to remain cautious in extrapolating results derived from murine studies to patients with chronic renal failure. Another limitation of our experimental setup is the inability to perform flow measurements and cannulations of the murine AVF, as an adequate blood flow volume and the cannulability of the AVF are the main characteristics of functional hemodialysis access. Nevertheless, the present study demonstrates the functional significance of the RXFP1 pathway in AVF remodeling, implying that the RLN2-RXFP1 pathway could be a novel therapeutic target to promote maturation and longevity of AVFs for hemodialysis.

Acknowledgements

This study was supported by a grant from Leiden University Medical Center. We would like to thank Reshma A. Lalai for her excellent assistance in performing experiments and data analysis.

References

1. Schinstock, C.A., *et al.* Outcomes of arteriovenous fistula creation after the Fistula First Initiative. *Clinical journal of the American Society of Nephrology : CJASN* **6**, 1996-2002 (2011).
2. Al-Jaishi, A.A., *et al.* Patency rates of the arteriovenous fistula for hemodialysis: a systematic review and meta-analysis. *American journal of kidney diseases : the official journal of the National Kidney Foundation* **63**, 464-478 (2014).
3. Rothuizen, T.C., *et al.* Arteriovenous access failure: more than just intimal hyperplasia? *Nephrology, dialysis, transplantation : official publication of the European Dialysis and Transplant Association - European Renal Association* **28**, 1085-1092 (2013).
4. Wong, C., *et al.* Liposomal prednisolone inhibits vascular inflammation and enhances venous outward remodeling in a murine arteriovenous fistula model. *Scientific reports* **6**, 30439 (2016).
5. Wong, C.Y., *et al.* Vascular remodeling and intimal hyperplasia in a novel murine model of arteriovenous fistula failure. *Journal of vascular surgery* (2013).
6. Bezhaeva, T., *et al.* Deficiency of TLR4 homologue RP105 aggravates outward remodeling in a murine model of arteriovenous fistula failure. *Scientific reports* **7**, 10269 (2017).
7. Krishnamoorthy, M.K., *et al.* Hemodynamic wall shear stress profiles influence the magnitude and pattern of stenosis in a pig AV fistula. *Kidney international* **74**, 1410-1419 (2008).
8. Liang, M., *et al.* Migration of smooth muscle cells from the arterial anastomosis of arteriovenous fistulas requires Notch activation to form neointima. *Kidney international* **88**, 490-502 (2015).
9. Roy-Chaudhury, P., *et al.* Cellular phenotypes in human stenotic lesions from haemodialysis vascular access. *Nephrology, dialysis, transplantation : official publication of the European Dialysis and Transplant Association - European Renal Association* **24**, 2786-2791 (2009).
10. Roy-Chaudhury, P., *et al.* Pathogenetic role for early focal macrophage infiltration in a pig model of arteriovenous fistula (AVF) stenosis. *The journal of vascular access* **15**, 25-28 (2014).
11. Zhao, J., *et al.* Dual Function for Mature Vascular Smooth Muscle Cells During Arteriovenous Fistula Remodeling. *Journal of the American Heart Association* **6**(2017).
12. Conrad, K.P., Debrah, D.O., Novak, J., Danielson, L.A. & Shroff, S.G. Relaxin modifies systemic arterial resistance and compliance in conscious, nonpregnant rats. *Endocrinology* **145**, 3289-3296 (2004).
13. Feng, S., Bogatcheva, N.V., Kamat, A.A., Truong, A. & Agoulnik, A.I. Endocrine effects of relaxin overexpression in mice. *Endocrinology* **147**, 407-414 (2006).
14. Cernaro, V., *et al.* Relaxin: new pathophysiological aspects and pharmacological perspectives for an old protein. *Medicinal research reviews* **34**, 77-105 (2014).
15. Jeyabalan, A., Shroff, S.G., Novak, J. & Conrad, K.P. The vascular actions of relaxin. *Advances in experimental medicine and biology* **612**, 65-87 (2007).
16. Sherwood, O.D. Relaxin's physiological roles and other diverse actions. *Endocrine reviews* **25**, 205-234 (2004).
17. Debrah, D.O., Conrad, K.P., Jeyabalan, A., Danielson, L.A. & Shroff, S.G. Relaxin increases cardiac output and reduces systemic arterial load in hypertensive rats. *Hypertension (Dallas, Tex. : 1979)* **46**, 745-750 (2005).
18. Conrad, K.P. & Shroff, S.G. Effects of relaxin on arterial dilation, remodeling, and mechanical properties. *Current hypertension reports* **13**, 409-420 (2011).
19. Debrah, D.O., *et al.* Relaxin regulates vascular wall remodeling and passive mechanical properties in mice. *Journal of applied physiology (Bethesda, Md. : 1985)* **111**, 260-271 (2011).

20. Chan, S.L. & Cipolla, M.J. Relaxin causes selective outward remodeling of brain parenchymal arterioles via activation of peroxisome proliferator-activated receptor-gamma. *FASEB journal : official publication of the Federation of American Societies for Experimental Biology* **25**, 3229-3239 (2011).
21. Samuel, C.S., Lekgabe, E.D. & Mookerjee, I. The effects of relaxin on extracellular matrix remodeling in health and fibrotic disease. *Advances in experimental medicine and biology* **612**, 88-103 (2007).
22. Samuel, C.S. & Hewitson, T.D. Relaxin and the progression of kidney disease. *Current opinion in nephrology and hypertension* **18**, 9-14 (2009).
23. Chow, B.S., *et al.* Relaxin requires the angiotensin II type 2 receptor to abrogate renal interstitial fibrosis. *Kidney international* (2014).
24. Zhou, X., *et al.* Relaxin inhibits cardiac fibrosis and endothelial-mesenchymal transition via the Notch pathway. *Drug design, development and therapy* **9**, 4599-4611 (2015).
25. Bennett, R.G., Heimann, D.G., Singh, S., Simpson, R.L. & Tuma, D.J. Relaxin decreases the severity of established hepatic fibrosis in mice. *Liver international : official journal of the International Association for the Study of the Liver* **34**, 416-426 (2014).
26. Chen, B., Wen, Y., Yu, X.Y. & Polan, M.L. Relaxin increases elastase activity and protease inhibitors in smooth muscle cells from the myometrium compared with cells from leiomyomas. *Fertility and sterility* **91**, 1351-1354 (2009).
27. Brecht, A., Bartsch, C., Baumann, G., Stangl, K. & Dschietzig, T. Relaxin inhibits early steps in vascular inflammation. *Regulatory peptides* **166**, 76-82 (2011).
28. Novak, J., *et al.* Evidence for local relaxin ligand-receptor expression and function in arteries. *FASEB journal : official publication of the Federation of American Societies for Experimental Biology* **20**, 2352-2362 (2006).
29. Jelinic, M., *et al.* Localization of relaxin receptors in arteries and veins, and region-specific increases in compliance and bradykinin-mediated relaxation after in vivo serelaxin treatment. *FASEB journal : official publication of the Federation of American Societies for Experimental Biology* **28**, 275-287 (2014).
30. Bathgate, R.A., *et al.* Relaxin family peptides and their receptors. *Physiological reviews* **93**, 405-480 (2013).
31. Horton, J.S., Yamamoto, S.Y. & Bryant-Greenwood, G.D. Relaxin modulates proinflammatory cytokine secretion from human decidual macrophages. *Biology of reproduction* **85**, 788-797 (2011).
32. Leo, C.H., *et al.* Vascular actions of relaxin: nitric oxide and beyond. *British journal of pharmacology* **174**, 1002-1014 (2017).
33. Kamat, A.A., *et al.* Genetic targeting of relaxin and insulin-like factor 3 receptors in mice. *Endocrinology* **145**, 4712-4720 (2004).
34. Wong, C.Y., *et al.* A Novel Murine Model of Arteriovenous Fistula Failure: The Surgical Procedure in Detail. *Journal of visualized experiments : JoVE*, e53294 (2016).
35. Shin, D., *et al.* Expression of ephrinB2 identifies a stable genetic difference between arterial and venous vascular smooth muscle as well as endothelial cells, and marks subsets of microvessels at sites of adult neovascularization. *Developmental biology* **230**, 139-150 (2001).
36. Owens, G.K., Kumar, M.S. & Wamhoff, B.R. Molecular regulation of vascular smooth muscle cell differentiation in development and disease. *Physiological reviews* **84**, 767-801 (2004).
37. Lacolley, P., Regnault, V., Nicoletti, A., Li, Z. & Michel, J.B. The vascular smooth muscle cell in arterial pathology: a cell that can take on multiple roles. *Cardiovascular research* **95**, 194-204 (2012).

38. Ichii, T.*, et al.* Fibrillar collagen specifically regulates human vascular smooth muscle cell genes involved in cellular responses and the pericellular matrix environment. *Circulation research* **88**, 460-467 (2001).
39. Thyberg, J. & Hultgardh-Nilsson, A. Fibronectin and the basement membrane components laminin and collagen type IV influence the phenotypic properties of subcultured rat aortic smooth muscle cells differently. *Cell and tissue research* **276**, 263-271 (1994).
40. Hocevar, B.A. & Howe, P.H. Analysis of TGF-beta-mediated synthesis of extracellular matrix components. *Methods in molecular biology* **142**, 55-65 (2000).
41. Kingsley, K.*, et al.* ERK1/2 mediates PDGF-BB stimulated vascular smooth muscle cell proliferation and migration on laminin-5. *Biochemical and biophysical research communications* **293**, 1000-1006 (2002).
42. Lee, T. & Misra, S. New Insights into Dialysis Vascular Access: Molecular Targets in Arteriovenous Fistula and Arteriovenous Graft Failure and Their Potential to Improve Vascular Access Outcomes. *Clinical journal of the American Society of Nephrology : CJASN* **11**, 1504-1512 (2016).
43. Guzman, R.J., Abe, K. & Zarins, C.K. Flow-induced arterial enlargement is inhibited by suppression of nitric oxide synthase activity in vivo. *Surgery* **122**, 273-279; discussion 279-280 (1997).
44. Chan, C.Y., Chen, Y.S., Ma, M.C. & Chen, C.F. Remodeling of experimental arteriovenous fistula with increased matrix metalloproteinase expression in rats. *Journal of vascular surgery* **45**, 804-811 (2007).
45. Burke SK, F.F., LaRochelle A, Mendenhall HV Local application of recombinant human type I pancreatic elastase (PRT-201) to an arteriovenous fistula (AVF) increases AVF blood flow in a rabbit model. . *J Am Soc Nephrol* **19: 252–253A** (2008)**.**
46. Peden, E.K.*, et al.* Arteriovenous fistula patency in the 3 years following vonapanitase and placebo treatment. *Journal of vascular surgery* **65**, 1113-1120 (2017).
47. Finlay, G.A., O'Donnell, M.D., O'Connor, C.M., Hayes, J.P. & FitzGerald, M.X. Elastin and collagen remodeling in emphysema. A scanning electron microscopy study. *The American journal of pathology* **149**, 1405-1415 (1996).
48. Chen, B., Wen, Y., Yu, X. & Polan, M.L. Elastin metabolism in pelvic tissues: is it modulated by reproductive hormones? *American journal of obstetrics and gynecology* **192**, 1605-1613 (2005).
49. Kang, L.*, et al.* A new model of an arteriovenous fistula in chronic kidney disease in the mouse: beneficial effects of upregulated heme oxygenase-1. *American journal of physiology. Renal physiology* **310**, F466-476 (2016).
50. Kang, L.*, et al.* Functioning of an arteriovenous fistula requires heme oxygenase-2. *American journal of physiology. Renal physiology* **305**, F545-552 (2013).
51. Juncos, J.P.*, et al.* MCP-1 contributes to arteriovenous fistula failure. *Journal of the American Society of Nephrology : JASN* **22**, 43-48 (2011).
52. Wolf, K.*, et al.* Physical limits of cell migration: control by ECM space and nuclear deformation and tuning by proteolysis and traction force. *The Journal of cell biology* **201**, 1069-1084 (2013).
53. Teerlink, J.R.*, et al.* Serelaxin, recombinant human relaxin-2, for treatment of acute heart failure (RELAX-AHF): a randomised, placebo-controlled trial. *Lancet* **381**, 29-39 (2013).
54. Xiao, J.*, et al.* Identification and optimization of small-molecule agonists of the human relaxin hormone receptor RXFP1. *Nat Commun* **4**(2013).

Supplementary material

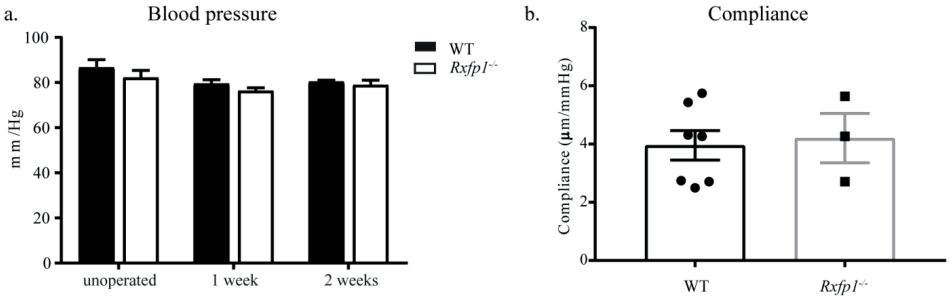

Supplementary Figure 1. (a) Arterial blood pressure levels did not differ between *Rxfp1*$^{-/-}$ and WT mice over the course of AVF maturation. n=5 per group. (b) Basal arterial compliance was also similar between *Rxfp1*$^{-/-}$ and WT mice. n=7 WT; n=3 *Rxfp1*$^{-/-}$.

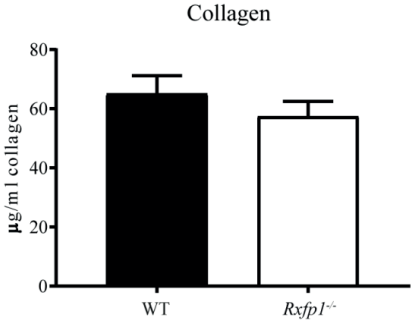

Supplementary Figure 2. Effect of RXFP1 deficiency on collagen content *in vivo*.
Collagen was analyzed in venous AVF sections from *Rxfp1*$^{-/-}$ and WT mice. Total collagen content did not differ between the groups. n = 10 per group.

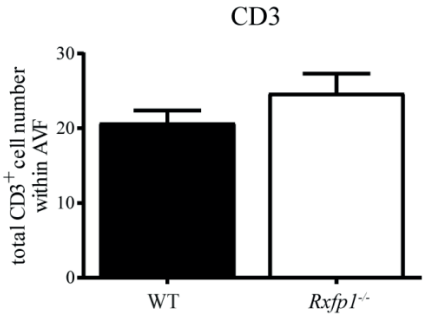

Supplementary Figure 3. Quantification of CD3⁺ T-cells in the AVF lesions 14 days after surgery. n=10 per group.

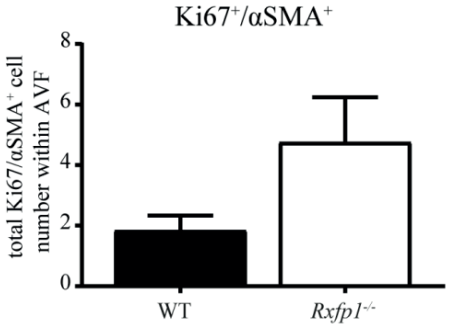

Supplementary Figure 4. Effect of RXFP1 deficiency on VSMCs proliferation *in vivo*.
Quantification of Ki67⁺/αSMA⁺ cells in AVF lesions of *Rxfp1*$^{-/-}$ and WT mice 14 days after AVF surgery. n=11 per group.

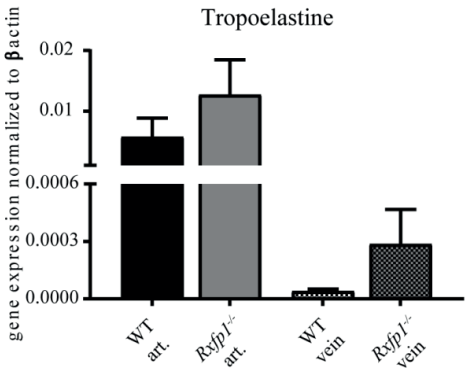

Supplementary Figure 5. Tropoelastine mRNA expression levels in cultured primary arterial and venous cells isolated from Rxfp1-/- and WT mice. n=4 per group.

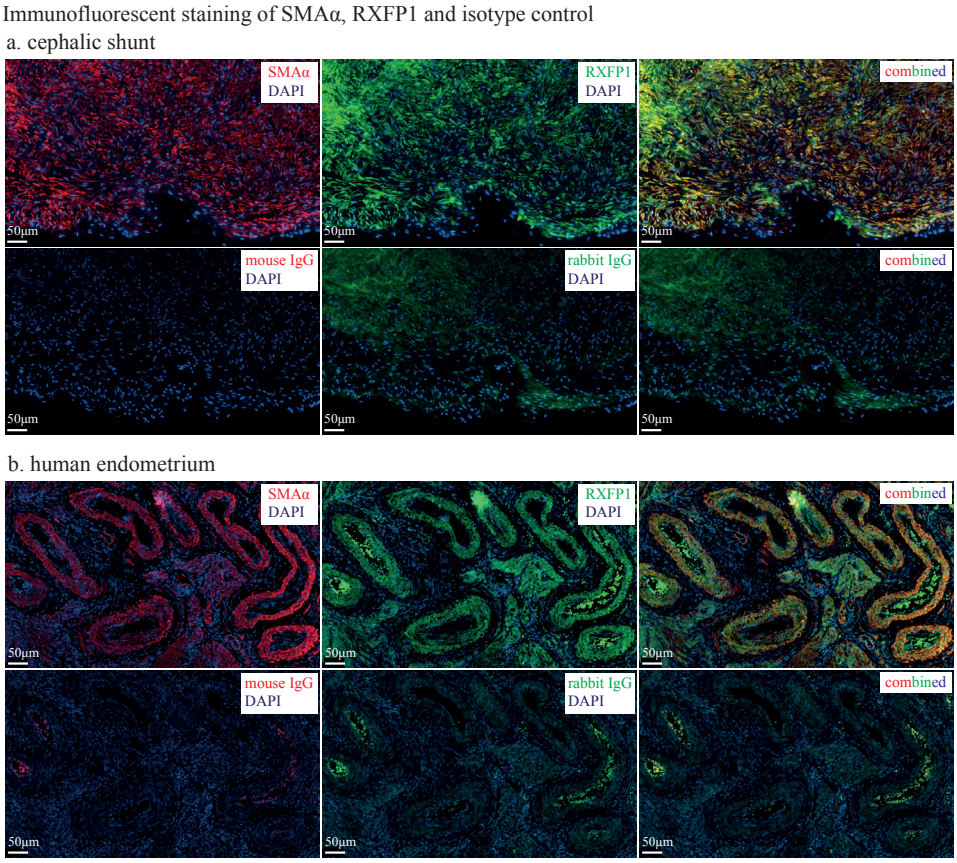

Supplementary Figure 6. Immunofluorescence RXFP1 antibody validation.
For immunofluorescent staining of double positive SMA$^+$, RXFP1$^+$ cells in (a) cephalic shunt and (b) endometrium after primary antibody sections were counterstained with Alexa 568 conjugated goat anti mouse IgG2a (1:250; Molecular probes A21134) for SMAα and Alexa 488 conjugated secondary goat anti rabbit IgG (1:250; Molecular probes A11008) for RXFP1. Mouse or rabbit IgG were used as negative controls. Nuclei were visualized with ProLong™ Gold Antifade Mountant with DAPI.

Table 1. Primers used for in vitro experiments

Gene	Forward primer	Reversed primer
ephrinB2	ACGGTCCAACAAGACGTCCA	GCTGTTGCCATCGGTGCTA
MyHC	TGGCTAGCAGCTTGTCAGGAA	GCCTTGCGTACTCTATCACTCATG
calponin	GAAGGCAGGAACATCATTGGA	CCTGCTGACTGGCAAACTTG
caldesmon	GCCGTTCAAGTGCTTCACTC	TGTCAATCTTGGAGACTACTGCT
Col1	TGACTGGAAGAGCGGAGAGT	GTTCGGGCTGATGTACCAGT
Fibronectin	ATGTGGACCCCTCCTGATAGT	GCCCAGTGATTTCAGCAAAGG
TGFβ	GCAACATGTGGAACTCTACCAGAA	GACGTCAAAAGACAGCCACTCA
PDGF	CAAGAAGCGGCCATGAATCAG	CGGCCCTAGTGAGTTGTTGT
tropoelastin	GGTTGTTCAGACTACAATCTGACC	CAACTTTGCCCAAATGACTCTCC
βactin	AGGTCATCACTATTGGCAACGA	CCAAGAAGGAAGGCTGGAAAA

Chapter 5

The battlefield at the arteriovenous crossroad: invading arterial SMCs occupy the venous outflow tract of fistulas

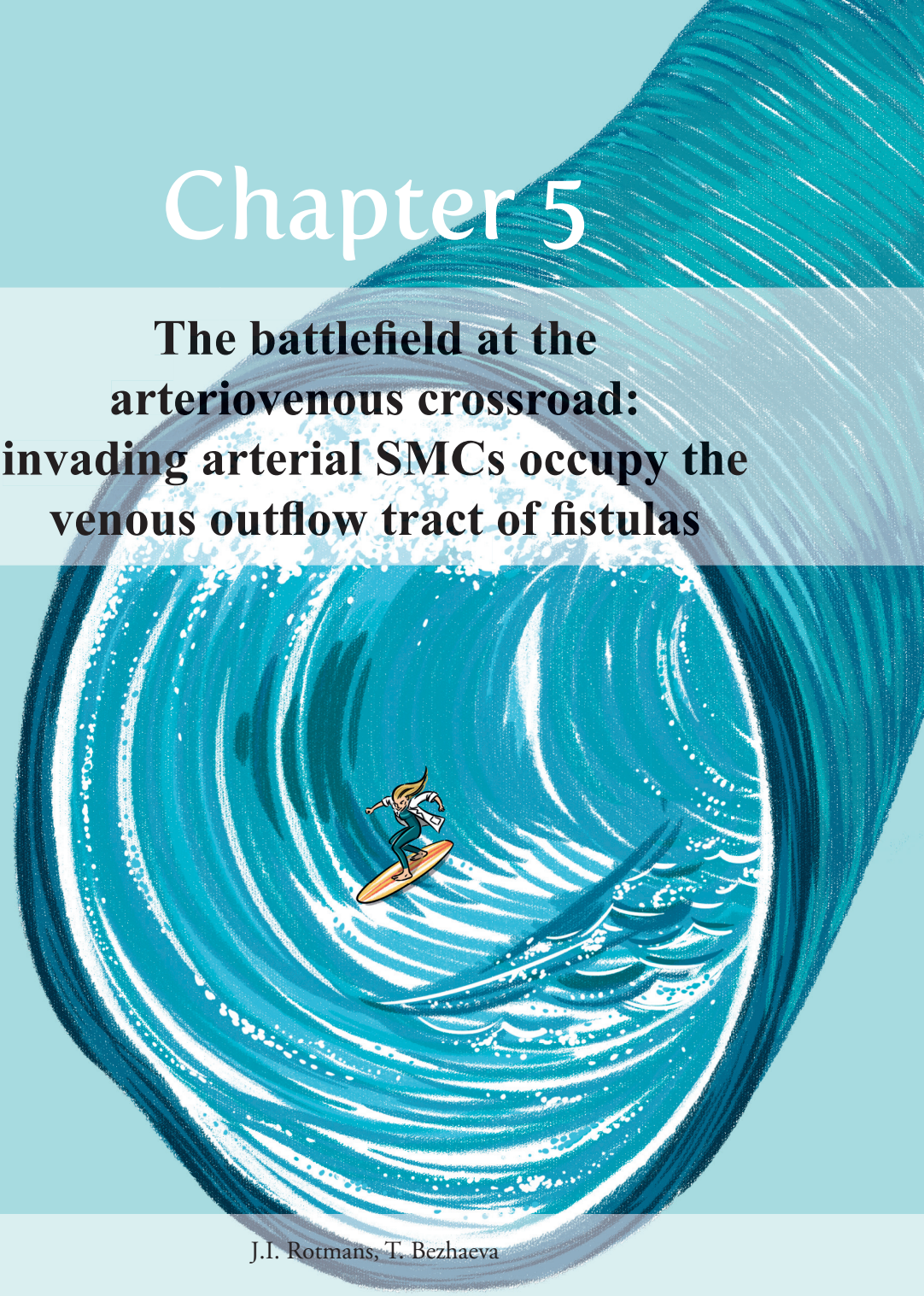

J.I. Rotmans, T. Bezhaeva

Kidney Int. 2015 Sep;88(3):431-3

Abstract

There is an ongoing debate about the anatomical origin of the neointimal cells that are responsible for venous stenotic lesions in arteriovenous fistulas. Liang and coworkers show that vascular smooth muscle cells from the feeding artery contribute substantially to venous intima hyperplasia in murine AVF model. In addition, they show that increased Notch-signaling is the driving force behind FSP-1 mediated migration of these cells to the venous outflow tract.

More than 50 years after the first vascular access device for maintenance hemodialysis was introduced by Scribner, the options for vascular access conduits have witnessed substantial improvements. Currently, native arteriovenous fistulas (AVFs) are considered the preferred option for vascular access in view of their lower complication rate, when compared to prosthetic arteriovenous grafts (AVG) and central venous catheters. However, AVF-related complications still constitute a major cause of morbidity for patients on chronic hemodialysis, as the durability of AVFs is far from optimal with 1-year primary patency rates of 60-65%[1].

The utility of AVFs is hampered by two distinct causes of failure: (1) initial failure to mature and (2) dysfunction of mature AVFs due to stenotic lesions in the venous outflow tract. The exact pathophysiology of both these types of AVF failure is unclear, although excessive intimal hyperplasia (IH) is thought to be a major cause of narrowing of the (venous) lumen, ultimately leading to AVF failure[2]. The vast majority of venous intimal cells are VSMCs and myofibroblasts, cells that both express alpha smooth muscle actin (α-SMA) whereas smooth muscle myosin heavy chain (SMMHC) is solely expressed by VSMCs. The stimuli responsible for the formation of IH in AVF are multifactorial and include hemodynamic factors such as turbulent flow, surgical injury as well as platelet activation due to repetitive cannulation. From an evolutionary point of view, veins are obviously not designed to cope with these excessive stimuli in AVF. To some extent, the outward remodeling and thickening of the intima in the venous outflow tract could therefore be considered as a physiological adaptive response that is needed to withstand the high hydrostatic pressure and flow.

Currently, there is an ongoing debate about the anatomical source of the neointimal cells in the venous outflow tract. While in the past, migrated VSMCs from the venous tunica media were considered to be the most prominent source of neointimal cells, more recent studies suggest that venous adventitial fibroblasts, circulating vascular progenitor cells as well as arterial VSMCs might contribute as well (Figure 1).

In a paper in the present issue of *Kidney International* [3], Liang and coworkers aimed to further unravel the cellular origin of venous intimal cells in a murine model of AVF failure. In a set of complex and elegant experiments in a murine uremic model of AVF failure, they focused on VSMCs in the feeding artery as important contributors to venous IH. For this purpose, transgenic mice were used that express green-fluorescent protein (GFP) in VSMCs in the carotid artery while venous VSMCs do not express GFP in these mice. This approach allowed the researchers to trace the arterial VSMCs in the development of venous IH in murine AVF. Histological analysis of the venous outflow tract of the murine AVFs at 2-4 weeks after surgery, revealed that half of intima cells in the AVF were GFP-positive and most of them expressed α-SMA, suggesting that VMSCs from the anastomosed artery contributed to as much as 50% of the VSMC compartment in the venous intima.

Next, the researchers aimed to identify the underlying mechanisms that stimulate arterial VSMCs to migrate to the venous intima. They hypothesized that increased Notch signaling could be the major driving force for arterial VSMC migration, as the Notch

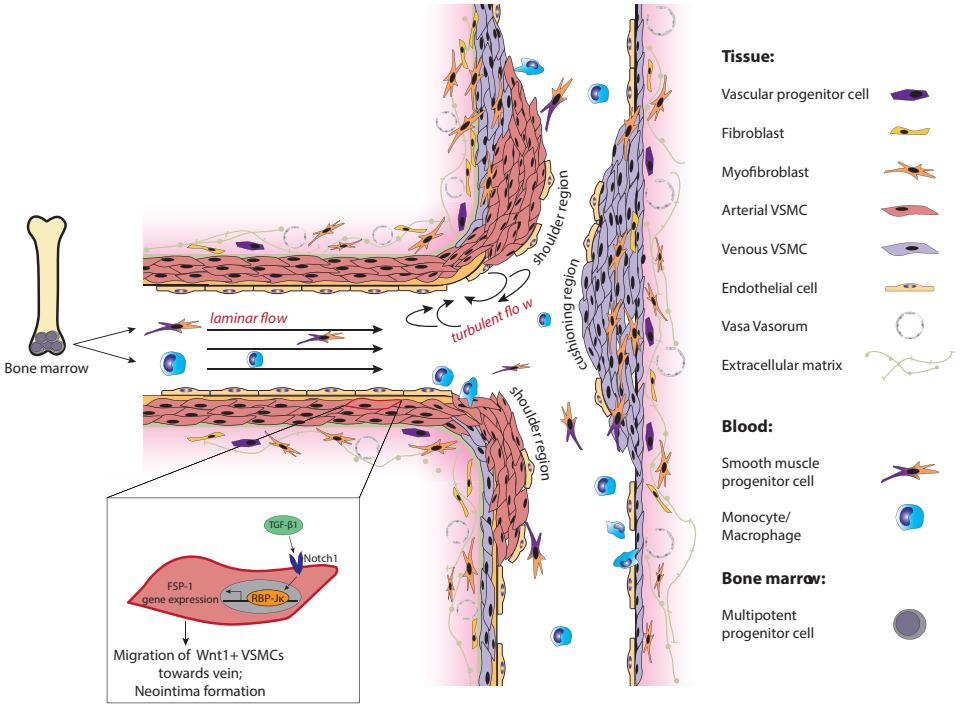

Figure 1. Schematic representation of peri-anastomotic neointima formation in AVFs.
A variety of cells have been designated as contributors to IH in AVF including venous VSMCs, venous fibroblasts that differentiate into myobroblasts, circulating vascular smooth muscle progenitor cells resident vascular progenitor cells and arterial VSMCs. With respect to the latter cells, FSP-1 mediates the migration towards the venous outflow tract in response to Notch activation. RBP-J: recombination signal binding protein for immunoglobulin kappa J region.

pathway plays a critical role in vascular development, for instance by determining arterial versus venous vessel formation. In addition, increased Notch signaling has previously been associated with neointima formation[4]. In their previous work in the murine AVF model, researchers from the group led by Jizhong Cheng in Houston have already shown that blockade of the Notch-signaling pathway in endothelial cells prevented AVF failure in uremic mice[5]. In their present paper, Liang and colleagues confirm that Notch activation is increased in AVFs created in CKD mice, when compared to AVF in mice with normal renal function. In additional *in vitro* experiments, they elegantly show that transforming growth factor β1 (TGF-β1)-mediated upregulation of fibroblast-specific protein-1 (FSP-1) in VSMCs is partly dependent on the same Notch-signaling pathway. The latter is of particular interest since FSP-1 is an important regulator of VSMC migration. Subsequently, the investigators provided additional evidence for a central role for FSP-1 in VSMCs migration in AVF, by showing that IH was significantly reduced in FSP-1 knock out mice when compared to wild type mice. Finally, they evaluated human venous samples of failed AVFs and AVGs which revealed marked expression of both N1ICD (a marker of Notch activation) as well as FSP-1 in α-SMA$^+$ venous neointimal

cells, thereby illustrating the clinical relevance of their observations in mice.

Altogether, Liang and colleagues' findings underscore the importance of the feeding artery as cellular source of migrating VSMCs that contribute to the formation of stenotic lesion in the venous outflow tract of AVFs. This observation might have important implications for local therapeutic strategies to inhibit IH, which thus far primarily focused on the draining vein as pivotal source of proliferating and migrating VSMCs and fibroblasts. However, one should be cautious in extrapolating promising results from murine studies to potential benefit for hemodialysis patients. In general, the translation rate from preclinical studies to the bedside remains low, most likely due to differences in physiology and molecular pathways. In this respect, it should be noticed that the end-to-end configuration that was utilized by Liang and coworkers for the construction of the murine AVFs, differs from the anatomical configuration that is commonly used in humans. Indeed, AVFs in hemodialysis patients are usually constructed by anastomosing the end of a vein to the side of an artery. The exact configuration is a crucial characteristic of the AVF since it determines the hemodynamic profile in the AVF and affects blood flow rate, wall shear stress (WSS) levels, endothelial dysfunction and subsequent development of IH[6]. To circumvent this limitation of the end-to-end configuration, we recently developed a novel murine AVF model with a configuration similar to the one used most frequently in humans[7]. In addition, we should keep in mind that the geometrical orientation of the arterial and venous parts of the AVF in the described end-to-end model differs from an end-to-side anastomosis. Indeed, arterial VSMCs can relatively easily migrate towards the venous segment in the end-to-end configuration, whereas in the end-to-side model, the anatomical distance between the arterial segment and especially the cushioning region of the vein (see Figure 1) is larger. Interestingly, previous studies that were performed using an end-to-side configuration in rats, failed to demonstrate a substantial contribution of arterial VSMCs to venous IH in AVF[8]. As Liang and coworkers primarily focused on peri-anastomotic IH, the contribution of arterial VSMCs in more downstream stenotic lesions as well as in venous lesion of AVGs, remains to be determined. Future studies should reveal if the arterial VSMCs indeed have the capacity to make such long-distance trips.

The question arises how the presented data on the Notch/FSP-1 signaling in arterial VSMCs could translate into novel therapeutic approaches to improve AVF patency. An interesting option would be to evaluate the efficacy of Notch-inhibitors that have been developed in the field of oncology. These small-molecules could be applied to the arterial adventitia during AVF surgery, for instance using a hydrogel-based local delivery system that facilitates sustained release of the compound. In this respect, it is important to recognize that complete inhibition of VSMC proliferation and migration in the early phase after AVF surgery do not necessarily translate into a better functional outcome of AVFs, as (limited) VSMC proliferation might be a prerequisite for adequate outward remodeling of the involved blood vessels[9]. Therefore, the timing of the application of novel interventions to inhibit VSMC proliferation could be crucial for its effect on the functional outcome of the AVF.

Nevertheless, the latter complicating issues should not distract from the fact that these mechanistic studies on the pathophysiology of AVF failure open up a new perspective on potential therapeutic strategies, aimed to modulate the suboptimal vascular response in AVFs for hemodialysis access. Liang and coworkers should be congratulated which their excellent work which hopefully can be translated into local interventions that improve the performance of this 'lifeline' of hemodialysis patients.

References

1. Tordoir JH, Rooyens P, Dammers R et al. Prospective evaluation of failure modes in autogenous radiocephalic wrist access for haemodialysis. Nephrol Dial Transplant 2003; 18: 378–383.
2. Rothuizen TC, Wong C, Quax PH, van Zonneveld AJ, Rabelink TJ, Rotmans JI. Arteriovenous access failure: more than just intimal hyperplasia? Nephrol Dial Transplant. 2013 May;28(5):1085-92.
3. Liang M, Wang Y, Liang A, Mitch WE, Roy-Chaudhury P, Han G, Cheng J. Migration of smooth muscle cells from the arterial anastomosis of arteriovenous fistulas requires Notch activation to form neointma. Kidney International 2015.
4. Li Y, Takeshita K, Liu P-Y, Satoh M, Oyama N, Mukai Y, Chin MT, Krebs L,Kotlikoff MI, Radtke F, Gridley T, Liao JK: Smooth muscle Notch1 mediates neointimal formation after vascular injury. Circulation 119: 2686–2692, 2009
5. Wang Y, Liang A, Luo J, Liang M, Han G, Mitch WE, Cheng J. Blocking Notch in Endothelial Cells Prevents Arteriovenous Fistula Failure Despite CKD. J Am Soc Nephrol 25: 773–783, 2014
6. Krishnamoorthy MK, Banerjee RK, Wang Y, Choe AK, Rigger D, Roy-Chaudhury P. Anatomic configuration affects the flow rate and diameter of porcine arteriovenous fistulae. Kidney Int. 2012 Apr;81(8):745-50.
7. Wong CY, de Vries MR, Wang Y, et al. Vascular remodeling and intimal hyperplasia in a novel murine model of arteriovenous fistula failure. J Vasc Surg 2014;59(1). 192e201.e1.
8. Skartsis N, Manning E, Wei Y, Velazquez OC, Liu ZJ, Goldschmidt-Clermont PJ, Salman LH, Asif A, Vazquez-Padron RI. Origin of neointimal cells in arteriovenous fistulae: bone marrow, artery, or the vein itself? Semin Dial. 2011 Mar-Apr;24(2):242-8.
9. De Mey JG, Schiffers PM, Hilgers RH, Sanders MM. Toward functional genomics of flow-induced outward remodeling of resistance arteries. Am J Physiol Heart Circ Physiol. 2005 Mar;288(3):H1022-7.

Chapter 6

Contribution of bone marrow-derived cells to in situ engineered tissue capsules in a rat model of chronic kidney disease

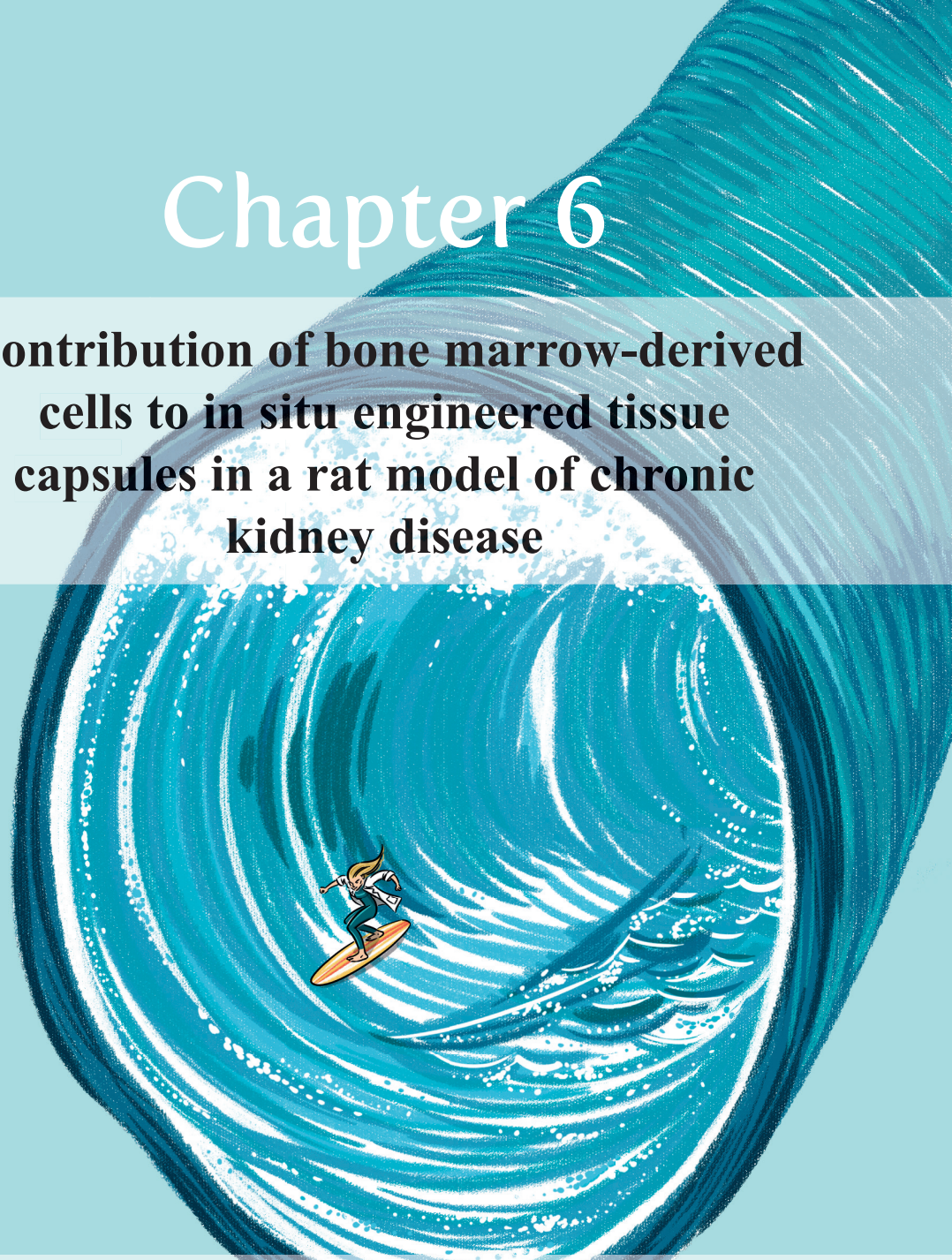

Taisiya Bezhaeva, Wouter J. Geelhoed, Dong Wang, Haoyong Yuan, Eric P. van der Veer, Carla M.A. van Alem, Febriyani F.R. Damanik, Xuefeng Qiu, Anton Jan van Zonneveld, Lorenzo Moroni, Song Li and Joris I. Rotmans

Biomaterials - In press (available online 15 December 2018)

Abstract

Tissue engineered blood vessels (TEBVs) hold great promise for clinical use in patients with end stage renal disease (ESRD) requiring vascular access for hemodialysis. A promising way to make TEBVs is to exploit foreign body response (FBR) of polymeric rods used as templates. However, since the FBR predominantly involves bone-marrow (BM) derived cells and ESRD coincides with impaired function of BM, it is important to assess the generation of TEBVs in conditions of renal failure. To this end, we implanted polymer rods in the subcutis of rats after BM-transplantation with GFP-labeled BM cells in a model of chronic kidney disease (CKD). At 3 weeks after implantation, rods were encapsulated by tissue capsule (TC) composed of collagen, myofibroblasts and macrophages. On average, 13% of $CD68^+$ macrophages were GFP^+, indicating BM origin. Macrophage-to-myofibroblasts differentiation appeared to play an important role in TC formation as 26% of SMA^+/GFP^+ myofibroblasts co-expressed the macrophage marker CD68. Three weeks after rod implantation, the cellular response changed towards tissue repair, characterized by 40% increase in $CD68^+/CD163^+$ repair associated macrophages and 95% increase in TGFβ and IL10 gene expression as compared to TCs harvested at 1 week. These results show that both BM derived and tissue resident cells, contribute to TC formation, whereas macrophages serve as precursors of myofibroblasts in mature TCs. Finally, the presence of CKD did not significantly alter the process of TC formation, which holds the potential to support our approach for future clinical use in ESRD patients.

Clinical problem:

Tissue engineered blood vessels for patients with end stage renal disease requiring vascular access for hemodialysis

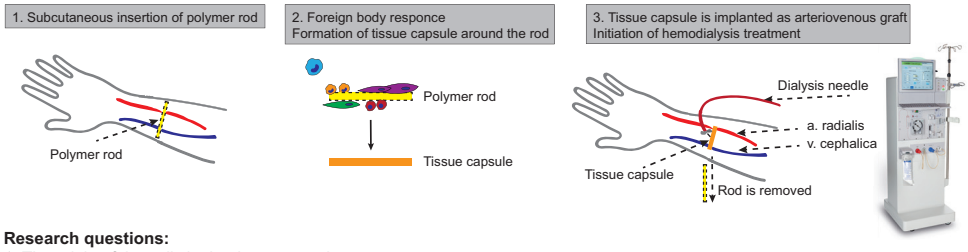

Research questions:

1. The origin of the cells in the tissue capsule
2. Effect of chronic kidney disease on tissue capsule formation

Methods:

Rat model of chronic kidney disease combined with a bone marrow transplantation using GFP-labeled cells

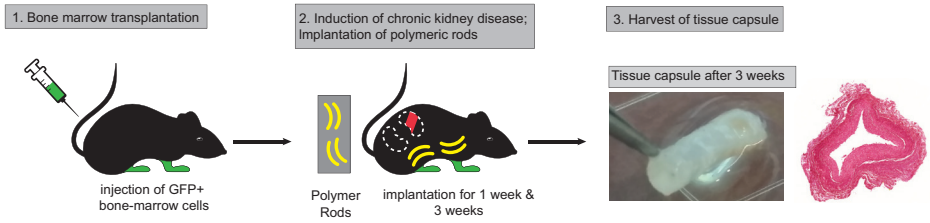

Results:

Cellular origin of cell within the tissue capsule

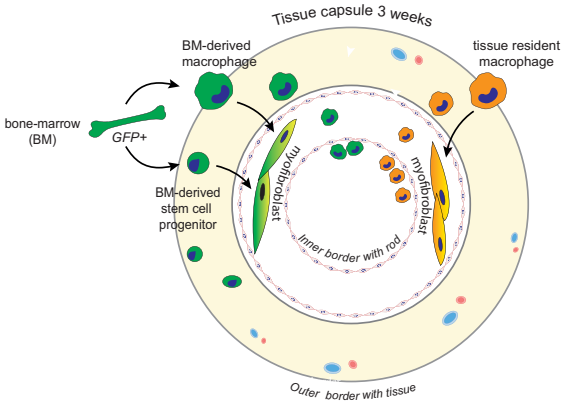

Conclusion:

1. Both bone-marrow derived and tissue resident cells contribute to tissue capsule formation
2. Macrophages serve as precursors of myofibroblasts
3. Chronic kidney disease does not alter process of tissue capsule formation

Introduction

Patients with cardiovascular disease (CVD) or end-stage renal disease (ESRD) frequently require surgery to either replace diseased blood vessels or create a vascular access site for hemodialysis[1-3]. For this purpose, native veins are generally preferred due to superior patency rates when compared to prosthetic grafts, but often unavailable due to preexisting vascular pathology[4,5]. The failure of synthetic vascular grafts predominantly results from the development of intimal hyperplasia ultimately leading to graft occlusion, and a relatively high risk of infectious complications[6-8]. In recent years, various strategies to create tissue engineered vascular grafts have been developed in an effort to overcome current limitations of synthetic grafts and diseased native blood vessels[9-11]. Indeed, tissue engineered blood vessels (TEBVs) can be tailor-made, do not have inconvenient valves and side-branches, are free from pre-existing vascular diseases and have the potential to adapt to changing hemodynamic conditions.

Our approach to generate autologous TEBVs *in vivo* is based on the foreign body response (FBR) directed to a subcutaneously implanted polymer rod that culminates in the formation of a fibrocellular tissue capsule (TC), that encapsulating the rod[12]. Upon extraction of the polymer rod several weeks after implantation, the remaining TC is grafted into the vasculature, whereupon it differentiates into a blood vessel. In this approach, the subcutaneous space is utilized as an *in situ* bioreactor to grow a completely autologous blood vessel. In a previous study in pigs, we demonstrated that upon vascular grafting, the TCs phenotypically differentiate towards a blood vessel, as demonstrated by enhanced matrix synthesis, differentiation of fibroblasts toward contractile vascular smooth muscle cells (VSMCs) and endothelialization of the luminal surface[13].

The dynamics of the FBR to implanted materials have been elucidated in detail[14]. The early phase of the FBR is characterized by the recruitment of inflammatory cells, which is followed by the formation of granulation tissue, ultimately resulting in a fibrocellular TC, which completely encapsulates the implanted foreign body[15]. However, the origin of the cells present within the TCs is still unknown. Understanding the origin of cells present in the TC is of vital importance for its application as vascular grafts, as various disease conditions such as diabetes mellitus, chronic kidney disease (CKD) and ischemic peripheral arterial disease coincide with impaired function of bone marrow (BM)-derived cells[16-18], which could hamper TC formation.

In the present study, we aimed to elucidate the contribution of BM-derived cells in TC formation in a rat model of green fluorescent protein (GFP) BM transplantation[19]. Furthermore, we combined this model with a model of CKD to investigate its effect on TC composition.

Material and Method

Study design

All the animal work was performed at the University of California, Los Angeles and

approved by the institutional animal care and use committee. Five-weeks old male Sprague Dawley (SD) rats (200-250 g) were purchased from Jackson Laboratory (USA) (n=27), transgenic enhanced GFP SD rats (SD-Tg(UBC-EGFP)2BalRrrc) were purchased from rat resource and resource center (University of Missouri, Columbia, USA) (n=9). All animals were housed in the local facilities accredited by the American Association for Accreditation of Laboratory Animal Care and were maintained under controlled conditions of light, temperature, and humidity.

Bone marrow transplantation

After 1-week acclimatization to the new environment, SD-Tg(UBC-EGFP)2BalRrrc rats were used as donor rats for the extraction of bone marrow cells (BMCs). BMCs were harvested from the femurs and tibias of 6 to 8-weeks-old SD-Tg(UBC-EGFP)2BalRrrc rats and the nucleated cells were enriched by lysing red blood cells with Red blood cell lysis buffer (1.2 mL, Sigma, St Louis, MO, USA). The recipient SD rats were lethally irradiated with two apart doses of 5.5 Gy each (11 Gy in total) with a 4h brake using a cobalt-60 gamma source. BMCs ($2*10^7$) were injected via tail vein into recipient rats 24 hours after irradiation. To prevent infections after BM transplantation antibiotic sulfamethoxazole and trimethoprim (0.5 mg/kg) was administrated via the drinking water for 12 days post transplantation. Three weeks after BM reconstitution peripheral blood (0.2 mL) was collected from the tail vein to determine enrichment in GFP^+ cells by fluorescence-activated cell sorting (FACS) analysis.

Model of chronic kidney disease

All operations were performed under isoflurane anesthesia. Three weeks after BM transplantation rats were randomly divided into two experimental groups: healthy controls (n=10) and rats with CKD (n=17). CKD was induced by two-stage subtotal nephrectomy (uninephrectomy of left kidney (UNX) followed 7 days later by 2/3 removal of right kidney), as described previously[20,21]. Two weeks later CKD was confirmed by measuring serum creatinine and blood urea nitrogen (BUN).

Implant material

Solid cylindrical-shaped rods composed of the elastomeric co-polymer PEOT/PBT of 1.75 – 0.25 mm in diameter and 1.5 cm in length were fabricated with a rapid prototyping unit[33] (Envisiontec GmbH, Gladbeck, Germany) used as melt extruder. Rods were composed of the co-polymer poly(ethylene oxide terephthalate)epoly(butylene terephthalate) (PEOT/PBT, Polyvation, The Netherlands), with a PEOT/PBT weight percentage of 55/45 and 300 g/mol molecular weight of the initial polyethylene glycol used for the copolymer reaction. The implant surface was modified by etching with chloroform as previously described[12,22]. Surface topography of all modified rods was evaluated using scanning electron microscopy (SEM). Rods were sterilized by gamma irradiation at a minimum dose of 25 kGy (Synergy Health Ede, the Netherlands). The effect of gamma-radiation on the surface was evaluated using scanning electron microscopy (SEM).

Implantation of polymeric rods

Per rat, four rods were implanted in the subcutaneous space of the abdominal area. First pair of rods were inserted at 2 weeks after CKD induction and 5 weeks after BM transplantation, and left in place for 3 weeks. One week before rods extrusion another pair of rods were inserted for 1-week time point. Following a small horizontal incision of ca. 0.5 cm, a longitudinal subcutaneous pocket was formed where the rods were inserted. The incision was closed using 4-0 vicryl sutures (Johnson & Johnson, NJ, USA). The skin was closed intracutaneously. Rats directly received post operational analgesia via pre-operative injection of buprenorphine (0.01-0.05 mg/kg) and 2 oz gel cups with Carprofen (5 mg/kg) were placed into the cages for up to 3 days post-surgery. One or three weeks after insertion of the rods, tissue capsules were harvested and animals were euthanized by CO2 asphyxiation. In short, a longitudinal incision lateral to the rod was made and the tissue capsule was gently removed from the surrounding tissue. After harvesting, rods could easily be extruded from the tissue capsule.

Morphometric and histological analysis

Tissue capsules containing rods were fixed in 4% paraformaldehyde. After extrusion of the rods, tissue capsules were processed and embedded in paraffin. Serial cross sections of 5 mm of two parts of each tissue capsule were made for immunohistochemical and immunofluorescence analysis. To characterize the extracellular matrix, serial sections of each tissue capsule were stained with picrosirius red for collagen and Movat's stain for other extracellular matrix (ECM) components. Total collagen content was analyzed using QuickZyme Total Collagen Assay Kit (Biosciences, the Netherlands) according to the manufacturer protocol. In brief, five to ten 10 μm tissue sections were hydrolyzed by o/n incubation at 95°C in a heat block. Upon hydrolysis, 35 μl was used for collagen quantification. The assay measured the total amount of hydroxyproline present in the sample after 90 min of incubation time, which represents all collagen-types present in the sample. The assay results in a chromogen with an absorbance maximum at 570 nm.

Cellular composition of tissue capsules was characterized using immunohistochemistry, with antibodies against a-smooth muscle actin (1:1000; Dako M0851, CA, USA) for myofibroblasts, CD68 (1:300; Abcam Ab31630, Cambridge, UK) for macrophages and Ki67 (1:100; BD-Pharmigen 550609, CA, USA) for proliferating cells and visualized with 3.3¢-diaminobenzadine (DAB).

To visualize GFP^+ cells sections were stained with anti-GFP antibody (1:100; Abcam, ab13970, Cambridge, UK) with secondary Cy5 conjugated Goat anti-Chk IgY (1:500; Abcam ab97147, Cambridge, UK). For immunofluorescent staining of CD68 after primary antibody Alexa 568 conjugated goat anti mouse IgG1 (1:300; Molecular Probes A21124, OR, USA) was used. SMA was counterstained with Alexa 488 conjugated secondary mouse IgG2a (1:250; Molecular Probes A21131, OR, USA). Stem/progenitor cell-like population was stained with CD133 (primary ab 1:200; Abcam Ab19898, Cambridge, UK) and secondary goat anti rabbit IgG Alexa 488 (1:250; Molecular Probes A11008, OR, USA). Anti-inflammatory macrophages were visualized by the double staining of CD68 and CD163 (1:400; Immunologic 1105-C01, the Netherlands; secondary goat anti rabbit IgG Alexa 488 (1:250; Molecular Probes

A11008, OR, USA). Nuclei were visualized with ProLong™ Gold Antifade Mountant with DAPI (Thermo Fisher P369, MA, USA). Negative controls were obtained using an isotype antibody and in addition for all stainings a positive control was taken along.

All slides were digitized using an automated microscopic scanner (Pannoramic digital MIDI, 3DHISTECH, Budapest, Hungary). For the quantification of all immunofluorescence staining, the number of positive cells was counted in 8 random fields of view within the TC area at 60x ($CD68^+$ and $CD68^+/GFP^+$) or 120x (SMA^+/GFP^+; $SMA^+/GFP^+/CD68^+$; $CD68^+/CD163^+$ and $CD133^+/GFP^+/SMA^+$) magnification, from which the mean was calculated. Quantification of bright field Ki67 staining was performed with HistoQuant software (3DHISTECH) by calculating % DAB positive area from the total tissue capsule area.

Flow Cytometry and Blood and BM Analysis

The peripheral blood was withdrawn from rat tail vein into tubes containing 15% EDTA for FACS analysis. For the analysis of GFP^+ cells in the BM, complete BM was flushed out from femurs and tibia of rats post-lethality. Red blood cell lysis buffer (1.2 mL, Sigma, St Louis, MO, USA) was added into the tubes containing 0.1 mL blood and/or BM and incubated at 37^0C for 5 minutes followed by addition of 10 mL PBS and centrifugation to remove the lysed red blood cells. The cells (10^6 cells/mL) were resuspended in 50 mL FACS buffer (PBS containing 1% BSA and 0.01% sodium azide) and incubated with Hoechst antibodies (Thermo Fisher, MA, USA) for life/dead cell gating. GFP fluorescence on the surface was determined by fluorescence-activated cell sorting analysis (FACS, LSR II; BD Biosciences, CA, USA). Data were analyzed using FACS-Diva software (BD Biosciences, CA, USA).

RNA isolation, cDNA synthesis and qPCR

Total RNA was extracted from VSMCs using Trizol reagent (Invitrogen, CA, USA) according to the manufacturer's protocol. RNA was reverse transcribed by M-MLV First-Strand Synthesis system (Invitrogen, CA, USA), and used for quantitative analysis of rat genes (Supplementary Table 1) with an SYBR Green Master Mix (Applied Biosystems, CA, USA). Ribosomal protein S15 (RPS15) was used as standard housekeeping gene. The relative mRNA expression levels were determined using $2[-\Delta\Delta C(T)]$ method.

Statistical analysis

Results are expressed as mean±SEM and considered statistically significant for $P<0.05$. T tests and Mann-Whitney tests for parametric and nonparametric data, respectively, were used as appropriate.

Results

Surgical procedure

Generation of rats with GFP-labeled hematopoietic cells and chronic kidney disease

To investigate the contribution of BM derived cells to TC formation, we established a rat model where cells of the hematopoietic lineage expressed GFP. SD rats were transplanted with BM cells derived from transgenic GFP-SD rats. No immunological rejection occurred, as all of the experimental animals underwent BM-transplantation survived and demonstrated high engraftment of donor-derived GFP^+ cells. Percentage of GFP^+ cells was evaluated by FACS analysis of the peripheral blood at three time points: 1) 3 weeks after BM transplantation; 2) 6 weeks later, when the polymeric rods were implanted; and 3) when the polymeric rods were excised from the TC, another 3 weeks later. The percentages of GFP^+ BMCs in the peripheral blood of the rats at these 3 time points were 74±1.6%; 80±1.5%; and 77±3%, respectively. The percentage of GFP^+ cells in the BM at time of TC harvest was 72±3.6%.

Three weeks after BM transplantation, 17 rats underwent a 5/6 nephrectomy procedure from which 8 rats survived (47%). The healthy control group (WT) comprised of 10 animals with BM transplant but without the 5/6 nephrectomy procedure.

The CKD condition was established and persisted for the duration of TC formation. At the time of TC harvest, histological analysis of the remaining kidney of CKD rats revealed enlarged sclerotic glomeruli, dilated tubuli, regions of tubular necrosis and cast formation (Supplementary Figure 1). These structural changes coincided with elevated serum creatinine and BUN levels at the time of rod implantation and rod extrusion (mean creatinine levels: implantation—WT 0.4 mg/dL, vs. CKD 0.94 mg/dL, P=0.0001; extrusion—WT 0.48 mg/dL vs. CKD 1.1 mg/dL P=0.0001; mean BUN levels: implantation—WT 15.2 mg/dL vs. CKD 31.1 mg/dL, P=0.0007; extrusion—WT 18.6 mg/dL vs. CKD 40.25 mg/dL, P=0.0005).

The high mortality rate (53%) of CKD animals was primarily due to uremia as creatinine and blood urea nitrogen levels in these animals were very high, emphasizing the severity of 5/6 nephrectomy model (data not shown).

Implantation of the rods and TC harvest

Fabrication of implanted material was performed as previously described[12]. To create a homogeneous porous surface along the rod, for optimal inflammatory cell recruitment and organization of collagen and myofibroblasts, rods were etched with chloroform. Chloroform etching was verified using SEM (Supplementary Figure 2).

Two weeks after induction of CKD, 4 polymer rods were implanted into the subcutis of the rats in the abdominal area. TCs were harvested at 1- and 3-weeks after subcutaneous implantation of the rods. The study design is summarized in figure 1.

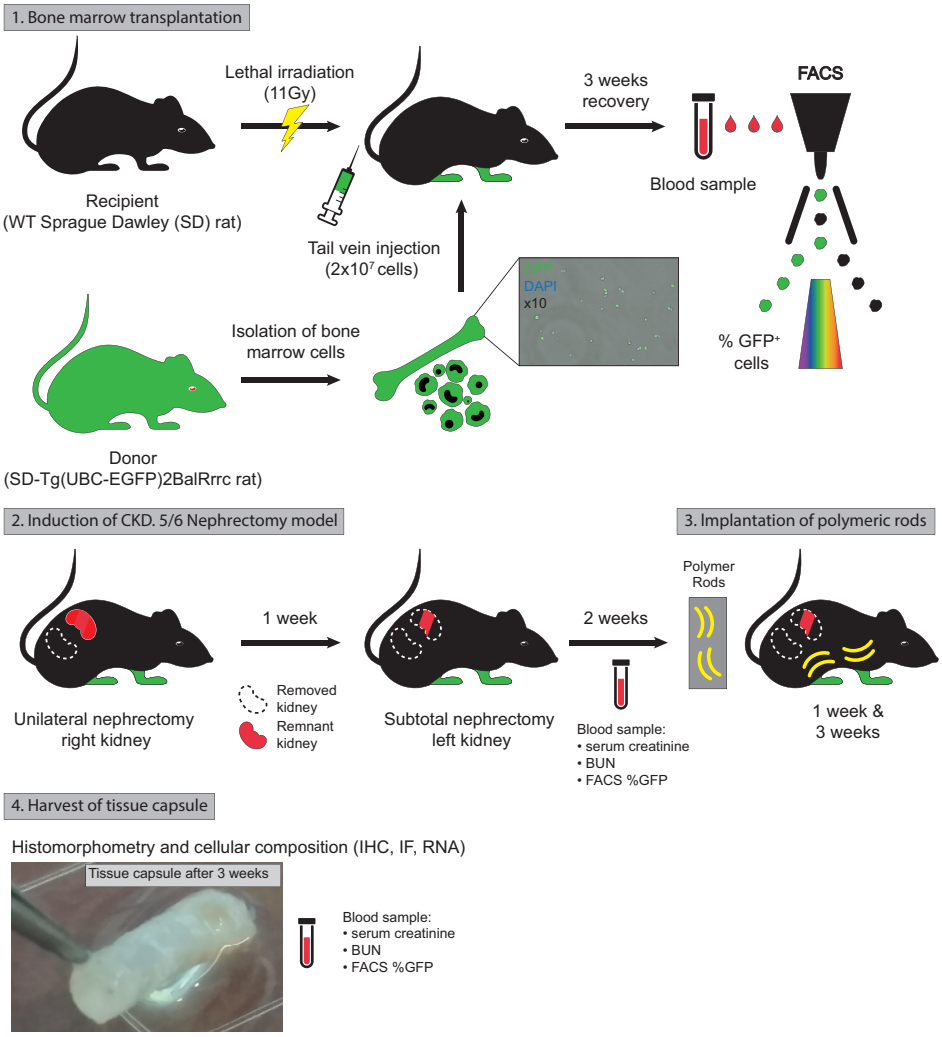

Figure 1. Schematic representation of the project work flow.
(1) 2*10^7 of total bone marrow cells harvested from transgenic Sprague Dawley (SD) rats ubiquitously expressing green fluorescent protein (GFP) were injected into the tail vein of wild-type (WT) SD recipient rats; n=27. Three weeks after the bone marrow reconstitution percentage of GFP$^+$ cells in the peripheral blood of recipient rats was measured by FACS analysis. (2) 2-step induction of chronic kidney disease (CKD); 1) unilateral right side nephrectomy and 2) 2/3 subtotal nephrectomy of the left kidney. Degree of CKD was confirmed by serum creatinine and blood urea nitrogen (BUN) levels 2 weeks after the procedure. (3) Polymeric rods were implanted into subcutaneous space of CKD and WT animals. (4) After 1 and 3 weeks implantation, rods together with formed fibrocellular tissue capsule were extruded and processed for further analysis. n=10 WT, n=8 CKD group.

Tissue capsule formation

Cellular organization within the TC gradually changed from a disorganized, highly nucleated structure at 1-week, to circumferentially aligned tissue at 3-weeks in both WT and CKD groups. TCs were mainly composed of extracellular matrix components (Figure 2a) and SMA$^+$ myofibroblasts (Figure 2b). The evolution of the TC formation was characterized by an initial accumulation of CD68$^+$ macrophages in proximity to the synthetic rod at the 1-week time point, whereas at 3-weeks CD68$^+$ cells were gradually dispersed through the entire TC volume (Figure 2c). Furthermore, the number of Ki67$^+$ proliferating cells at 3-weeks reduced by 40% and 67% (P=0.03) in WT and CKD animals, respectively, when compared to the 1-week time point (Figure 2d). The collagen density gradually increased as the TC maturated, forming a well-defined circular structure at 3-weeks in both WT and CKD animals (Figure 3a). Analysis of the total collagen content revealed increase in total collagen amount in the TCs at 3 weeks in both WT and CKD animals (WT: 54% increase, P=0.02; CKD: 61% increase, P=0.01) when compared to TCs obtained at 1 week after rod implantation (Figure 3b). No difference in collagen content was detected between WT and CKD animals, indicating that CKD state has no major influence on collagen synthesis in the TCs.

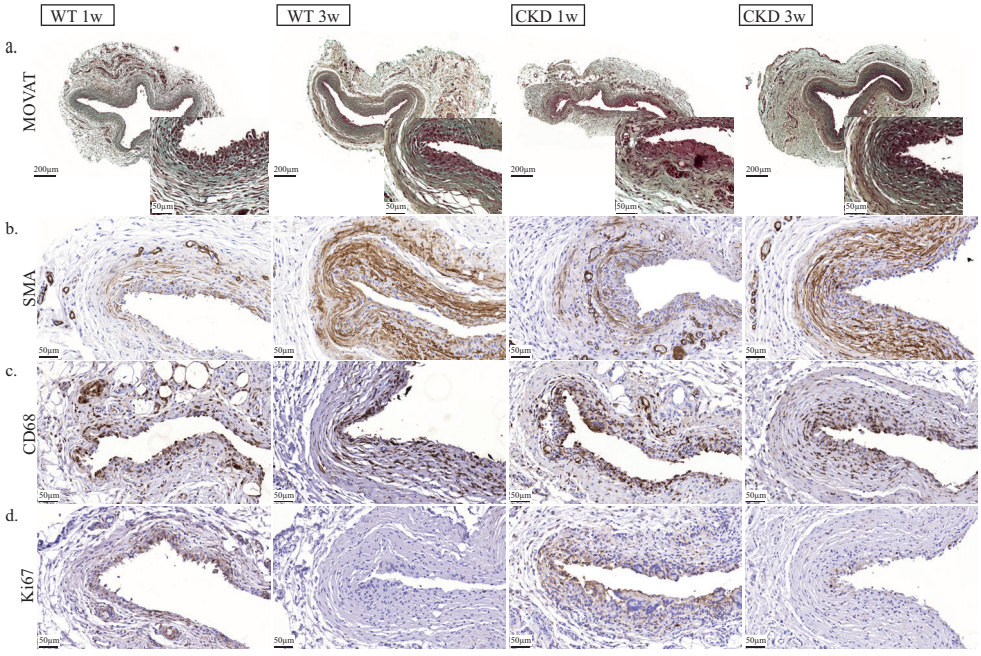

Figure 2. Cellular composition of tissue capsule at 1 and 3 weeks post-implantation. Immunohistochemical staining of (a) various constituents of connective tissues by MOVAT; (b) SMA$^+$ myofibroblasts, (c) CD68$^+$ macrophages and (d) Ki67$^+$ proliferating cells in the TC from healthy controls (WT) and chronic kidney disease (CKD) rats harvested at 1 and 3 weeks post-implantation. n=10 WT, n=8 CKD group.

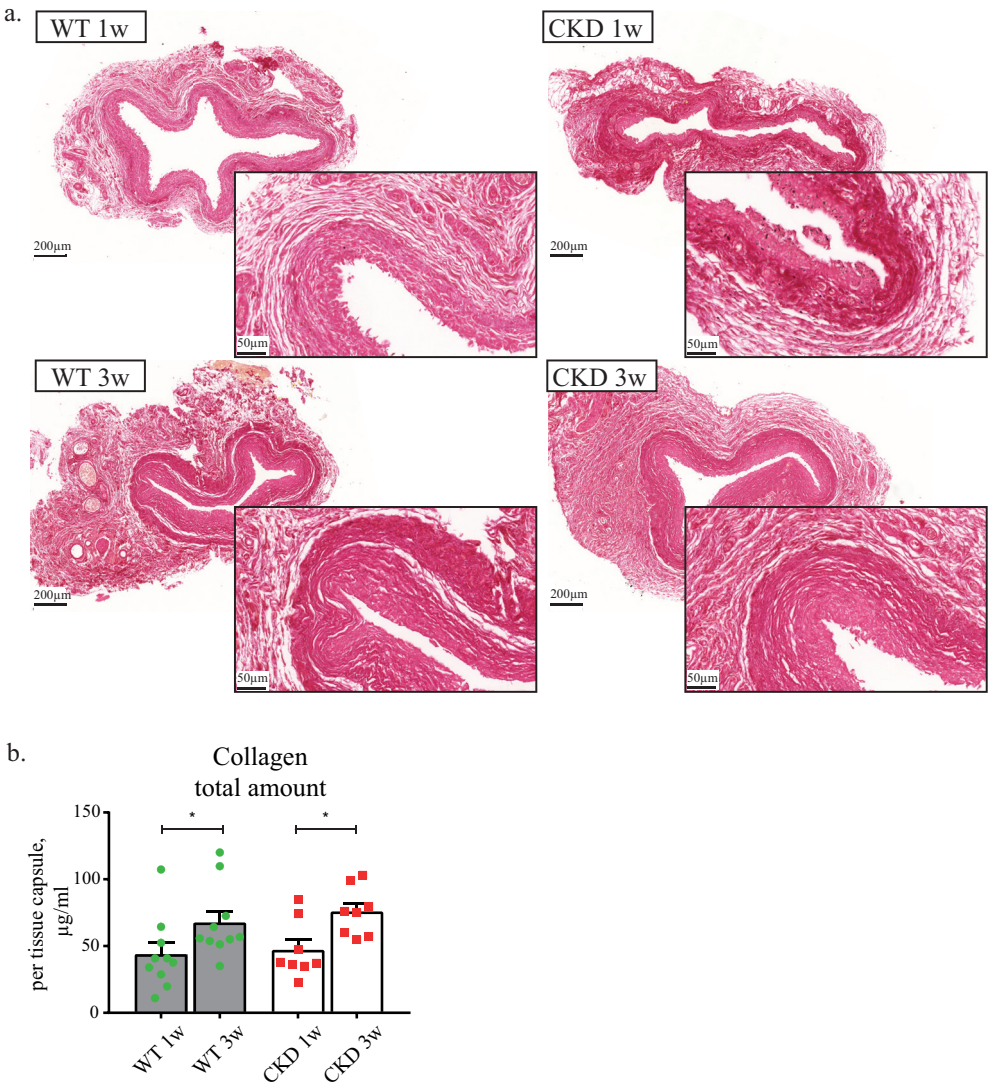

Figure 3. Changes in collagen content over the time course of tissue capsule maturation.
(a) Picrosirius red staining of the collagen. The collagen density gradually increased forming a well-defined circular structure at 3 weeks in both WT and CKD animals. (b) Analysis of the total collagen amount measured by QuickZyme Total Collagen Assay Kit. Significant increase in collagen content within WT and CKD groups was observed. (*) $P<0.05$; n=10 WT, n=8 CKD group.

A minority of inflammatory cells within TCs originates from the bone marrow

The number of CD68⁺ macrophages in the TCs at 3-weeks increased by 28% (P=0.03) and 82% (P=0.0006) in WT and CKD animals respectively, as compared to 1-week (Figure 4a,b).

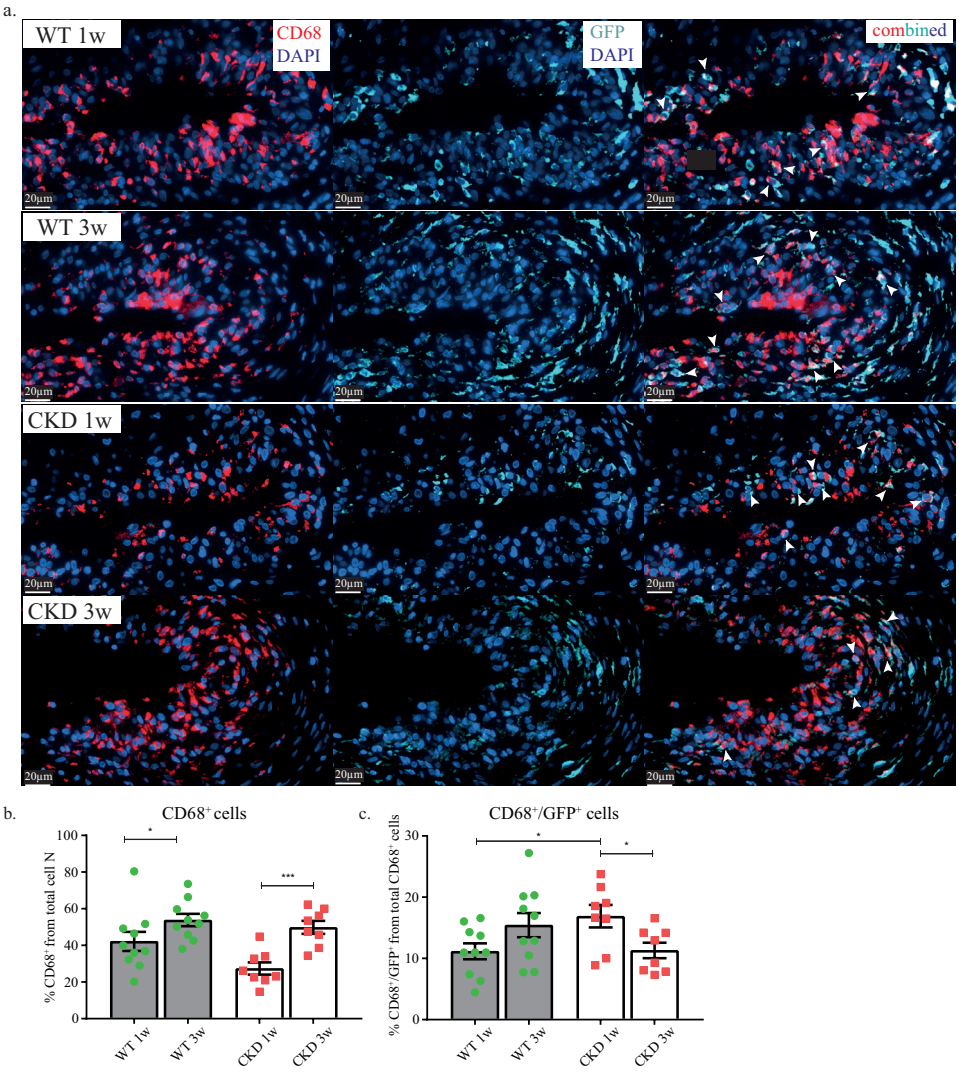

Figure 4. Macrophages in tissue capsule formation.

(a) Immunofluorescence staining of CD68⁺ macrophage marker (red color) and bone marrow derived GFP marker (light blue color). CD68⁺/GFP⁺ bone marrow derived macrophages (white arrows) was detected in the TC harvested at 1 and 3 weeks in WT and CKD group. (b) Quantification of total CD68⁺ macrophages within TC harvested at 1 and 3 weeks in WT and CKD animals. (c) Quantification of CD68⁺/GFP⁺ bone marrow derived macrophages from total CD68⁺ population. Nuclei DAPI (blue color). (*) P<0.05; (***) P<0.001; n=10 WT, n=8 CKD group.

Analysis of CD68⁺/GFP⁺ cells within TC at 1-week revealed that 11.2±1% and 16.9±2% of CD68⁺ cells originated from the bone marrow in WT and CKD group, respectively (Figure 4a,c). The percentage of BM-derived CD68⁺/GFP⁺ macrophages in TC at 3-weeks was 15.4±2% and 11.3±1.3% in WT and CKD group, respectively (Figure 4a,c). At 1-week time point, the percentage of CD68⁺ cells that expressed GFP was 1.5 times higher in the CKD group as compared to WT animals (P=0.03), whereas at 3-weeks this trend reversed (Figure 4c). The percentage of CD68⁺/GFP⁺ cells, from the CKD group, detected in the TC harvested at 3-weeks, was reduced by 33% as compared to the 1-week time point (P=0.02), (Figure 4c).

Contribution of bone marrow derived cells to myofibroblasts population in mature TCs

As described above, the TC harvested at 3-weeks was characterized by an increase in SMA⁺ myofibroblasts and accumulation of collagen and as compared to TCs obtained at 1-week after rod implantation (Figure 2b; 3a,b). Analysis of the TC harvested at 3-weeks revealed that 36% and 35% of SMA⁺ cells were originating from the BM as they were positive for GFP in WT and CKD group, respectively (Figure 5a,b). Moreover, 29% and 23% of SMA⁺/GFP⁺ myofibroblasts co-expressed a macrophage marker CD68 in the WT and CKD group, respectively (Figure 5a,c), suggesting a role for macrophage to myofibroblasts transition in TC formation.

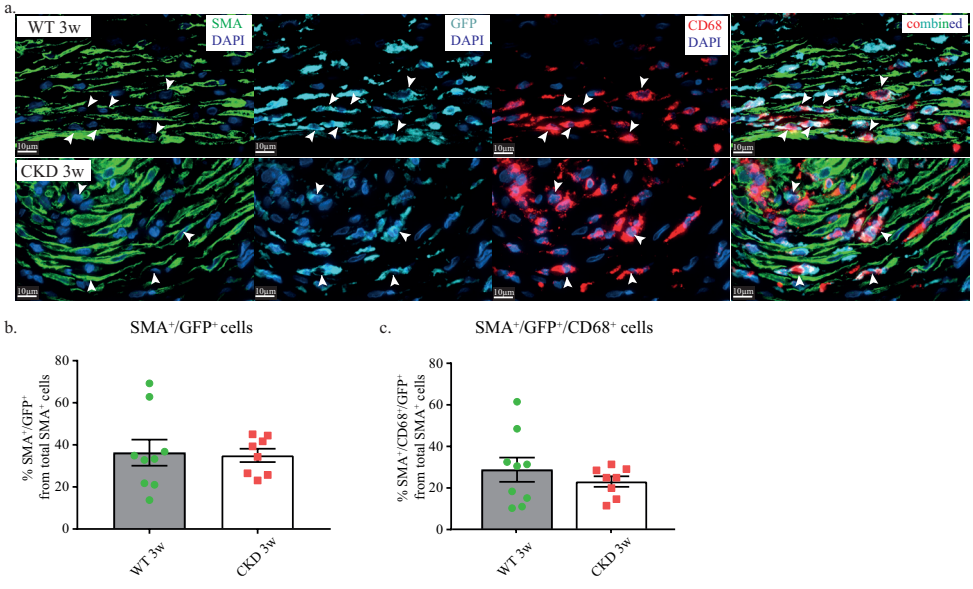

Figure 5. Macrophage to myofibroblasts transition.
(a) Immunofluorescence staining of SMA⁺ myofibroblasts (green color) co-expressing bone marrow derived GFP marker (light blue color) and CD68⁺ macrophage marker (red color). Population of SMA⁺/GFP⁺/CD68⁺ myofibroblasts (white arrows) was detected in TC at 3 weeks in both groups. Quantification of (b) SMA⁺/GFP⁺ and (c) SMA⁺/GFP⁺/CD68⁺ myofibroblasts from total SMA⁺ population within TC harvested at 3 weeks in WT and CKD group. Nuclei DAPI (blue color). n=9 WT, n=8 CKD group.

Tissue-resident macrophages in TC formation

There is accumulating evidence that tissue-resident macrophages orchestrate tissue-repair responses[23]. Immunohistochemical analysis of the TCs obtained at 3 weeks after rod implantation revealed that 53% and 58% of CD68$^+$ macrophages expressed the anti-inflammatory marker CD163$^+$, in WT and CKD animals respectively (Figure 6a,b). Gene expression analysis confirmed the repair-associated phenotype of these cells, as mRNA levels of transforming growth factor beta (TGFβ) in WT group was elevated by 2-fold (P=0.03), whereas mRNA levels of the anti-inflammatory cytokine IL10 in CKD group was 2-fold higher (P=0.04) in the TCs harvested at 3-weeks as compared to 1-week time point (Figure 6b).

Discrete population of cells positive for stem/progenitor-cell marker CD133

We observed a population of GFP$^+$/CD68$^-$ cells that accumulated predominantly at the outside border of the TC (Supplementary Figure 3). Interestingly, nearly all of these GFP$^+$/CD68$^-$ cells expressed CD133, a marker of progenitor cells of various origin[24], in both WT and CKD animals. Moreover, 24% of the CD133$^+$/GFP$^+$ cells co-expressed SMA (Figure 7a, b) indicating that BM derived hematopoietic stem cells can serve as direct precursors to myofibroblasts in mature TCs.

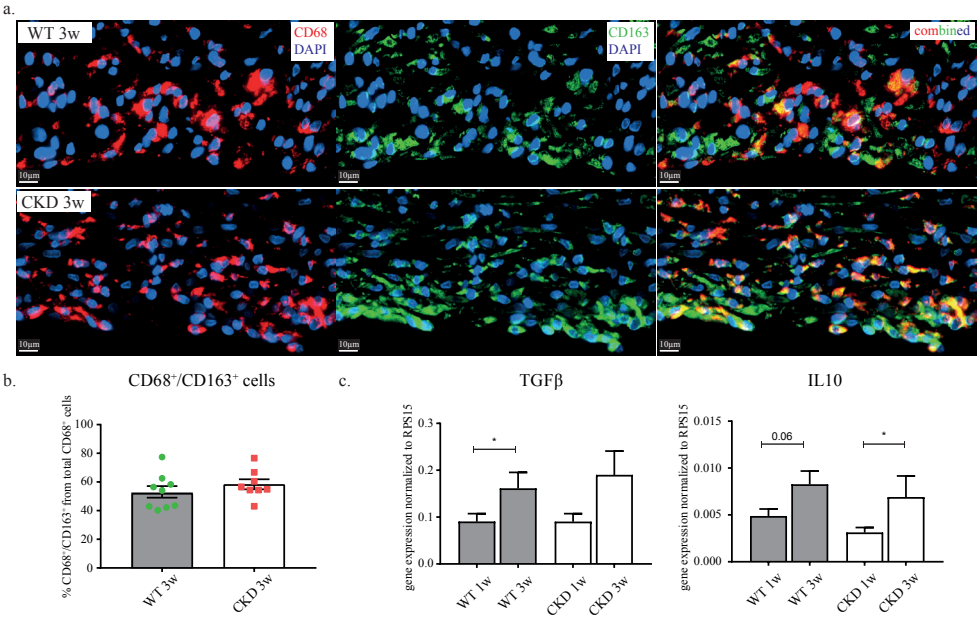

Figure 6. Tissue resident macrophages in tissue capsule formation.
(a) Immunofluorescence staining of CD68$^+$ macrophages (red color) positive for tissue resident marker CD163 (green color). (b) Quantification of the CD68$^+$/CD163$^+$ tissue resident macrophages from total CD68$^+$ cells. (c) Gene expression analysis of transforming growth factor beta (TGFβ) and anti-inflammatory cytokine IL10 in the TC at 1 and 3 weeks in WT and CKD group. Nuclei DAPI (blue color). (*) P=0.05; n=8 WT, n=8 CKD group.

Discussion

In the present study, we showed that both BM-derived and tissue-resident cells contribute to TC formation upon subcutaneous polymeric rod implantation. Surprisingly, only 13% of the macrophages within the TC originated from the BM, whereas 36% of the myofibroblast originated from BM precursors. A substantial number of SMA$^+$ bone marrow derived myofibroblasts co-expressed CD68, highlighting the role of the macrophage-to-myofibroblast transition in the formation of the TC. During the maturation of the TC, the cellular response predominantly displayed repair associated characteristics. Importantly, the CKD condition did not significantly affect the process of TC formation.

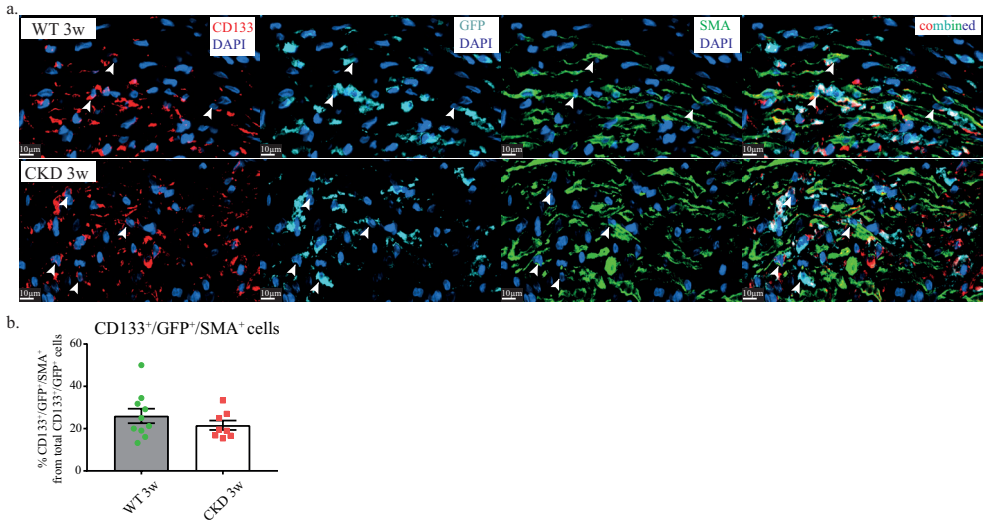

Figure 7. Expression of CD133 and GFP proteins by SMA$^+$ myofibroblasts in TC.
(a) Immunofluorescence staining of SMA$^+$ myofibroblasts (green color) originating from GFP$^+$ bone marrow (light blue color) derived CD133$^+$ stem/progenitor-cells (red color). CD133$^+$/GFP$^+$/SMA$^+$ cells (white arrows) were detected in the TC at 3 weeks in both experimental groups detected. (b) Quantification of CD133$^+$/GFP$^+$/SMA$^+$ within the TC at 3weeks in WT and CKD group. DAPI-nuclei blue. n=10 WT, n=8 CKD group.

Tissue-resident and BM-derived cells both contribute to the inflammatory response upon polymer rod implantation

Several studies have shown that the encapsulation of the foreign body is initiated with an inflammatory response, mainly through the activity of macrophages[14,15,25-27]. In this study, we also observed that along the inner border – adjacent to the polymeric rod – the tissue capsules were mainly composed of CD68$^+$ macrophages. Remarkably, only a minority of the macrophages within the TC originated from the bone marrow, as only 13% of the total CD68$^+$ population co-expressed GFP. Several studies suggest that cells within the local tissue environment, such as tissue-resident macrophages, also contribute to the foreign body response and play major role in the formation of

engineered tissue[28-30]. Tissue-resident macrophages consist of a mixture of embryonic- and adult-hematopoietic stem cell-derived macrophages, which have the capacity to self-renewal throughout adulthood[31,32].

Here, we show that the maturation of the TC is associated with a 40% increase in tissue-resident $CD68^+/CD163^+$ macrophages along with increase in IL10 and pro-fibrotic TGFβ mRNA levels within TCs. Besides, we did not observe a significant difference in $CD68^+/CD163^+$ macrophage population between CKD (46% of total macrophages) and WT animals (38%). Myofibroblast content was also similar between the groups. The latter most likely explains the similarity in collagen content in TCs as collagen is predominantly synthesized by (myo)fibroblasts.

Macrophages as precursors of myofibroblasts

During the development of the TC, we observed a gradual transition from granulation tissue towards circumferentially aligned SMA^+ myofibroblasts, whereas a substantial proportion of the myofibroblasts in the TCs were derived from hematopoietic BMCs. The ability of BM-derived cells to differentiate into smooth muscle-like cells was first described by Campbell and coworkers in their experimental work on TC formation in the peritoneal cavity[33]. Subsequent studies from the same group confirmed the plasticity of peritoneal macrophages and their ability to transdifferentiate from a myeloid to mesenchymal phenotype[34]. In our model, 26% of myofibroblasts originated from BM-derived macrophages, which illustrates the importance of macrophage-to-myofibroblast transition during the TC development.

Contribution of bone marrow progenitor cells to TC formation

Possibly, other than BM-derived and/or tissue resident macrophages can contribute to TC formation. A recent study by Wang *et al.* showed that $Sox10^+$ adult mouse stem cells found within the stroma of subcutaneous loose connective tissues, can contribute to encapsulation, fibrosis, and microvascularization of biomaterials upon implantation[35]. Interestingly, we observed a population of $CD133^+/GFP^+$ cells at the outer border of the TCs. Previous studies revealed that the membrane bound glycoprotein CD133 is expressed in mesenchymal stem cells (MSCs)[36] and stromal cells[37] within the BM. Both MSCs and stromal cells can give rise to human osteoblasts, adipocytes, chondrocytes as well as fibroblasts[38,39]. In this study, 24% $CD133^+/GFP^+$ cells were positive for SMA^+ suggesting that $CD133^+$ BM-derived cells can contribute to the myofibroblast population in mature tissue capsules.

CKD does not influence the cellular response during TC formation

As discussed above, the process of TC formation involves an acute inflammatory response, followed by chronic inflammation and fibrosis culminating in the encapsulation of the implanted biomaterial. CKD is a pro-fibrotic condition associated with tissue scarring as well as kidney and cardiac fibrosis[40-42]. Excessive TGFβ signaling, which has been implicated in epithelial cells and fibroblasts in CKD[41], can potentially enhance the process of TC formation in the subcutaneous space. On the other hand, CKD is associated with impaired function of both the innate and adaptive immune systems[17]. Circulating $CD34^+$ progenitor cells are markedly reduced in patients with CKD. In

addition, monocyte-macrophages are more prone to apoptosis in CKD patients[43], which could also negatively influence TC formation in CKD patients.

In the present study, we did not observe a significant effect of CKD on the cellular response upon implantation of the polymer rod. We hypothesize that the local foreign body response upon implantation of the polymer rod substantially differs from chronic inflammation and subsequent tissue fibrosis as observed in various organs of patients with CKD.

After only 3 weeks, tissue capsules were well matured, indicating the importance of the acute response and that the local environment within subcutaneous space is sufficient to maintain the process of TC formation.

Some aspects of our study require further discussion. One limitation in particular is the imperfect efficacy of the bone marrow transplantation, as only 75-80% of the cells in the peripheral blood were GFP^+ after BM-transplantation. As a consequence, the contribution of bone marrow derived cells in TC formation might be underestimated.

Our technology of tissue engineered blood vessels is aimed for patients with stage 5 of CKD which is defined as ESRD, when renal replacement therapy is required to survive. It needs to be emphasized that the 5/6-nephrectomy model used in the current study does not fully resemble ESRD, as the glomerular filtration rate (GFR) is this model is around 29-15% of normal (CKD stage 4). Thus, when extrapolating results to humans one should be cautious as TC formation in these rats might be slightly different when compared to dialysis patients. The pathophysiological mechanisms underlying CKD are also different between 5/6 nephrectomy animals and patients with CKD. Nevertheless, the 5/6-nephrectomy model in rats remains the most valuable and extensively investigated animal model mimicking human CKD[44-47].

Another limitation of this study is the inability to measure the mechanical strength of the TCs, an important parameter defining TC suitability for vascular grafting. However, a recent study performed in pigs demonstrates that the burst pressure and suture retention strength of the autologous TCs are sufficient to allow safe implantation in the arterial circulation[13].

Conclusion

This study illustrates that both BM-derived and resident cells contribute to the process of tissue response directed to a polymer rod that culminates in the formation of a collagen rich fibrocellular tissue capsule. BM-derived- as well as tissue resident macrophages serve as precursors of myofibroblasts in matured TCs. Notably, the presence of CKD does not significantly alter the process of TC formation, which supports the suitability of our autologous vascular tissue engineering approach for future clinical use in CKD patients.

Acknowledgements

This study was supported by a VIDI grant (016.156.328) awarded to J.I. Rotmans and funding from the National Institute of Health (EB012240 and HL083900) awarded to S. Li. We would like to thank Reshma A. Lalai for her excellent assistance in performing experiments and data analysis. Dr. Kei S. Iwamoto, from UCLA Radiation Oncology department for his excellent assistance in bone marrow transplantation experiments.

Flow cytometry was performed in the UCLA Jonsson Comprehensive Cancer Center (JCCC) and Center for AIDS Research Flow Cytometry Core Facility that is supported by National Institutes of Health awards P30 CA016042 and 5P30 AI028697, and by the JCCCJCCC, the UCLA AIDS Institute, the David Geffen School of Medicine at UCLA, the UCLA Chancellor's Office, and the UCLA Vice Chancellor's Office of Research.

Reference List

1. Diodato, M. & Chedrawy, E.G. Coronary artery bypass graft surgery: the past, present, and future of myocardial revascularisation. *Surgery research and practice* **2014**, 726158 (2014).
2. Kainz, A.*, et al.* Prediction of prevalence of chronic kidney disease in diabetic patients in countries of the European Union up to 2025. *Nephrology, dialysis, transplantation : official publication of the European Dialysis and Transplant Association - European Renal Association* **30 Suppl 4**, iv113-118 (2015).
3. Lloyd-Jones, D.*, et al.* Heart disease and stroke statistics--2010 update: a report from the American Heart Association. *Circulation* **121**, e46-e215 (2010).
4. Lee, T.*, et al.* Comparative analysis of cellular phenotypes within the neointima from vein segments collected prior to vascular access surgery and stenotic arteriovenous dialysis accesses. *Seminars in dialysis* **27**, 303-309 (2014).
5. Friedl, R.*, et al.* Intimal hyperplasia and expression of transforming growth factor-beta1 in saphenous veins and internal mammary arteries before coronary artery surgery. *The Annals of thoracic surgery* **78**, 1312-1318 (2004).
6. Rotmans, J.I.*, et al.* Hemodialysis access graft failure: time to revisit an unmet clinical need? *Journal of nephrology* **18**, 9-20 (2005).
7. Aslam, S., Vaida, F., Ritter, M. & Mehta, R.L. Systematic review and meta-analysis on management of hemodialysis catheter-related bacteremia. *Journal of the American Society of Nephrology : JASN* **25**, 2927-2941 (2014).
8. Roy-Chaudhury, P.*, et al.* Venous neointimal hyperplasia in polytetrafluoroethylene dialysis grafts. *Kidney international* **59**, 2325-2334 (2001).
9. Pashneh-Tala, S., MacNeil, S. & Claeyssens, F. The Tissue-Engineered Vascular Graft-Past, Present, and Future. *Tissue engineering. Part B, Reviews* (2015).
10. Yu, J.*, et al.* The effect of stromal cell-derived factor-1alpha/heparin coating of biodegradable vascular grafts on the recruitment of both endothelial and smooth muscle progenitor cells for accelerated regeneration. *Biomaterials* **33**, 8062-8074 (2012).
11. Geelhoed, W.J., Moroni, L. & Rotmans, J.I. Utilizing the Foreign Body Response to Grow Tissue Engineered Blood Vessels in Vivo. *Journal of cardiovascular translational research* **10**, 167-179 (2017).
12. Rothuizen, T.C.*, et al.* Tailoring the foreign body response for in situ vascular tissue engineering. *Tissue engineering. Part C, Methods* **21**, 436-446 (2015).
13. Rothuizen, T.C.*, et al.* Development and evaluation of in vivo tissue engineered blood vessels in a porcine model. *Biomaterials* **75**, 82-90 (2016).
14. Anderson, J.M., Rodriguez, A. & Chang, D.T. Foreign body reaction to biomaterials. *Seminars in immunology* **20**, 86-100 (2008).
15. Kenneth Ward, W. A review of the foreign-body response to subcutaneously-implanted devices: the role of macrophages and cytokines in biofouling and fibrosis. *Journal of diabetes science and technology* **2**, 768-777 (2008).
16. Westerweel, P.E.*, et al.* Impaired endothelial progenitor cell mobilization and dysfunctional bone marrow stroma in diabetes mellitus. *PloS one* **8**, e60357 (2013).
17. Kato, S.*, et al.* Aspects of immune dysfunction in end-stage renal disease. *Clinical journal of the American Society of Nephrology : CJASN* **3**, 1526-1533 (2008).
18. Teraa, M.*, et al.* Bone marrow alterations and lower endothelial progenitor cell numbers in critical limb ischemia patients. *PloS one* **8**, e55592 (2013).

19. Lois, C., Hong, E.J., Pease, S., Brown, E.J. & Baltimore, D. Germline transmission and tissue-specific expression of transgenes delivered by lentiviral vectors. *Science (New York, N.Y.)* **295**, 868-872 (2002).
20. van Koppen, A.*, et al.* Healthy bone marrow cells reduce progression of kidney failure better than CKD bone marrow cells in rats with established chronic kidney disease. *Cell transplantation* **21**, 2299-2312 (2012).
21. van Koppen, A., Verhaar, M.C., Bongartz, L.G. & Joles, J.A. 5/6th nephrectomy in combination with high salt diet and nitric oxide synthase inhibition to induce chronic kidney disease in the Lewis rat. *Journal of visualized experiments : JoVE*, e50398 (2013).
22. Damanik, F.F., Rothuizen, T.C., van Blitterswijk, C., Rotmans, J.I. & Moroni, L. Towards an in vitro model mimicking the foreign body response: tailoring the surface properties of biomaterials to modulate extracellular matrix. *Scientific reports* **4**, 6325 (2014).
23. Mantovani, A.*, et al.* The chemokine system in diverse forms of macrophage activation and polarization. *Trends in immunology* **25**, 677-686 (2004).
24. Yin, A.H.*, et al.* AC133, a novel marker for human hematopoietic stem and progenitor cells. *Blood* **90**, 5002-5012 (1997).
25. Miller, K.M., Huskey, R.A., Bigby, L.F. & Anderson, J.M. Characterization of biomedical polymer-adherent macrophages: interleukin 1 generation and scanning electron microscopy studies. *Biomaterials* **10**, 187-196 (1989).
26. Patino, M.G., Neiders, M.E., Andreana, S., Noble, B. & Cohen, R.E. Cellular inflammatory response to porcine collagen membranes. *Journal of periodontal research* **38**, 458-464 (2003).
27. Lucas, T.*, et al.* Differential roles of macrophages in diverse phases of skin repair. *Journal of immunology (Baltimore, Md. : 1950)* **184**, 3964-3977 (2010).
28. Davies, L.C., Jenkins, S.J., Allen, J.E. & Taylor, P.R. Tissue-resident macrophages. *Nature immunology* **14**, 986-995 (2013).
29. Okabe, Y. & Medzhitov, R. Tissue biology perspective on macrophages. *Nature immunology* **17**, 9-17 (2015).
30. Cailhier, J.F.*, et al.* Conditional macrophage ablation demonstrates that resident macrophages initiate acute peritoneal inflammation. *Journal of immunology (Baltimore, Md. : 1950)* **174**, 2336-2342 (2005).
31. Hashimoto, D.*, et al.* Tissue-resident macrophages self-maintain locally throughout adult life with minimal contribution from circulating monocytes. *Immunity* **38**, 792-804 (2013).
32. Dollinger, C.*, et al.* Incorporation of resident macrophages in engineered tissues: Multiple cell type response to microenvironment controlled macrophage-laden gelatine hydrogels. *Journal of tissue engineering and regenerative medicine* **12**, 330-340 (2018).
33. Campbell, J.H., Efendy, J.L., Han, C., Girjes, A.A. & Campbell, G.R. Haemopoietic origin of myofibroblasts formed in the peritoneal cavity in response to a foreign body. *Journal of vascular research* **37**, 364-371 (2000).
34. Mooney, J.E.*, et al.* Cellular plasticity of inflammatory myeloid cells in the peritoneal foreign body response. *The American journal of pathology* **176**, 369-380 (2010).
35. Wang, D.*, et al.* Sox10(+) adult stem cells contribute to biomaterial encapsulation and microvascularization. *Scientific reports* **7**, 40295 (2017).
36. Tondreau, T.*, et al.* Mesenchymal stem cells derived from CD133-positive cells in mobilized peripheral blood and cord blood: proliferation, Oct4 expression, and plasticity. *Stem cells (Dayton, Ohio)* **23**, 1105-1112 (2005).

37. Bakondi, B. & Spees, J.L. Human CD133-derived bone marrow stromal cells establish ectopic hematopoietic microenvironments in immunodeficient mice. *Biochemical and biophysical research communications* **400**, 212-218 (2010).
38. Bianco, P., Riminucci, M., Gronthos, S. & Robey, P.G. Bone marrow stromal stem cells: nature, biology, and potential applications. *Stem cells (Dayton, Ohio)* **19**, 180-192 (2001).
39. Jiang, Y.*, et al.* Pluripotency of mesenchymal stem cells derived from adult marrow. *Nature* **418**, 41-49 (2002).
40. Charytan, D.M.*, et al.* Increased concentration of circulating angiogenesis and nitric oxide inhibitors induces endothelial to mesenchymal transition and myocardial fibrosis in patients with chronic kidney disease. *International journal of cardiology* **176**, 99-109 (2014).
41. Xavier, S.*, et al.* Curtailing endothelial TGF-beta signaling is sufficient to reduce endothelial-mesenchymal transition and fibrosis in CKD. *Journal of the American Society of Nephrology : JASN* **26**, 817-829 (2015).
42. Mutsaers, H.A., Stribos, E.G., Glorieux, G., Vanholder, R. & Olinga, P. Chronic Kidney Disease and Fibrosis: The Role of Uremic Retention Solutes. *Frontiers in medicine* **2**, 60 (2015).
43. Bahlmann, F.H., Speer, T. & Fliser, D. Endothelial progenitor cells in chronic kidney disease. *Nephrology, dialysis, transplantation : official publication of the European Dialysis and Transplant Association - European Renal Association* **25**, 341-346 (2010).
44. Lu, H., Lei, X. & Klaassen, C. Gender differences in renal nuclear receptors and aryl hydrocarbon receptor in 5/6 nephrectomized rats. *Kidney international* **70**, 1920-1928 (2006).
45. Yang, H.C., Zuo, Y. & Fogo, A.B. Models of chronic kidney disease. *Drug discovery today. Disease models* **7**, 13-19 (2010).
46. Tsuprykov, O.*, et al.* The dipeptidyl peptidase inhibitor linagliptin and the angiotensin II receptor blocker telmisartan show renal benefit by different pathways in rats with 5/6 nephrectomy. *Kidney international* **89**, 1049-1061 (2016).
47. Bai, J.*, et al.* Netrin-1 attenuates the progression of renal dysfunction by blocking endothelial-to-mesenchymal transition in the 5/6 nephrectomy rat model. *BMC nephrology* **17**, 47 (2016).

Supplementary material

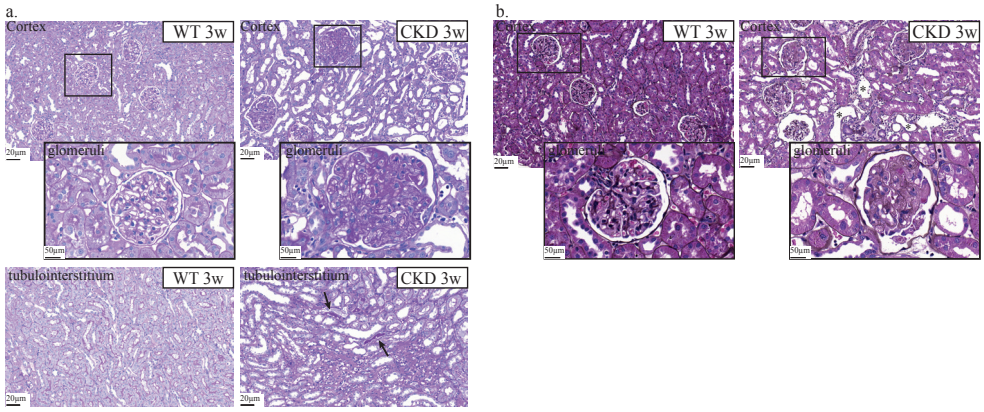

Supplementary Figure 1. Comparison of kidney histology between controls and rats underwent 5/6 nephrectomy.
(a.) Staining of kidney cortex with PAS (periodic acid-Schiff) highlights basement membranes of glomerular capillary loops. The capillary loops of WT glomerulus are well-defined an thin, as compared to enlarged sclerotic glomeruli, regions of tubular necrosis and tubular cast formation (black arrows) in CKD rats 5 weeks after 5/6 nephrectomy. (b.) Silver-stained kidney sections show pronounced glomerulosclerosis with dilated tubuli (black asterisks).

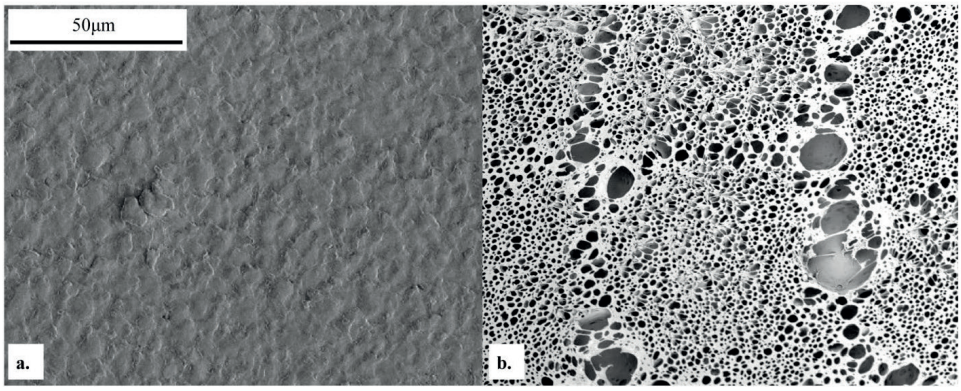

Supplementary Figure 2. Scanning electron microscopy images of (a) unmodified Pa300, (b) Pa300 chloroform-treated surface. Unmodified rods have smooth surfaces while chloroform etching resulted in porous structures on the surface.

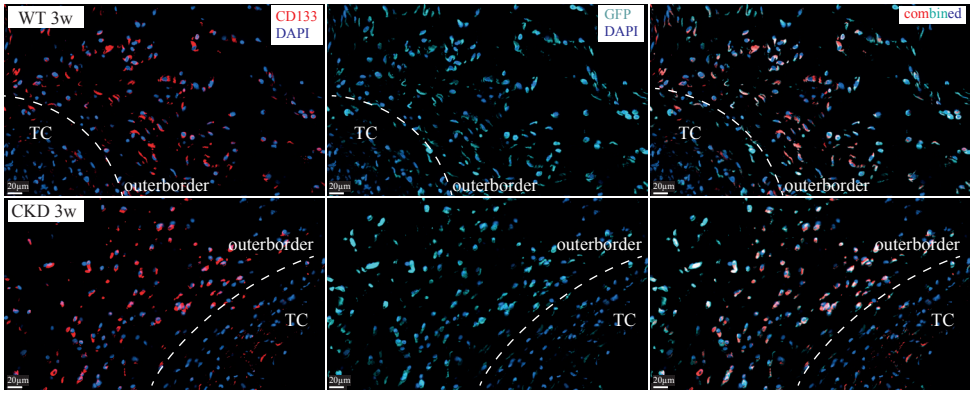

Supplementary Figure 3. Progenitor CD133⁺ bone marrow derived cells in tissue capsule.
Immunofluorescence staining of CD133⁺ stem/progenitor-cells (red color) originated from the GFP⁺ bone marrow (light blue color) detected in the TC at 3 weeks in WT and CKD groups. DAPI-nuclei blue.

Table 1 Primers used for *in vitro* experiments

Gene	Forward primer	Reversed primer
RPS15	CGTCACCCGTAATCCACC	CAGCTTCGCGTATGCCAC
IL10	AAAGCAAGGCAGTGGAGCAG	TCAAACTCATTCATGGCCTTGT
TGFβ	TGGCGTTACCTTGGTAACC	GGTGTTGAGCCCTTTCCAG

Chapter 7

Summary and Discussion

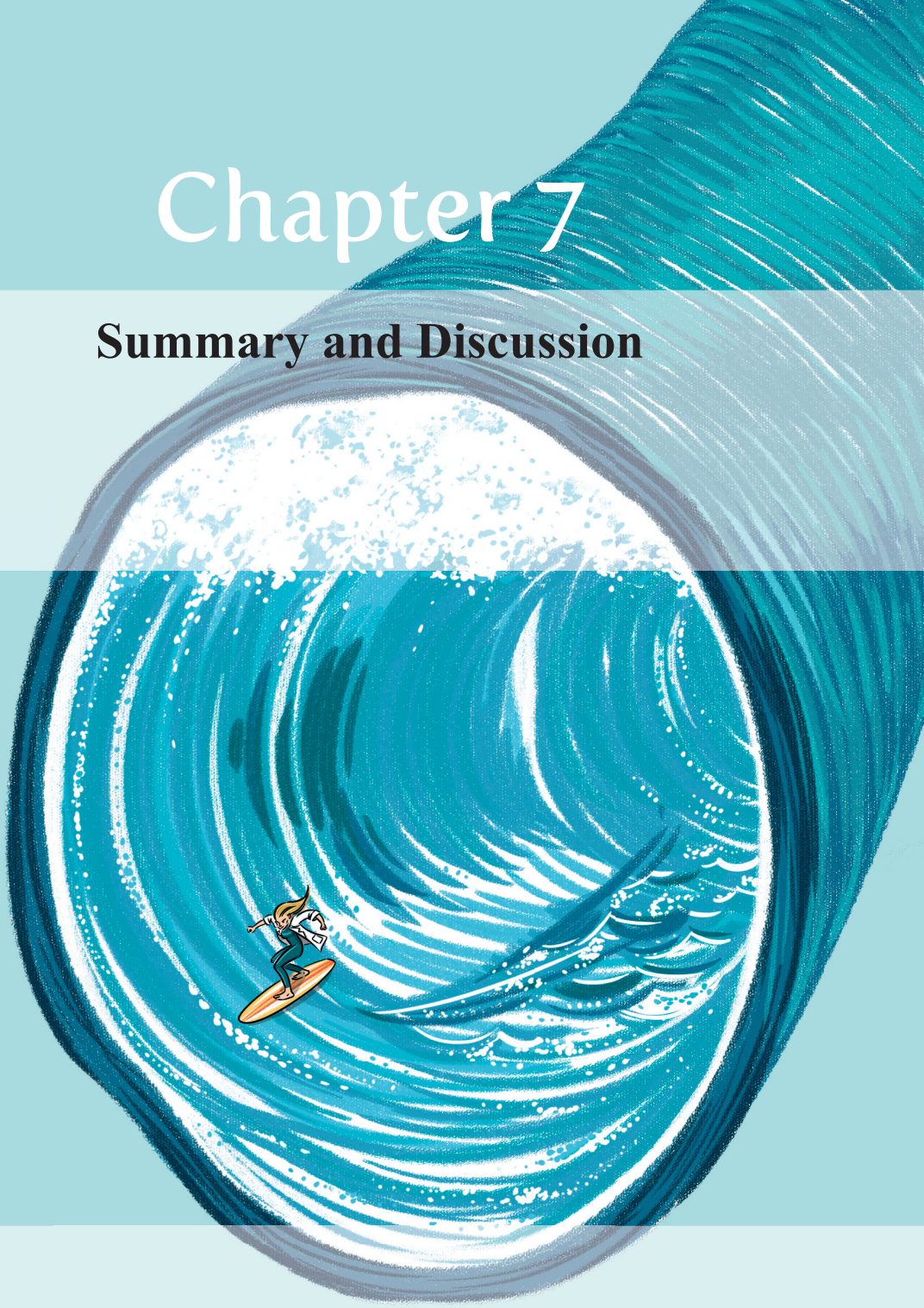

How it all started?

The view on renal replacement therapy was revolutionized in 1943 when the Dutch physician Dr. Willem Kollf built a first prototype of a dialyzer[1,2]. The first dialysis machines could get acute renal failure patients through a crisis until renal recovery, but the Achilles heel was a reliable access to the circulation for multiple dialysis sessions, which did not yet exist. Dialysis therapy for ESRD was first successfully attempted by Scribner in 1960 (Seatle, USA) after Quinton built the first shunt, based on a teflon-siliac loop externally placed between artery and vein of a patient[3]. Clyde Shields, a Boeing machinist, survived for 11 years after the insertion of Scribner's first AV shunt on 9 March 1960. Yet, Scribner-Quinton shunts usually lasted a few months or less, and were prone to clotting, skin necrosis, bleeding, and infection.

James E. Cimino and Michael J. Brescia (New York, USA) first described a 'simple venipuncture for hemodialysis'[4] followed by the historical paper 'Chronic hemodialysis using venipuncture and a surgically created arteriovenous fistula'[5] published in 1966 in NEJM. Dr. Cimino says. "We were bold in using a procedure that had always been considered physiologically abnormal, but without adequate vascular access our patients were doomed." Later, recalling the development of the AV fistula, Dr. Cimino adds "I had no idea our technique would continue to be popular for so many years later. I thought the real advances were going to be in chemistry, and that scientists would develop a pill to help patients with end-stage renal disease".

Where do we stand right now?

Even though at present kidney transplantation has become the preferred modality in kidney replacement therapy, the shortage of suitable donors is still persist. A considerable 40% of ESRD patients still depend on dialysis[6]. An adequately functioning AVF, described by Brescia and Cimino, remains the first choice for chronic HD serving as a lifeline for a lifetime in hemodialysis patients. Up to now, international guidelines strongly encourage the creation of AVFs for HD vascular access over prosthetic AV grafts and CVCs[7]. Ironically, being preferred and most commonly used vascular access point, AVFs dysfunction remains a major source of morbidity for patients with ESRD. At current, only few effective therapies for this clinical problem are available. One of the reasons is limited understanding of the underlying mechanisms that lead to AVF failure. The availability of animal models made it possible to study the pathogenesis of vascular access failure and to evaluate new treatment candidates.

Although the exact pathophysiology of AVF failure is not completely understood, there is a general consensus between researchers that IH and inadequate OR are two main processes that contribute to AVF failure[8,9]. Recent studies have shown that the process of vascular adaptation is mainly driven by altered hemodynamics after AVF creation and is associated with an excessive inflammatory response and proliferation and migration of arterial and venous VSMCs towards the intima at the site of anastomosis[10-14].

The work described in this thesis aimed to further understand the pathobiology of

vascular access dysfunction and identify new therapeutic candidates to improve the current status of hemodialysis vascular access.

New insights into the pathobiology of AVF

Targeting inflammation in AVF maturation

Although several studies have shown that the adaptive response upon AVF creation triggers infiltration of macrophages and lymphocytes[11] as well as upregulation of pro-inflammatory cytokine production[14], the role of inflammation in vascular remodeling upon AVF surgery has not been unraveled. Based on the previous knowledge that the TLR4 mediated inflammatory response contributes to several vascular pathologies[15-17], in **chapter 2** of this thesis we addressed the specific role of TLR4 homologue RP105 in vascular remodeling, inflammation and VSMCs function in a murine model of AVF failure. We clearly show that RP105 deficiency affects the inflammatory and VSMC-mediated response to injury during the course of AVF maturation, accumulating in an impaired outward remodeling of the venous outflow track of the AVF.

More detailed analysis of the effects of RP105 deficiency on the inflammatory response revealed strong accumulation of anti-inflammatory macrophages and an unexpected decrease in pro-inflammatory macrophages. The dominance of anti-inflammatory macrophages (> 90% of total macrophages) in the lesions at 2 weeks after AVF creation suggest either that in the current model pro-inflammatory response is completed at earlier time points, or that anti-inflammatory macrophages play a dominant role in the tissue response in murine AVF. Unfortunately, we did not study macrophage subpopulations at earlier time points. Concurrently, we observed a 50% decrease in MMP-activity *in vivo*, suggesting that the attenuation of vessel wall MMP activity limits venous OR in maturating AVFs.

VSMC content in AVFs from RP105 deficient mice was markedly decreased. *In vitro*, proliferation of venous VSMCs from RP105 deficient mice was reduced by 50%, whereas arterial VSMCs displayed a 50% decrease in migration. While VSMC proliferation in IH is generally considered to be detrimental, the process might be beneficial for OR, especially in the early phase of AVF maturation. In this respect, the observed reduction in venous outward remodeling, coupled with a reduction in proliferating venous VSMCs within AVFs, suggests that new drug targets designed to inhibit VSMCs proliferation could be detrimental for AVF maturation.

A striking observation in our studies was that RP105 diminution differentially affected arterial and venous VSMCs, as evidenced by RP105-specific effects on migration, proliferation and inflammatory cytokine production that differed substantially between these two cell sources. The endogenous expression levels of RP105 in arterial and venous VSMCs support this finding, along with differential expression profiles of associating TLR4-family members (including TLR4 and MD1). These findings illustrate the need for continued investigation of the phenotypic properties and functional characteristics of VSMCs in AVFs, in particular due to the contrasting lineage tracing studies detailing a predominance of arterial VSMCs[18] versus venous VSMCs[19] in venous IH following

AVF placement. This issue is further discussed in **chapter 5** of this thesis.

Overall, results of this study demonstrate that deletion of TLR4 homologue RP105 trigger alterations on various cell types involved in AVF maturation. In order to improve AVF outcomes, future therapeutic interventions targeting the TLR4/RP105 axis must include time-dependent and cell specific targeting approaches to steer the vascular remodeling response in the proper direction.

Our next step in understanding the role of inflammation in AVF maturation was aimed to understand whether inhibition of early inflammatory response triggered by AVF surgery directly contributes to maturation failure. Glucocorticoids (GCs) are well known anti-inflammatory drugs that bind to cytosolic glucocorticoid receptors in target cells, leading to the down-regulation in inflammatory cytokine production and reduction in inflammatory cell recruitment[20,21]. Despite being potent anti-inflammatory drugs chronic and systemic use of GCs is limited due to high incidents of severe side-effects[22]. In **chapter 3** of this thesis we aimed to test whether administration of liposomal prednisolone (L-Pred) will result in local inhibition of inflammatory response and, consequently, better AVF maturation. Targeted drug delivery achieved by incorporation of prednisolone into the liposomes hold great potential. As a result of enhanced vascular permeability caused by AVF surgery, circulating liposomal nanoparticles will extravasate and accumulate in the area around AV-anastomosis. To maximize efficacy and minimize toxicity of prednisolone is extremely important in such vulnerable patients as with ESRD.

First, using near infrared microscopy we demonstrated that liposomes extravasate in macrophages in the post-anastomotic area of the venous outflow tract—the most prone area of IH formation. As expected, we observed an 83% reduction in infiltrating leukocytes from which subpopulation of T-lymphocytes and granulocytes were reduced by 86% and 51% respectively. Treatment of macrophages with L-Pred *in vitro* induced transition towards an anti-inflammatory phenotype. Overall shift towards anti-inflammatory state might have inhibited the recruitment of lymphocytes and granulocytes to the AV-anastomosis. Alternatively, release of prednisolone from macrophages might have had a direct effect on lymphocytes and granulocytes.

At a morphometrical level, treatment with L-Pred resulted in a 27% increase in outward remodeling and 47% increase in luminal area. Control mice treated with unencapsulated prednisolone or liposomes loaded with PBS did not show any effect on morphometry. The exact mechanism by which liposomal prednisolone resulted in increased OR in murine AVF is not clear. We speculate that matrix metalloproteinases might contribute to this vascular response. The effect of MMPs on the vascular remodeling depend on the specific MMPs that are activated and the type of vascular injury[23]. Elegant study by Nieves Torres and coworkers[24] suggests effect of MMP inhibition on venous outward remodeling in AVF. Indeed, adventitial delivery of a small hairpin RNA against the MMP ADAMTS-1, resulted in reduced macrophage infiltration, decreased MMP9 activity and enhanced outward remodeling in murine AVF.

In our study, *in vitro* treatment of macrophages with L-Pred resulted in decreased MMP2 and MMP9 gene expression. Although we were not able to quantify MMP activity *in vivo*, we speculate that enhanced outward remodeling upon L-Pred treatment is mediated by the inhibition of inflammatory response and decrease MMP activity in macrophages.

In contrast to its effect on outward remodeling, no inhibitory effect of L-Pred on IH in the venous outflow tract was observed. These results deviate from other preclinical studies that evaluated the therapeutic effect of GCs in other vascular injury models, that have reported a strong inhibitory effect of dexamethasone on IH[25-27]. This discrepancy may result from a difference in potency between prednisolone and dexamethasone to inhibit VSMC proliferation[28]. Alternatively, it may relate to the difference in pathophysiological stimuli that contribute to IH after arterial injury, when compared to venous IH in AVF. While hemodynamic stimuli are considered to be of vital importance for IH[29,30], the contribution of inflammation to IH in AVF might be limited, as suggested by our results. As a consequence, interventions that facilitate OR might therefore also result in a (modest) stimulation of IH. Ultimately, the net result of vascular remodeling in the AVF was increased luminal area of the venous outflow tract, that was mainly accountable by the OR process alone. Of note, a stimulatory effect of an intervention on OR is more important for the ultimate luminal surface area than the coinciding effect on IH, as there is a quadratic relationship between radius and surface area of the vessel.

In conclusion, liposomal prednisolone reduces the local inflammatory response and stimulates venous outward remodeling in murine AVF. Therefore, treatment with liposomal prednisolone might be valuable strategy to reduce AVF non-maturation. The efficacy of liposomal prednisolone to enhance radiocephalic AVF maturation in ESRD patients is currently being evaluated in the LIPMAT trial (clinicaltrial.gov ID NCT0249566), a double-blind, randomized, placebo-controlled trial[31].

Targeting outward remodeling—a new direction for drug development?

While previous studies focused mainly on the development of strategies that aimed to reduce intimal hyperplasia, the current view on AVF maturation underscores the link between impaired outward remodeling and AVF failure[8,32]. Investigation of new targets that may promote outward remodeling might be of a great interest.

One of the appealing candidates is hormone relaxin (RLN2), originally known for its role in the growth and differentiation of the reproductive tract, and systemic hemodynamic adaptations during pregnancy, in particular vasodilatation[33-35]. In the context of AVF maturation, it is important to emphasize that RLN2 is expressed in the vessel wall[36,37] and that the observed vascular effects of RLN2 are mediated though an interaction with RXFP1 (relaxin/insulin-like peptide family receptor 1, original abbreviation LGR7), a G-protein-coupled receptor. In **chapter 4** of this thesis we examined the consequences of disturbing this hormone-receptor balance in murine model of AVF failure. Our hypothesis was that RXFP1 deficiency disables local signal transduction from endogenous relaxin after AVF surgery resulting in reduced OR. Indeed, deficiency of RXFP1 resulted in a 22% decrease in vessel size at the venous outflow tract 14 days after AVF surgery.

One of the main physiological actions of relaxin is its ability to remodel extracellular matrix components such as collagen and elastin in the cervix and myometrium during pregnancy[38,39]. In the settings of AVF, MMPs expression must be augmented to degrade and restructure the vascular matrix[40] to promote outward remodeling. Interestingly, peri-adventitial application of recombinant elastase has been shown to stimulate outward remodeling in a rabbit-model of AVF[41]. In our study we observed a 43% increase in elastin content in the lesions of RXFP1 deficient mice which coincided with a 41% reduction in elastase activity, suggesting that RXFP1 is an important regulator of elastin degradation during AVF maturation. Furthermore, it supports the concept that venous outward remodeling requires relaxin axis-mediated augmentation of elastase activity.

Interestingly, relaxin-relaxin receptor interactions are known to mitigate vascular inflammation, by inhibiting the upregulation of pro-inflammatory cytokines[42]. In line with these observations, we found that RXFP1 deficiency augments vascular inflammation in AVFs, as illustrated by a 6-fold increase in $CD45^+$ leukocytes, along with a 2-fold increase in MCP1 expression in the venous outflow tract.

Despite elevated levels of MCP1 in AVF lesions of RXFP1 deficient mice, we unexpectedly did not observe effects on venous intimal hyperplasia. Further *in vitro* experiments revealed that RXFP1 ablation caused a phenotypic switch of both arterial and venous VSMCs from a contractile towards a synthetic phenotype, as illustrated by augmentation of collagen, fibronectin, TGFβ and PDGF mRNA expression levels. Functional studies revealed elevated migration of arterial and venous VSMCs isolated form RXFP1 deficient mice. The question arises why RXFP1 deficiency *in vivo* resulted in decreased outward remodeling and had no effect on intimal hyperplasia, whereas *in vitro* functional studies clearly show impact of RXFP1 deficiency on VSMCs migration. In this respect, it is important to notice that the efficacy of cell migration *in vivo* strongly depends on the balance between cell deformability and ECM density, of which the latter is governed by the capacity of proteolytic enzymes to degrade matrix components[43]. Interestingly, RXFP1 deficiency resulted in a significant increase in elastin content as a result of decreased elastase activity. This preserved elastin density most likely explains why the increased migratory capacity of RXFP1 deficient VSMCs *in vitro*, did not translate into enhanced intima hyperplasia in the venous outflow tract of AVF in RXFP1 deficient mice. Finally, RXFP1 and RLN expression levels were increased in human AVFs, as compared to unoperated cephalic veins, strongly suggesting that therapeutic targeting of this pathway in the context of AVF maturation could be beneficial.

In conclusion, RXFP1 deficiency hampers elastin degradation and results in induced vascular inflammation after AVF surgery. These processes impair outward remodeling in murine AVF, suggesting that the relaxin-axis could be a potential therapeutic target to promote AVF maturation.

Remaining questions, points of consideration

One of the puzzling observations coming across this thesis is the difference in anatomical origin, gene expression profile and functional behavior of arterial and venous VSMCs. As the VSMCs and myofibroblasts are the main cell types contributing to intimal hyperplasia formation, it is of vital importance to gain more insights on the source of these cells within the neointima.

In **chapter 5** of this thesis, the anatomical origin of VSMCs that are responsible for venous stenotic lesions in arteriovenous fistulas is discussed. In the past, migrated VSMCs from the venous tunica media were considered to be the most prominent source of neointimal cells, more recent studies suggest that venous adventitial fibroblasts, circulating vascular progenitor cells, and arterial VSMCs might contribute as well.

Liang and coworkers in an elegant lineage tracing study suggested that VSMCs from the anastomosed artery contributed to as much as 50% of the VSMC compartment in the venous intima. The underlying mechanism was increased Notch signaling—a pathway critical in vascular development, in particular determining arterial versus venous vessel formation.

Not only different origin of VSMCs, but their physiological state might steer the cellular response in AVF maturation, as recent study from Zhao *et al.* suggests. Genetic mapping displayed a dual function of mature VSMCs in AVF maturation, with differentiated/contractile VSMCs contributing to medial wall thickening towards beneficial venous maturation and dedifferentiated/proliferative VSMCs contributing to detrimental neointimal hyperplasia[44].

These findings underscore importance to further understand the role of different VSMCs in AVF maturation. While discussing implementation of the inhibitors of VSMCs proliferation, such as Notch/FSP-1, to improve AVF patency we should keep in mind that complete inhibition of VSMC proliferation and migration in the early phase after AVF surgery does not necessarily translate into a better functional outcome of AVFs. In previous chapters of this thesis we have already discussed importance of VSMC proliferation as a prerequisite for adequate outward remodeling of the involved blood vessels. Therefore, the timing of the application of novel interventions to inhibit VSMC proliferation could be crucial for its effect on the functional outcome of the AVF. Another attractive aim for the future studies is to optimize venous adaptation to the arterial environment during postsurgical processes.

Beyond arteriovenous fistula

Even though AVF is preferred modality of hemodialysis vascular access site, native veins are often unavailable due to preexisting vascular pathology[12]. Utilization of synthetic vascular grafts predominantly results from the development of intimal hyperplasia ultimately leading to graft occlusion, and a relatively high risk of infectious

complications[45,46]. To create tissue engineered vascular grafts is one of the promising solutions to overcome current limitations of synthetic grafts and diseased native blood vessels. Previously, we developed a method to generate autologous TEBVs *in vivo*, which is based on the FBR directed to a subcutaneously implanted polymer rod that culminates in the formation of a fibrocellular TC[47]. Thus far, the origin of the cells present within the TCs remains unknown. Understanding the origin of cells present in the TC is of vital importance for its application as vascular grafts, as various disease conditions such as diabetes mellitus and CKD coincide with impaired function of BM-derived cells[48,49], which could hamper TC formation.

In **chapter 6** of this thesis, we elucidated the contribution of BM-derived cells in TC formation. For this purpose, we implanted polymer rods in the subcutis of rats after receiving BM-transplants with GFP-labeled BM cells. In addition, a CKD model was incorporated, as we aim to utilize the engineered vascular grafts for patients with ESRD requiring vascular access for hemodialysis.

In the early phase after rod implantation, TCs were mainly composed of $CD68^+$ macrophages which where predominantly located along the inner border, adjacent to the polymeric rod. On average, 13% of $CD68^+$ macrophages were GFP^+ cells, indicating BM origin. Several studies suggest that cells within the local tissue environment, such as tissue-resident macrophages, also contribute to the foreign body response and play major role in the formation of engineered tissue[50,51]. Here, we show that the maturation of the TC is associated with a 40% increase in repair associated $CD68^+/CD163^+$ macrophages along with increase in IL10 and pro-fibrotic TGFβ mRNA levels within TCs.

During the development of the TC, we observed a gradual transition from granulation tissue towards circumferentially aligned SMA^+ myofibroblasts. Macrophage-to-myofibroblasts differentiation appeared to play an important role in TC formation as 26% of SMA^+/GFP^+ myofibroblasts co-expressed macrophage marker CD68. Interestingly, we detected a population of $CD133^+$ bone marrow progenitor cells, positive for GFP, from which 24% were positive for SMA^+ suggesting that $CD133^+$ BM-derived cells can also contribute to the myofibroblast population in mature TC.

Finally, we did not observe a significant effect of CKD on the cellular response upon implantation of the polymer rod. We hypothesize that the local foreign body response upon implantation of the polymer rod is substantially differs from chronic inflammation and subsequent tissue fibrosis as observed in various organs of patients with CKD. After only 3 weeks, tissue capsules were well matured, indicating the importance of the acute response and that the local environment within subcutaneous space is sufficient to maintain the process of TC formation.

Overall results from our study show that both BM-derived, as well as tissue resident cells, contribute to TC formation, whereas macrophages serve as precursors of myofibroblasts in mature TCs. The presence of CKD did not significantly alter the process of TC formation, which supports our approach for future clinical use in ESRD patients.

Final conclusion

Dysfunction of vascular access remains a major clinical problem responsible for high morbidity and substantial health care costs in patients required chronic hemodialysis treatment. Despite the magnitude of this clinical problem, there have been no major novel therapeutic interventions in the field of hemodialysis access for the past few decades.

Even though nowadays more and more attention is drawn onto importance to understand pathobiology of vascular access dysfunction the complete picture is still missing.
In our group, we developed a unique murine AVF model, which has a configuration similar to the one used most frequently in humans (venous end-to-arterial side). This work has revealed that stenotic lesions in this murine AVF model closely resemble that in human failed fistulas. Specifically, pathological lesions are localized near the venous anastomosis and are characterized by proliferating VSMCs, infiltration of leukocytes and accumulation of extracellular matrix components.

Work described in this thesis, further shed light onto our understanding of the pathophysiology of AVF failure and identified new therapeutic targets aimed to improve patency of AV-fistula.

We first explored the role of inflammation in vascular remodeling upon AVF surgery. We unraveled the complex role of natural agonist of TLR4–RP105 in the pathophysiology of AVF failure identifying a novel relationship between inflammation and VSMC function.

Knowing that AVF surgery triggers influx of inflammatory cells in the vessel wall, in our subsequent study we focused on the strategy to reduce inflammation by administering liposomal prednisolone. We observed reduction in the local inflammatory response and increase in the venous outward remodeling, suggesting that local delivery of prednisolone via liposomes is beneficial for AVF maturation.

Based on the evolving concept of the importance of the outward remodeling in AVF maturation next, we evaluated the role of relaxin pathway as potential contributor to OR in AVF maturation. Deficiency of the relaxin receptor resulted in an impaired outward remodeling in the murine AVF, suggesting that the relaxin-axis could be a potential therapeutic target to promote AVF maturation. Together with our collaborators at the university Miami, Florida in near future we aim to test therapeutic agonist of relaxin in our AVF model and in hemodialysis patients.

In parallel with testing new therapeutics to improve maturation and patency of native AVFs, our group is working on developing TEBVs which could offer a suitable alternative for arteriovenous conduits. In collaboration with University of California, Los Angeles, we performed a lineage tracing to study the contribution of bone marrow derived cells to TEBV formation and the impact of CKD onto the process of TEBV formation. Importantly, the CKD condition did not significantly alter the process of

TEBV formation, supporting our technology to be relevant for future clinical use in ESRD patients.

Some aspects of our studies require further discussion. One of the limitations in our experimental setup is the inability to perform flow measurements and cannulations of the murine AVF, as an adequate blood flow volume and the cannulability of the AVF are the main characteristics of functional hemodialysis access.

Another point to consider is that our studies were performed in healthy mice. Recently established CKD model described by Kang *et al.* demonstrated that fistula maturation is affected by CKD, specifically the chronic accumulation of waste products and uremic toxins in the blood impacted AVF flow, resulting in increased venous wall thickness and thrombus formation[52].

However, we believe that decision on combining AVF model with CKD, should be well-reasoned and based not only on blind faith, but ethical justification. Welfare of laboratory animals is an important parameter of consideration while designing a new study. In studies aimed to identify new pathways involved in the pathobiology of AVF, the relevance of CKD implementation should be questioned.

For many years, vascular access was regarded as an exclusively surgical problem. Up to now, advances in vascular access treatments are limited. Medical professionals often focusing on the one-center experience and neglect importance to study the fundamental mechanisms leading to an arteriovenous fistula failure. It is time to recognize vascular access as truly multi-disciplinary science and to bring fields of molecular biology, medicine and new advances of biomaterials for local drug delivery to improve current patient care.

Reference List

1. Kolff, W.J. The artificial kidney. *Journal of the Mount Sinai Hospital, New York* **14**, 71-79 (1947).
2. Cooley, D.A. In Memoriam: Willem Johan Kolff 1911–2009. *Texas Heart Institute Journal* **36**, 83-84 (2009).
3. Scribner, B.H., Buri, R., Caner, J.E., Hegstrom, R. & Burnell, J.M. The treatment of chronic uremia by means of intermittent hemodialysis: a preliminary report. *Transactions - American Society for Artificial Internal Organs* **6**, 114-122 (1960).
4. Cimino, J.E. & Brescia, M.J. Simple venipuncture for hemodialysis. *The New England journal of medicine* **267**, 608-609 (1962).
5. Brescia, M.J., Cimino, J.E., Appel, K. & Hurwich, B.J. Chronic hemodialysis using venipuncture and a surgically created arteriovenous fistula. *The New England journal of medicine* **275**, 1089-1092 (1966).
6. Renine.nl. RENINE-year-report. *Online Source* (2016).
7. Clinical practice guidelines for vascular access. *American journal of kidney diseases : the official journal of the National Kidney Foundation* **48 Suppl 1**, S248-273 (2006).
8. Lee, T. & Misra, S. New Insights into Dialysis Vascular Access: Molecular Targets in Arteriovenous Fistula and Arteriovenous Graft Failure and Their Potential to Improve Vascular Access Outcomes. *Clinical journal of the American Society of Nephrology : CJASN* **11**, 1504-1512 (2016).
9. Rothuizen, T.C., *et al.* Arteriovenous access failure: more than just intimal hyperplasia? *Nephrology, dialysis, transplantation : official publication of the European Dialysis and Transplant Association - European Renal Association* **28**, 1085-1092 (2013).
10. Wong, C.Y., *et al.* Vascular remodeling and intimal hyperplasia in a novel murine model of arteriovenous fistula failure. *Journal of vascular surgery* (2013).
11. Wang, Y., *et al.* Venous stenosis in a pig arteriovenous fistula model--anatomy, mechanisms and cellular phenotypes. *Nephrology, dialysis, transplantation : official publication of the European Dialysis and Transplant Association - European Renal Association* **23**, 525-533 (2008).
12. Lee, T., *et al.* Comparative analysis of cellular phenotypes within the neointima from vein segments collected prior to vascular access surgery and stenotic arteriovenous dialysis accesses. *Seminars in dialysis* **27**, 303-309 (2014).
13. Lee, T. & Haq, N.U. New Developments in Our Understanding of Neointimal Hyperplasia. *Advances in chronic kidney disease* **22**, 431-437 (2015).
14. Nath, K.A., Kanakiriya, S.K., Grande, J.P., Croatt, A.J. & Katusic, Z.S. Increased venous proinflammatory gene expression and intimal hyperplasia in an aorto-caval fistula model in the rat. *The American journal of pathology* **162**, 2079-2090 (2003).
15. Hollestelle, S.C., *et al.* Toll-like receptor 4 is involved in outward arterial remodeling. *Circulation* **109**, 393-398 (2004).
16. Karper, J.C., *et al.* Blocking toll-like receptors 7 and 9 reduces postinterventional remodeling via reduced macrophage activation, foam cell formation, and migration. *Arteriosclerosis, thrombosis, and vascular biology* **32**, e72-80 (2012).
17. Vink, A. In Vivo Evidence for a Role of Toll-Like Receptor 4 in the Development of Intimal Lesions. *Circulation* **106**, 1985-1990 (2002).
18. Liang, M., *et al.* Migration of smooth muscle cells from the arterial anastomosis of arteriovenous fistulas requires Notch activation to form neointima. *Kidney international* **88**, 490-502 (2015).
19. Skartsis, N., *et al.* Origin of neointimal cells in arteriovenous fistulae: bone marrow, artery, or the vein itself? *Seminars in dialysis* **24**, 242-248 (2011).

20. Cronstein, B.N., Kimmel, S.C., Levin, R.I., Martiniuk, F. & Weissmann, G. A mechanism for the antiinflammatory effects of corticosteroids: the glucocorticoid receptor regulates leukocyte adhesion to endothelial cells and expression of endothelial-leukocyte adhesion molecule 1 and intercellular adhesion molecule 1. *Proceedings of the National Academy of Sciences of the United States of America* **89**, 9991-9995 (1992).
21. Rhen, T. & Cidlowski, J.A. Antiinflammatory action of glucocorticoids--new mechanisms for old drugs. *The New England journal of medicine* **353**, 1711-1723 (2005).
22. Oray, M., Abu Samra, K., Ebrahimiadib, N., Meese, H. & Foster, C.S. Long-term side effects of glucocorticoids. *Expert opinion on drug safety* **15**, 457-465 (2016).
23. Galis, Z.S. & Khatri, J.J. Matrix metalloproteinases in vascular remodeling and atherogenesis: the good, the bad, and the ugly. *Circulation research* **90**, 251-262 (2002).
24. Nieves Torres, E.C.*, et al.* Adventitial Delivery of Lentivirus-shRNA-ADAMTS-1 Reduces Venous Stenosis Formation in Arteriovenous Fistula. *PloS one* **9**, e94510 (2014).
25. Pires, N.M.*, et al.* Histopathologic alterations following local delivery of dexamethasone to inhibit restenosis in murine arteries. *Cardiovascular research* **68**, 415-424 (2005).
26. Schepers, A.*, et al.* Short-term dexamethasone treatment inhibits vein graft thickening in hypercholesterolemic ApoE3Leiden transgenic mice. *Journal of vascular surgery* **43**, 809-815 (2006).
27. Villa, A.E.*, et al.* Local delivery of dexamethasone for prevention of neointimal proliferation in a rat model of balloon angioplasty. *The Journal of clinical investigation* **93**, 1243-1249 (1994).
28. Reil, T.D., Sarkar, R., Kashyap, V.S., Sarkar, M. & Gelabert, H.A. Dexamethasone suppresses vascular smooth muscle cell proliferation. *The Journal of surgical research* **85**, 109-114 (1999).
29. Roy-Chaudhury, P., Spergel, L.M., Besarab, A., Asif, A. & Ravani, P. Biology of arteriovenous fistula failure. *Journal of nephrology* **20**, 150-163 (2007).
30. Asif, A., Roy-Chaudhury, P. & Beathard, G.A. Early arteriovenous fistula failure: a logical proposal for when and how to intervene. *Clinical journal of the American Society of Nephrology : CJASN* **1**, 332-339 (2006).
31. Voorzaat, B.M.*, et al.* Improvement of radiocephalic fistula maturation: rationale and design of the Liposomal Prednisolone to Improve Hemodialysis Fistula Maturation (LIPMAT) study - a randomized controlled trial. *The journal of vascular access* **18**, 114-117 (2017).
32. Guzman, R.J., Abe, K. & Zarins, C.K. Flow-induced arterial enlargement is inhibited by suppression of nitric oxide synthase activity in vivo. *Surgery* **122**, 273-279; discussion 279-280 (1997).
33. Conrad, K.P., Debrah, D.O., Novak, J., Danielson, L.A. & Shroff, S.G. Relaxin modifies systemic arterial resistance and compliance in conscious, nonpregnant rats. *Endocrinology* **145**, 3289-3296 (2004).
34. Feng, S., Bogatcheva, N.V., Kamat, A.A., Truong, A. & Agoulnik, A.I. Endocrine effects of relaxin overexpression in mice. *Endocrinology* **147**, 407-414 (2006).
35. Jeyabalan, A., Shroff, S.G., Novak, J. & Conrad, K.P. The vascular actions of relaxin. *Advances in experimental medicine and biology* **612**, 65-87 (2007).
36. Novak, J.*, et al.* Evidence for local relaxin ligand-receptor expression and function in arteries. *FASEB journal : official publication of the Federation of American Societies for Experimental Biology* **20**, 2352-2362 (2006).
37. Jelinic, M.*, et al.* Localization of relaxin receptors in arteries and veins, and region-specific increases in compliance and bradykinin-mediated relaxation after in vivo serelaxin treatment. *FASEB journal : official publication of the Federation of American Societies for Experimental Biology* **28**, 275-287 (2014).

38. Finlay, G.A., O'Donnell, M.D., O'Connor, C.M., Hayes, J.P. & FitzGerald, M.X. Elastin and collagen remodeling in emphysema. A scanning electron microscopy study. *The American journal of pathology* **149**, 1405-1415 (1996).
39. Chen, B., Wen, Y., Yu, X. & Polan, M.L. Elastin metabolism in pelvic tissues: is it modulated by reproductive hormones? *American journal of obstetrics and gynecology* **192**, 1605-1613 (2005).
40. Chan, C.Y., Chen, Y.S., Ma, M.C. & Chen, C.F. Remodeling of experimental arteriovenous fistula with increased matrix metalloproteinase expression in rats. *Journal of vascular surgery* **45**, 804-811 (2007).
41. Peden, E.K.*, et al.* Arteriovenous fistula patency in the 3 years following vonapanitase and placebo treatment. *Journal of vascular surgery* **65**, 1113-1120 (2017).
42. Brecht, A., Bartsch, C., Baumann, G., Stangl, K. & Dschietzig, T. Relaxin inhibits early steps in vascular inflammation. *Regulatory peptides* **166**, 76-82 (2011).
43. Wolf, K.*, et al.* Physical limits of cell migration: control by ECM space and nuclear deformation and tuning by proteolysis and traction force. *The Journal of cell biology* **201**, 1069-1084 (2013).
44. Zhao, J.*, et al.* Dual Function for Mature Vascular Smooth Muscle Cells During Arteriovenous Fistula Remodeling. *Journal of the American Heart Association* **6**(2017).
45. Rotmans, J.I.*, et al.* Hemodialysis access graft failure: time to revisit an unmet clinical need? *Journal of nephrology* **18**, 9-20 (2005).
46. Roy-Chaudhury, P.*, et al.* Venous neointimal hyperplasia in polytetrafluoroethylene dialysis grafts. *Kidney international* **59**, 2325-2334 (2001).
47. Rothuizen, T.C., et al. Development and evaluation of in vivo tissue engineered blood vessels in a porcine model. *Biomaterials* 75, 82-90 (2016).
48. Westerweel, P.E.*, et al.* Impaired endothelial progenitor cell mobilization and dysfunctional bone marrow stroma in diabetes mellitus. *PloS one* **8**, e60357 (2013).
49. Kato, S.*, et al.* Aspects of immune dysfunction in end-stage renal disease. *Clinical journal of the American Society of Nephrology : CJASN* **3**, 1526-1533 (2008).
50. Okabe, Y. & Medzhitov, R. Tissue biology perspective on macrophages. *Nature immunology* **17**, 9-17 (2015).
51. Cailhier, J.F.*, et al.* Conditional macrophage ablation demonstrates that resident macrophages initiate acute peritoneal inflammation. *Journal of immunology (Baltimore, Md. : 1950)* **174**, 2336-2342 (2005).
52. Kang, L.*, et al.* A new model of an arteriovenous fistula in chronic kidney disease in the mouse: beneficial effects of upregulated heme oxygenase-1. *American journal of physiology. Renal physiology* **310**, F466-476 (2016).

Chapter 8

Nederlandse Samenvatting

Curriculum Vitae

List of Publications

Acknowledgement

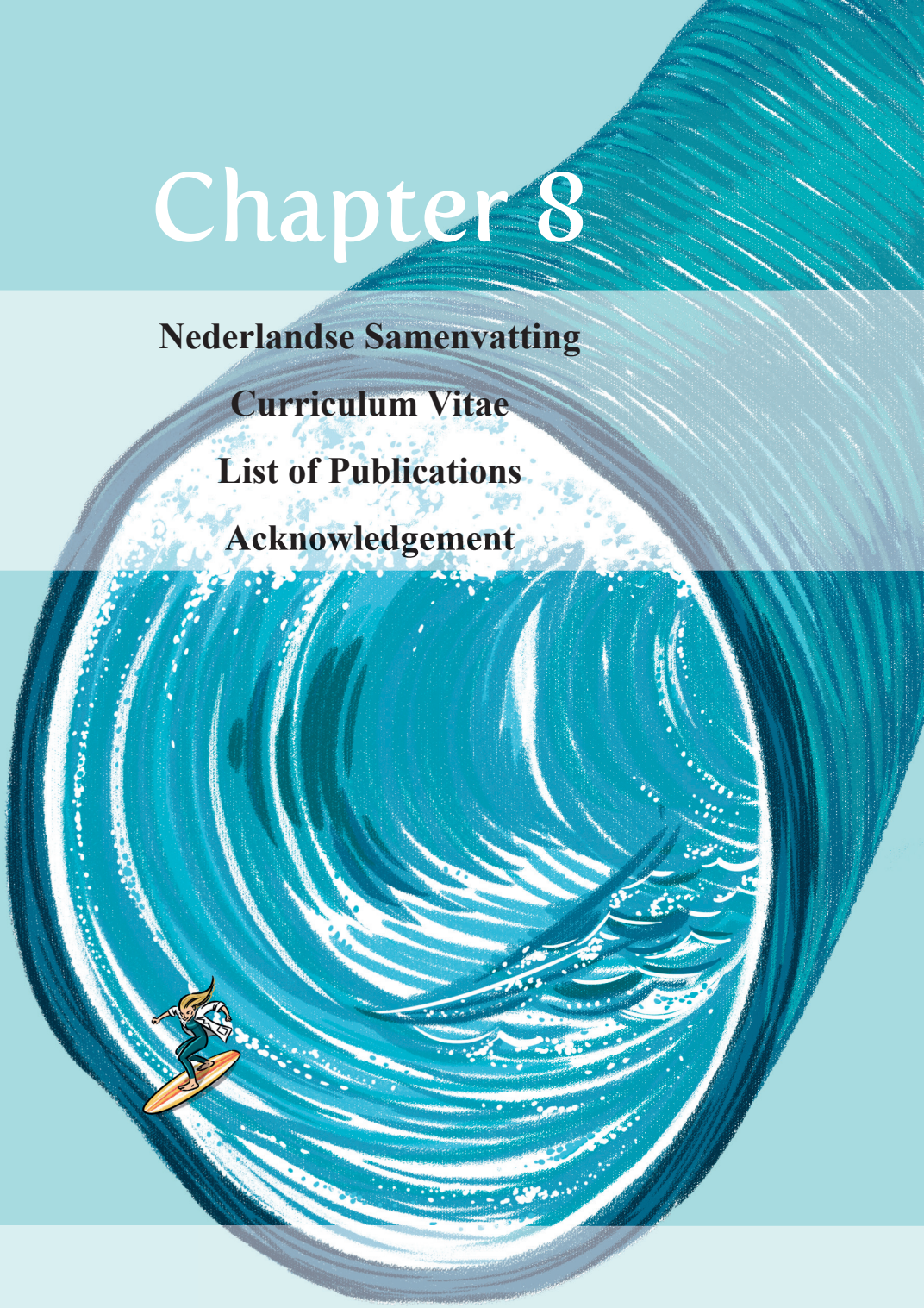

Nederlandse Samenvatting

Niertransplantatie is momenteel de beste behandeling voor chronisch nierfalen, er is echter een groot tekort aan donoren en sommige patiënten zijn niet in de conditie om veilig een niertransplantatie te ondergaan. Derhalve zijn 40% van de patiënten met eindstadium nierfalen nog steeds afhankelijk van dialyse. De meest voorkomende vorm van dialyse is hemodialyse. Tijdens de hemodialyse behandeling wordt het extracorporaal verwijderen van afvalstoffen en het verwijdering van vloeistoffen direct via het bloed uitgevoerd. Om de hemodialyse procedure te beginnen, is er een toegang tot een bloedvat met een hoge bloedstroomsnelheid nodig. Tot op het heden is de arterioveneuze fistel (AVF), een directe verbinding tussen een arterie en een vene, de gouden standaard van hemodialyse vaattoegang.

Complicaties van de vaattoegang zijn een belangrijke oorzaak van morbiditeit voor patiënten met eindstadium nierfalen. Om de vaattoegang te kunnen verbeteren is het van groot belang om de onderliggende mechanismen achter AVF dysfunctie beter te begrijpen. Alleen dan kunnen nieuwe effectieve therapieën worden ontwikkeld.

Het onderzoek in dit proefschrift is gericht op het beter begrijpen van de pathofysiologie van vaattoegang disfunctie, en nieuwe therapeutische targets te identificeren om de vaattoegang voor dialyse te verbeteren.

Nieuwe inzichten in de pathobiologie van AVF

Inflammatie in AVF maturatie

Eerder onderzoek heeft aangetoond dat het proces van vaatadaptatie na het maken van de AVF gepaard gaat met een excessieve inflammatoire response.

In **hoofdstuk 2 en 3** van dit proefschrift zal de bijdrage van inflammatie op AVF maturatiefalen worden bestudeerd.

Gebaseerd op bestaande kennis dat de toll-like receptor 4 (TLR4) gemedieerde inflammatoire response bijdraagt aan verschillende vaatziekten, wordt in **hoofdstuk 2** van dit proefschrift de specifieke rol van TLR4 homoloog RP105 met betrekking tot vaatremodelering, inflammatie, en gladde spiercelfunctie in een muis model van AVF falen beschreven.

Een meer gedetailleerde analyse van het effect van RP105 deficiëntie op de inflammatoire response toonde een sterke accumulatie van anti-inflammatoire macrofagen en een vermindering in de hoeveelheid pro-inflammatoire macrofagen. Daarnaast resulteerde de afwezigheid van RP105 in een duidelijke vermindering van de hoeveelheid gladde spiercellen in de AVF in muizen. Een onverwachte bevinding in deze studie was dat RP105 vermindering de veneuze en arteriële gladde spiercellen anders beïnvloed. Samenvattend heeft de deletie van RP105 impact op de verschillende celtypes die betrokken zijn bij AVF maturatie. Om de uitkomsten van AVFs te verbeteren is het van

belang om toekomstige TLR4/RP105 gerichte therapieën cel specifiek te maken om de vasculaire response in de juiste richting te leiden.

De volgende stap in het begrijpen van de rol van inflammatie in AVF maturatie was om te testen of het remmen van de vroege inflammatoire response in de vaatwand resulteert in een betere uitkomst van AVFs. In **hoofdstuk 3** van dit proefschrift wordt liposomaal prednisolon, een bekende anti-inflammatoire stof, toegediend in muizen met een AVF. Door de incorporatie van prednisolon in de liposomen wordt een optimale locatie-specifieke concentratie van het geneesmiddel bereikt waardoor minder systemische bijwerkingen optreden van prednisolon. Dit onderzoek liet zien dat behandeling met liposomaal prednisolon resulteert in een 83% verminderingen van ontstekingscellen in de vaatwand en een bijna 50% toename in het lumenoppervlak van de AVF. Daarom zou liposomaal prednisolon een strategie kunnen zijn om de bruikbaarheid van AVFs als vaattoegang voor dialyse te verbeteren. Het effect van liposomaal prednisolon om AVFs te verbeteren in patiënten met nierfalen wordt momenteel geëvalueerd in de LIPMAT studie (clinicaltrial.gov ID NCT0249566), een dubbel geblindeerde, gerandomiseerde, placebo gecontroleerde klinische studie.

Stimulatie van outward remodeling - een nieuwe optie om AVFs te verbeteren?
De meeste studies die zijn verricht om AVF functie te verbeteren richten zich op de ontwikkeling van strategieën ter vermindering van intimal hyperplasie. Er zijn echter steeds meer aanwijzingen dat het bevorderen van de groei van de betrokken bloedvaten (outward remodeling) een goede optie zou kunnen helpen om AVF falen te voorkomen.

Het hormoon relaxin (RLN2) speelt mogelijk een rol in de groei van bloedvaten. Relaxin draagt immers in belangrijke mate bij aan de aanpassing van bloedvaten tijdens de zwangerschap (met name vasodilatatie). Zowel RLN2 als de relaxin-receptor (RXFP1) komen tot expressie in de wand van bloedvaten. In **hoofdstuk 4** van dit proefschrift wordt onderzocht wat het effect is van het wegnemen van relaxin op AVFs in muizen die geen relaxin-receptor hebben. Onze hypothese is dat het ontbreken van RXFP1 resulteert in een verminderde outward remodeling. In dit onderzoek leidde een tekort aan RXFP1 inderdaad tot een 22% vermindering in vaatoppervalk ter plaatse van veneuze component van de AVF.

Een van de voornaamste fysiologische werkingen van relaxin is het remodelleren van extracellulaire matrix componenten zoals collageen en elastine in de cervix en myometrium tijdens de zwangerschap. In ons onderzoek observeerden wij een 43% vermindering in de hoeveelheid elastine in de lesies van RXFP1 deficiënte muizen. Dit kwam overeen met een 41% reductie in elastase activiteit, wat aangeeft dat RXFP1 en belangrijke regulator is van elastine degradatie tijdens AVF maturatie.

De interacties van relaxin met de relaxin receptor bevordert inflammatie. In ons onderzoek ontdekten we dat RXFP1 deficiëntie ook de vaatinflammatie in AVF beïnvloedt, geïllustreerd door een 6-voudige toename van leukocyten in de vaatwand, en een 2-voudige verhoging van MCP-1 expressie, een belangrijk pro-inflammatoir cytokine. Ook in humane AVFs konden we aantonen dat de expressie niveaus van

RXFP1 en RLN verhoogd zijn ten opzicht van normale bloedvaten. Deze bevinding ondersteunt de potentie van relaxin als therapeutisch target bij het stimuleren van AVF maturatie.

Vervolgonderzoek
Een van de meest opmerkelijke bevindingen in dit proefschrift is het verschil tussen de anatomische origine, genexpressie profiel en functioneel gedrag van arteriële en veneuze gladde spiercellen.

In **hoofdstuk 5** van deze thesis wordt de anatomische origine van VSMCs in stenotische lesies besproken. Tot het heden werden gladde spiercellen die migreerde van de middenlaag van bloedvaten (tunica media) gezien als de meest prominente oorsprong van neointimal cellen. Recent onderzoek wijst echter uit dat veneuze adventitiele fibroblasten, circulerende progenitor cellen, en arteriële gladde spiercellen ook bijdragen aan stenose in AVFs.

Beyond arteriovenous fistulas

Hoewel een AVF de meest gebruikte vorm van vaattoegang is, zijn geschikte venen niet altijd beschikbaar. Het gebruik van kunststof bloedvaten wordt beperkt door slechte uitkomsten, waarbij de kunststof vaten veelal dichtgroeien en verstopt raken en een hoog risico van infectie met zich mee brengen. Tissue-engineered bloedvaten zijn een veelbelovende oplossing om de nadelen van synthetische, en pathologische vaten omzeilen.

De afgelopen jaren hebben wij een methode ontwikkeld waarbij nieuwe bloedvaten worden gemaakt door de patiënt zelf, door een polymeer staafje onderhuids te implanteren. De zogenaamde vreemd lichaamsreactie leidt tot de formatie van een fibrocellulaire weefselcapsule, die gebruikt kan worden als lichaamseigen bloedvat. Tot op het heden blijft de origine van de cellen in deze weefselcapsule onbekend. In **hoofdstuk 6** van dit proefschrift wordt de contributie van beenmerg cellen in weefsel capsule vorming onderzocht. Polymere staafjes werden onderhuids geïmplanteerd in ratten die een beenmerg transplantatie van speciaal-gelabelde cellen (met GFP) hebben gekregen. Een nierfalenmodel werd ook geïncorporeerd, aangezien het doel is om deze weefsel capsules te implementeren als vaat toegang in patiënten met eindstadium nierfalen.

In de vroege fase na het implanteren van de staafjes bestaan de weefselcapsules grotendeels uit macrofagen. Gemiddeld bleek 13% van de macrofagen in de weefselcapsules afkomstig uit het beenmerg. Tijdens de ontwikkeling van de weefselcapsule veranderd het weefsel van ontstekingsweefsel met macrofagen in granulatieweefsel, vooral bestaand uit myofibroblasten. De macrofaag naar myofibroblast differentiatie leek een belangrijke rol te spelen in de vorming van de weefsel capsule aangezien 26% van de GFP- myofibroblasten een macrofaag marker tot expressie brachten.

Deze resultaten geven aan dat cellen vanuit het beenmerg en lokale cellen uit de

onderhuid bijdragen aan de weefselcapsule vorming. De aanwezigheid van nierfalen had geen invloed op de vorming van de weefselcapsules, wat aangeeft ons doel versterkt van het toepassen van deze techniek in patiënten met eind stadium niet falen.

Tot slot geeft **hoofdstuk 7** een beschouwing en discussie van alle studies die in dit proefschrift zijn beschreven.

Curriculum Vitae

Taisiya Bezhaeva was born on 10 December 1986 in Moscow, Soviet Union (present Russian Federation). In 2003 she began her study in Moscow Medical Academy in the faculty of Pharmaceutical Sciences. In 2008 she obtained a master's degree in pharmacy and started to work in the field of drug development. During the following three years, while working as a monitor of clinical trials, she developed a strong interest in pre-clinical research aimed towards understanding the molecular mechanisms of drug action and underlying disease pathobiology. This experience resulted in her decision to obtain a second master's degree. In 2011 she was accepted into an international master program in Molecular Medicine at Charite University, Berlin, Germany.

During this two year degree, she became actively engaged in research on vascular biology and inflammation. First, Taisiya joined the laboratory of Prof. dr. med. Philipp Stawowy at the German Heart Institute, Berlin where she studied the role of PCSK9 in atherosclerosis. Later, she performed an internship in the group of "Inflammation biology" headed by Prof. dr. Sergei A. Nedospasov at the German Rheumatism Research Center (DRFZ), a Leibniz Institute, Berlin. Under the supervision of Dr. Yuri Schebzukov she successfully completed her master thesis on the transcriptional regulation of tumor necrosis factor (TNFα).

In October 2013 Taisiya received her second M.Sc. in Molecular Medicine and in December same year became a PhD candidate at the Department of Internal Medicine and Einthoven Laboratory for Vascular and Regenerative Medicine at Leiden University Medical Centre.

In following years, Taisiya focused on hemodialysis vascular access dysfunction. To untangle this major clinical problem: Taisiya designed, performed and coordinated several *in vivo* and *in vitro* studies under the supervision of Prof. dr. A.J. van Zonneveld, Prof. dr. P.H.A. Quax and Dr. J.I. Rotmans.

During her Doctoral degree, Taisiya spent eight months at the University California, Los Angeles at the Department of Bioengineering. Under the supervision of Prof. dr. Song Li she performed a research project in the field of vascular tissue engineering.
The results of her research are published in peer-reviewed international scientific journals and presented in this thesis.

Her work was presented in number of national and international conferences, including an oral presentation at the Kidney Week of the American Society of Nephrology (2016). At the congress of European Renal Association – European Dialysis and Transplant Association (ERA-EDTA) Taisiya won a price in a category Best Abstracts presented by Young Authors.

Supplementary to her research, Taisiya is involved in teaching activities, providing lectures and supervision to medical and biomedical students of the "Heart and blood vessels" and "Biomedical Translational Research in Surgery" minors.

It is her sincere desire and ambition to improve current patient care therapies through translational medical research. Taisiya remains passionate towards development of her career in academia, and currently continues her work in the vascular biology field as a postdoctoral fellow.

List of publications:

1. Rotmans JI, **Bezhaeva T.**
The battlefield at arteriovenous crossroads: invading arterial smooth muscle cells occupy the outflow tract of fistulas.
Kidney Int. 2015 Sep;88(3):431-3.

2. Wong C, **Bezhaeva T**, Rothuizen TC, Metselaar JM, de Vries MR, Verbeek FP, Vahrmeijer AL, Wezel A, van Zonneveld AJ, Rabelink TJ, Quax PH, Rotmans JI.
Liposomal prednisolone inhibits vascular inflammation and enhances venous outward remodeling in a murine arteriovenous fistula model.
Sci Rep. 2016 Jul 27;6:30439.

3. Grune J, Meyborg H, **Bezhaeva T**, Kappert K, Hillmeister P, Kintscher U, Pieske B, Stawowy P.
PCSK9 regulates the chemokine receptor CCR2 on monocytes.
Biochem Biophys Res Commun. 2017 Apr 1;485(2):312-318.

4. Shebzukhov YV, Stanislawiak S, **Bezhaeva T**R, Nedospasov SA, Kuprash DV.
Low level of Lck kinase in Th2 cells limits expression of CD4 co-receptor and S73 phosphorylation of transcription factor c-Jun.
Sci Rep. 2017 May 24;7(1):2339.

5. **Bezhaeva T**, Wong C, de Vries MR, van der Veer EP, van Alem CMA, Que I, Lalai RA, van Zonneveld AJ, Rotmans JI, Quax PHA.
Deficiency of TLR4 homologue RP105 aggravates outward remodeling in a murine model of arteriovenous fistula failure.
Sci Rep. 2017 Aug 31;7(1):10269.

6. van Alem CMA, Boonstra M, Prins J, **Bezhaeva T**, van Essen MF, Ruben JM, Vahrmeijer AL, van der Veer EP, de Fijter JW, Reinders ME, Meijer O, Metselaar JM, van Kooten C, Rotmans JI.
Local delivery of liposomal prednisolone leads to an anti-inflammatory profile in renal ischaemia-reperfusion injury in the rat.
Nephrol Dial Transplant. 2018 Jan 1;33(1):44-53.

7. **Bezhaeva T**, de Vries MR, Geelhoed WJ, van der Veer EP, Versteeg S, van Alem CMA, Voorzaat BM, Eijkelkamp N, van der Bogt KE, Agoulnik AI, van Zonneveld AJ, Quax PHA, Rotmans JI.
Relaxin receptor deficiency promotes vascular inflammation and impairs outward remodeling in arteriovenous fistulas.
FASEB J. 2018 Jun 8.

8. **Taisiya Bezhaeva**, Wouter J. Geelhoed, Dong Wang, Haoyong Yuan, Eric P. van der Veer, Carla M.A. van Alem, Febriyani F.R. Damanik, Xuefeng Qiu, Anton Jan van Zonneveld, Lorenzo Moroni, Song Li and Joris I. Rotmans.
Contribution of bone marrow-derived cells to in situ engineered tissue capsules in a rat model of chronic kidney disease.
Biomaterials - In press (available online 15 December 2018).

Acknowledgement

Every single step of this thesis was done in a very collaborative and supportive environment. Here, I would like to reflect upon the people who have supported and helped me so much throughout this entire period.

My thesis advisors **Prof. Anton Jan van Zonneveld** and **Prof. Paul Quax**.
Anton Jan. A professor who can really "rock-and-roll". Thank you for your inspiring guidance. Our Monday group meetings provided me with very insightful discussions.

Paul. You are truly a visionary of science and have been an exemplary mentor for me. I appreciate and value everything you have taught me. Our interesting and long-lasting chats and insightful discussions were always very motivating and inspiring.

I would like to thank my dear mentor **Dr. Joris Rotmans**.
Joris, you are everything one could look for in a good mentor and I could not have imagined having a better advisor and supervisor for my Ph.D. than you. Your invaluable feedback to all of my scientific drafts were always full of enthusiasm and motivation. Your critical analysis and excellent advice during the entire period make the completion of this thesis successful and groomed me to be sound professional. Special thanks for your personal support, in times of my scientific or personal black holes. After meetings with you there was always a light at the end of the tunnel.

My sincere thanks also go to **Prof. Song Li**, for offering me the 8-month internship opportunity in your group. It was an unforgettable time in sunny California for me. To work under your supervision at UCLA helped me to realize what interdisciplinary cutting edge research truly means.

Prof. Cees van Kooten, dear Cees. The immunology guru and an extremely friendly professor whose door is always open for questions. Thank you for your time, your insightful suggestions and support of my research.

Margreet. Magician of mouse surgery, great scientists, colleague and a friend. Thank you for always giving me your honest advice. It was a pleasure to have you by my side during all these years and I really value all the scientific and personal contribution from your side.

Carla. Wonderful and generous friend who has always been ready to support and help me. I admire your positive, honest and loyal outlook. I will never forget the many wonderful lunches, trips and fun activities we have done together. Black humor is a sign of high intelligence, as a recent study in the journal *Cognitive Processing* suggests. I think you get it all.

Wouter. "Als je wilt chillen, is het geen probleem." Great colleague, who can construct almost anything ranging from a homemade fish smoker to highly-tech medical devises. It was always a lot of fun to plan and to perform experiments with you.

Reshma. Your willingness to give your time for my research so generously has been very much appreciated. Not to forget, your Surinamese treats definitely had a positive influence on the quality of the research I was doing.

Eric. One of the most enthusiastic, life-energizing, funny and intelligent person I know. Eric you were someone who was always ready to brainstorm on science and give me a fresh look, when I felt stuck. Special thanks to all your proofreading.

C7 senior crew: **Janine, Hetty, Catelijne, Bernard, Roel, Marten** each of you has given of your time, energy, and expertise and I am grateful for it.

All the past **Carolien, Margien, Danielle, Jonna, ChunYu, Bram, Ruben** and present members of C7 Island: What welcoming people you are.

K5 Island: **Sophie, Dianne, Franca, Gesa, Barend, Jurjen, Huayu, Gangqi** you are the dream team. I would like to thank you all for your support in my work and also when I had personal troubles.

D2 Island: **Jaq, Anne-Marie, Wendy Sol, Wendy Stam, Loes. People from thrombosis and hemostasis department. Wonderful colleagues from** D3 Island. Former P1 Island: **Erna, Rob;**

I know that I could always ask them for advice and opinions on lab related issues and they are always there to help me.

I would like to thank my colleagues **Dong, Jennifer, Danny, Zhang, Jun, LeeAnn** from my internship at UCLA for their wonderful collaboration.

Yury Shebzukhov, my first science-coach and one of the most creative scientists with a great sense of humor I have ever met. Thank you for enlightening upon me the first glance on real science.

Here, there are my friends.

Russian block:
Lenoki Puris, my forever interested, cheering and always enthusiastic real friend. One of the few people who were always keen to know what I was doing and how I was proceeding with my science.

To my soul mates, **Iriza and Tanjuk**. Thank you for your thoughts, well-wishes, texts, visits, and being there whenever I needed a friend.

My former study mates 15-16 and kozyavki crew.

Amsterdam block:
Ilusha, Ksju, Irisha and Oksana

Berlin block:
Dan. Does not matter where you are or what you are up to, we are always on the same frequency**.**

Los Angeles block:
Anna Tarasyuk and Mike Miroshnikov, true angels I found in LA. Thank you for taking care.
Basti and Sam, thank you for your support and for showing me beautiful California state and beyond.
Cary for your hospitality and making me feel home.

Finally, there is my family.
My grandfather **Ivan Bezhaev** (dedushka Vanya) who was always truly appreciating any of my achievements. I am sure that he would be one of the few people who would read this thesis from the beginning until the end although it is likely that he would not have grasped what it was all about!

Nicolino a true and great supporter. It is very important for me, to have you - the person with whom I can share my thoughts and doubts. Thank you for making home a place where you want to come back.

My eternal cheerleader and my best friend, my sister **Olyas** and her family **Mills** and **Hugh** who have provided for me through moral and emotional support in my life. Olyas has always faith in me and my intellect. Thank you for being non-judgmental and accepting all my freak-ins and outs.

I am especially grateful to my parents, **maman- Irina Bezhaeva** and **papan- Rostislav Bezhaev** who supported me emotionally and financially. I always knew that you wanted the best for me.

Thank you very much, everyone!